TECHNISCHE UNIVERSITÄT DRESDEN

Faculty of Environmental Sciences

Integrated watershed modeling in Central Brazil: Toward robust process-based predictions

A dissertation submitted in partial fulfillment of the requirements for the degree of Doctor rerum naturalium (Dr. rer. nat.) by

Dipl.-Geogr. Michael Strauch

born on October 9, 1981 in Marienberg/Sa., Germany

Reviewed by

Prof. (em.) Dr. Franz Makeschin

Dresden University of Technology, Chair of Soil Science and Site Protection

Prof. Dr. Nicola Fohrer

Kiel University, Department Hydrology and Water Resources Management

PD Dr. Martin Volk

UFZ Leipzig, Department Computational Landscape Ecology

Date of defense: April 16, 2014 (Tharandt, Germany)

Declaration of the candidate

I confirm that this copy is identical with the original dissertation titled:

„Integrated watershed modeling in Central Brazil: Toward robust process-based predictions."

I hereby declare that this thesis is my own work and effort. Where other sources of information have been used, they have been acknowledged.

Leipzig, 30.01.2014

. . . . . .

Michael Strauch

The more I see the less I know for sure.
John Lennon

Acknowledgments

I would like to express my gratitude to all those who have contributed to the completion of this thesis.

Firstly, I wish to thank Franz Makeschin for his supervision and the tremendous confidence he has placed in me. Within our project working group, he gave me the freedom to explore the scientific questions that I found most interesting and also to find solutions to problems that I encountered.

My special thanks go to Martin Volk, who took me seven years ago on the path of watershed modeling and supported and encouraged me from then onwards. I owe him much, for good advice and access to his extensive network, but foremost for his open-minded warmth that makes working with him a true pleasure.

Carsten Lorz must be mentioned in the same breath, who has been my mentor since I was an undergraduate at the TU Dresden and whose continuing support was absolutely essential for my professional development. I fondly remember our joint work in Dresden and Tharandt including the journeys to Brazil, as colleagues and friends.

I wish to thank all my Brazilian colleagues, in particular Jorge Werneck Lima and Fábio Bakker, for providing data and organizational efforts, for fruitful discussions and for supporting social events, above and beyond the context of work.

Following is a list of persons to which I am deeply grateful for discussion as well as sharing their ideas and time: Ameur Manceur, Claudia Franz, Daniel Hawtree, Daniel Doktor, Filipa Tavares Wahren, Felix Witing, Friedrich Koch, Pablo Borges, René Schulze, René Höfer, and Sven Lautenbach. I greatly appreciated your friendly support.

I would like to thank all other colleagues at the Institute of Soil Science and Site Ecology (TU Dresden) and the Department of Landscape Ecology (UFZ Leipzig) for providing a pleasant working atmosphere.

I gratefully acknowledge the financial support by the BMBF for the IWAS-ÁGUA DF project (FKZ: 02WM1166 and 02WM1070) and wish to thank everyone involved in the project for good cooperation.

Special thanks go to the SWAT model community and in particular to the developers group in Temple, TX. Their feedback on my work at conferences, workshops, and external meetings was always encouraging me.

I also thank Nicola Fohrer for agreeing to serve as a reviewer and I am deeply grateful to the anonymous researchers that critically reviewed and thus improved the articles included here.

Last but not least, my dear family and friends: thanks for always being there for me!

Abstract

Over the last decades, fast growing population along with urban and agricultural sprawl has drastically increased the pressure on water resources of the Federal District (DF), Brazil. Various socio-environmental problems, such as soil erosion, non-point source pollution, reservoir silting, and conflicts among water users evoked the need for more efficient and sustainable ways to use land and water. Due to the complexity of processes relevant at the scale of river basins, a prior analysis of impacts of certain land use and/or land management changes is only feasible by means of modeling. The Soil and Water Assessment Tool (SWAT) has been proven to be useful in this context, across the globe and for different environmental conditions. In this thesis, the SWAT model is utilized to evaluate the impact of Best Management Practices (BMPs) on catchment hydrology and sediment transport. However, model applications in tropical regions, such as the DF, are hampered by severe challenges, (i) the lack of input and control data in an adequate temporal and spatial resolution and (ii) model structural failures in representing processes under tropical conditions. The present (cumulative) thesis addresses these challenges in model simulations for two contrasting watersheds, which both are important sources of the DF's drinking water supply, i.e. (i) the agriculture-dominated Pipiripau river basin where conflicting demands put immense pressure on the available water resources and (ii) the Santa Maria / Torto river basin, which is to large parts protected as national park and, thus, covered by native vegetation of the Cerrado biome.

Perhaps one of the most challenging issues facing watershed modelers in tropical regions is the fact that rain gauge networks can usually not reflect the high spatio-temporal variability of mostly convective precipitation patterns. Therefore, an ensemble of different reasonable input precipitation data-sets was used to examine the uncertainty in parameterization and model output. Acceptable streamflow and sediment load predictions could be achieved for each input data-set. However, the best-fit parameter values varied widely across the ensemble. Due to its enhanced consideration of parameter uncertainty, this ensemble approach provides more robust predictions and hence is reasonable to be used also for scenario simulations. BMP scenarios for the Pipiripau River Basin revealed that erosion control constructions, such as terraces and small retention basins along roads (Barraginhas) are promising measures to reduce sediment loads (up to 40%) while maintaining streamflow. Tests for a multi-diverse crop rotation system, in contrast, showed a high vulnerability of the hydrologic system against any increase in irrigation. Considering the BMP implementation costs, it was possible to estimate cost-abatement curves, which can provide useful information for watershed managers, especially when BMPs are supported by Payments for Environmental Services as it is the case in the study area due to the program *Produtor de Água*. While for agricultural areas the model has proven to gen-

erate plausible results, the plant growth module of SWAT was found to be not suitable for simulating perennial tropical vegetation, such as Cerrado (savanna) or forest, which can also play a crucial role in river basin management. For temperate regions SWAT uses dormancy to terminate growing seasons of trees and perennials. However, there is no mechanism considered to reflect seasonality in the tropics, i.e. the phenological change between wet and dry season. Therefore, a soil moisture based approach was implemented into the plant growth module to trigger new growing cycles in the transition period from dry to wet season. The adapted model was successfully tested against LAI and ET time series derived from remote sensing products (MODIS). Since the proposed changes are process-based but also allow flexible model settings, the modified plant growth module can be seen as a fundamental improvement useful for future model application in the tropics.

The present thesis shows insights into the workflow of a watershed model application in the semi-humid tropics – from input data processing and model setup over source code adaptation, model calibration and uncertainty analysis to its use for running scenarios. It depicts region-specific challenges but also provides practical solutions. Hence, this work might be seen as one further step toward robust and process-based model predictions to assist land and water resources management.

Zusammenfassung

Starkes Bevölkerungswachstum, ungeplante Suburbanisierung und Landnutzungsänderungen (z.B. Intensivierung in der Landwirtschaft) verstärkten innerhalb der letzten Jahrzehnte zunehmend den Druck auf die Wasserressourcen des Bundesdistrikts Brasilien (zentralbrasilianisches Hochland), in dessen Mitte die junge Hauptstadt Brasília liegt. Damit verbundene negative Umweltauswirkungen, wie Bodenerosion, Stoff- und Sedimenteinträge in Fließgewässer und Talsperren sowie Konflikte zwischen den Wassernutzern erfordern daher dringend effektive und nachhaltige Lösungen im Land- und Wasserressourcenmanagement.

Der Einfluss von möglichen zukünftigen Landnutzungs- und Bewirtschaftungsänderungen auf Wasserverfügbarkeit und -qualität hängt vom jeweiligen, oftmals sehr komplexen, landschaftsökologischen Prozessgefüge ab und kann nur mithilfe von prozessbasierten Simulationsmodellen quantitativ auf der Ebene von Einzugsgebieten abgeschätzt werden. Das "Soil and Water Assessment Tool" (SWAT) ist ein solches Modell. Es findet weltweite Anwendung für verschiedene Umweltbedingungen in Einzugsgebieten der Meso- bis Makroskala, um Landnutzungseffekte auf den Wasserhaushalt und den Transport von Nährstoffen, Pestiziden und Sedimenten zu prognostizieren. Seine Anwendung in tropischen Regionen, wie etwa in Zentralbrasilien, ist jedoch mit erheblichen Herausforderungen verbunden. Das betrifft sowohl die Verfügbarkeit von Eingangs- und Referenzdaten in ausreichender raum-zeitlicher Auflösung, als auch modellstrukturelle Unzulänglichkeiten bei der Prozessabbildung. Die vorliegende kumulative Dissertation zeigt dies anhand von Modellanwendungen für zwei unterschiedliche wasserwirtschaftlich relevante Einzugsgebiete (EZG): Das landwirtschaftlich intensiv genutzte EZG des Rio Pipiripau mit aktuell besonders konfliktträchtiger Wassernutzung, und das Santa Maria/Torto-EZG, welches - geschützt als Nationalpark - durch größtenteils natürliche Vegetationsformationen der brasilianischen Savanne (Cerrado) gekennzeichnet ist.

Eine der größten Herausforderungen für die Einzugsgebietsmodellierung in tropischen Regionen liegt in der Abschätzung des Gebietsniederschlages, da vorhandene Messstationsdichten oft nicht ausreichen, um die hohe räumliche und zeitliche Variabilität der meist konvektiven Niederschläge zu erfassen. Mithilfe eines Ensembles verschiedener, plausibel generierter Niederschlagsreihen ist der Einfluss von Niederschlagsdaten-Unsicherheit auf die Modellparametrisierung und -vorhersage explizit berücksichtigt und untersucht worden. Zufriedenstellende Abfluss- und Sedimentfrachtsimulationen waren mit jeder der als Modelinput verwendeten Niederschlagsreihen möglich, jedoch nur bei entsprechender, z.T. stark voneinander abweichender Einstellung der Kalibrierungsparameter. Da diese umfassendere Betrachtung von Parameterunsicherheit zu robusteren Modellvorhersagen führt, wurde der Ensemble-Ansatz auch in der Simulation von Bewirtschaftungsszenarien, dem eigentlichen Modellzweck, verwendet. Die Szenariosimulationen zeigten, dass

Maßnahmen zur Erosionsvermeidung (Terrassierung) und zum Sedimentrückhalt (kleine Sedimentrückhaltebecken entlang von Straßen - *Barraginhas*) die Sedimentfracht des Rio Pipiripau durchschnittlich um bis zu 40% reduzieren können, ohne dabei die Wasserverfügbarkeit zu beeinträchtigen. Modellszenarien mit einer vielgliedrigen Fruchtfolge auf großer Fläche verdeutlichten dagegen die hohe Vulnerabilität des Niedrigwasserabflusses in der Trockenzeit gegenüber jedweder Erhöhung der Bewässerungsmenge. Auf Grundlage von Kostenschätzungen für einzelne Maßnahmen konnten Kostenkurven zur Verringerung der Sedimentfracht und damit nützliche Informationen für das Wasserressourcen-Management abgeleitet werden, insbesondere weil eine Auswahl solcher Agrar-Umweltmaßnahmen im Pipiripau-EZG durch das Programm *Produtor de Agua* finanziell gefördert werden sollen. Während das Modell in landwirtschaftlich genutzten Gebieten plausible Ergebnisse produzierte, wurden erhebliche Schwachstellen in der Simulation ausdauernder Vegetation (z.B. Cerrado) identifiziert. Zur Unterbrechung jährlicher Vegetationszyklen verwendet SWAT eine tageslängenabhängige Dormanzperiode. Diese ist zwar zweckmäßig zur Abbildung der Vegetationsdynamik in den gemäßigten Breiten, steuert aber nicht tropische Vegetationszyklen. Um den Wechsel zwischen Trocken- und Regenzeit in der pflanzenphänologischen Simulation in SWAT abzubilden, wurde daher im Rahmen dieser Arbeit das Pflanzenwachstumsmodul modifiziert, und zwar unter anderem durch Einbeziehung der simulierten Bodenfeuchte zur Unterbrechung der Wachstumszyklen. Das angepasste Modul wurde erfolgreich anhand von Fernerkundungsdaten (MODIS) zum zeitlichen Verlauf von Blattflächenindex und Evapotranspiration getestet. Es ist prozessbasiert und erlaubt flexible Einstellungen, so dass es als grundlegende Modellverbesserung auch für andere SWAT-Anwender von großem Nutzen sein kann.

Die vorliegende Dissertation bringt neue Einsichten in verschiedene wichtige Aspekte der integrierten Modellierung tropischer Einzugsgebiete, von der Eingangsdatenaufbereitung über Quellcode-Anpassung, Modellkalibrierung und Unsicherheitsanalyse bis hin zu Szenariosimulationen. Sie veranschaulicht regionsspezifische Herausforderungen, liefert gleichzeitig aber auch praktikable Lösungen und damit einen wichtigen Beitrag für robustere prozessbasierte Modellanwendungen als Entscheidungsunterstützung im Bereich Land- und Wasserressourcenmanagement.

Contents

List of Figures

List of Tables

1 Introduction

1.1 Motivation: The *Distrito Federal*

In 1960, a new city and a new federal state were plotted on each map of Latin America's largest country. Brazil's planned capital city, Brasília, and the surrounding district, *Distrito Federal* – DF (Fig. 1.1), were placed in the interior of the Brazilian Central Plateau, at that time referred to as *nowhere land* (Madaleno, 1996). Until now, the DF has become a metropolitan area inhabiting nearly 2.6 million residents (IBGE, 2011); and its population is projected to grow continuously in future decades (GDF, 2012). As a consequence, the existing system of water supply has approached its limits and cannot provide water security in future decades (ANA, 2009).

There is broad political and scientific consensus that the concept of Integrated Water Resources Management (IWRM) is most suitable to generate and implement efficient, equitable and sustainable solutions for problems related to water scarcity (Biswas, 2004; Rahaman and Varis, 2005; UN-Water, 2008). IWRM is defined as "a process which promotes the coordinated development and management of water, land and related resources, in order to maximize the resultant economic and social welfare in an equitable manner without compromising the sustainability of vital ecosystems" (GWP, 2000). In contrast to sectoral management approaches, decision making in IWRM is based on participation of all relevant stakeholders (UNESCO et al., 2009) as well as on integrative scientific knowledge and understanding (Liu et al., 2008).

Such a widened integrated approach includes green water as an additional resource to be managed (Hoff, 2009). Green water refers to the flows of water vapour in the form of transpiration, interception and evaporation from the soil and vegetation and thus explicitly refers to land use and land management, while runoff and groundwater recharge is considered as blue water (Jewitt, 2006). Compared to conventional infrastructure and blue water solutions, best practices accounting for both blue and green water, provide more degrees of freedom for increasing water productivity and enhancing water-related ecosystem services[1] (Hoff, 2009). Considering green water flows is especially important in the DF. Along with the growing population, land cover and land use have changed tremendously over the last 50 years, similarly to regions in southern Brazil (Simon et al., 2010). Before Brasília was constructed, the area was almost fully covered by native vegetation of the Cerrado biome, i.e. savanna and gallery forests. Nowadays, agricultural areas producing crops and livestock occupy about 45% and urban areas 11% of the DF (Felizola et al., 2001; Fortes et al., 2007).

[1] Ecosystem services are defined as the benefits humans obtain from ecosystems (Millenium Ecosystem Assessment, 2005).

Lorz et al. (2011b) studied the effects of this land use/cover change on the DF's water resources by analyzing historical hydro-climatic time series. Although they found no significant precipitation changes for the last decades, low flow during dry season decreased substantially in many areas, especially in watersheds[2] which had a strong increase in both agricultural and urban water use. The degradation of water quality including sediment pollution and the silting of reservoirs are thought to be mainly related to urban processes[3], but might be also caused by diffuse pollution from agriculture (Franz et al., 2013; Lorz et al., 2011b). Hence, the pressure on DF's water resources has not only increased due to water supply demands of a steadily growing population, it is also forced by a huge transformation of the landscape and its management. Even though additional water resources will be made available, including the Lakes Paranoá and Corumbá, it needs more efficient ways to use and distribute water in order to avoid conflicts among water users (GDF, 2012).

In this context, incentive-based policy instruments, such as Payments for Ecosystem Services (PES), can effectively help to adopt green-blue water principles. As an example, upstream farmers that switch to more sustainable management practices (e.g. by applying less irrigation water, pesticides and fertilizer) might suffer less income from agriculture, but would be paid for the benefits (improved water supply) they provide for downstream water users. PES can thus bridge the gap between field-scale soil and water conservation and basin-scale IWRM (Hoff, 2009).

In 2007, the Brazilian National Water Agency (ANA) has launched an initiative called Produtor de Água (Water Producer) to establish PES schemes in priority river basins. The Pipiripau catchment (Fig. 1.1), northeast of Brasília, is one of these priority river basins since it is intensively used for both, crop production and urban water supply. Recently, DF's water supply and treatment company (CAESB) has faced increasing treatment costs for the withdrawals from the Pipiripau River due to soil erosion and nutrient runoff from surrounding agricultural lands (Buric and Gault, 2011). Therefore, the Water Producer program will compensate rural landowners in the catchment who help to improve water quality and quantity by restoring or preserving (semi-)natural vegetation along streams and by implementing Best Management Practices (BMPs) on cropland and pastures (BRASIL, 2010; Buric and Gault, 2011). As a consequence, the PES schemes planned for the Pipiripau catchment formed an excellent research subject for the project IWAS-Água DF[4], which aimed at creating a scientific base to support IWRM in the DF. The project was subdivided into three major complexes, i.e., (1) river basins and water bodies, (2) waste water, and (3) drinking water (Lorz et al., 2011a). Complex (1) and in particular the aspect land management formed the scope of this doctoral thesis.

[2] Watershed, the area of land draining into a common body of water, is also labelled variously as catchment or river basin (throughout the world and also in this thesis).

[3] For example, nutrient pollution due to insufficient sewage treatment or soil erosion in construction sites due to the removal of vegetation.

[4] IWAS (Internationale Wasserforschungs-Allianz Sachsen) and the companion project Água DF were funded by the German Ministry of Education and Science (BMBF; FKZ: 02WM1166 and 02WM1070) for a 5-year run-time (2008 – 2013).

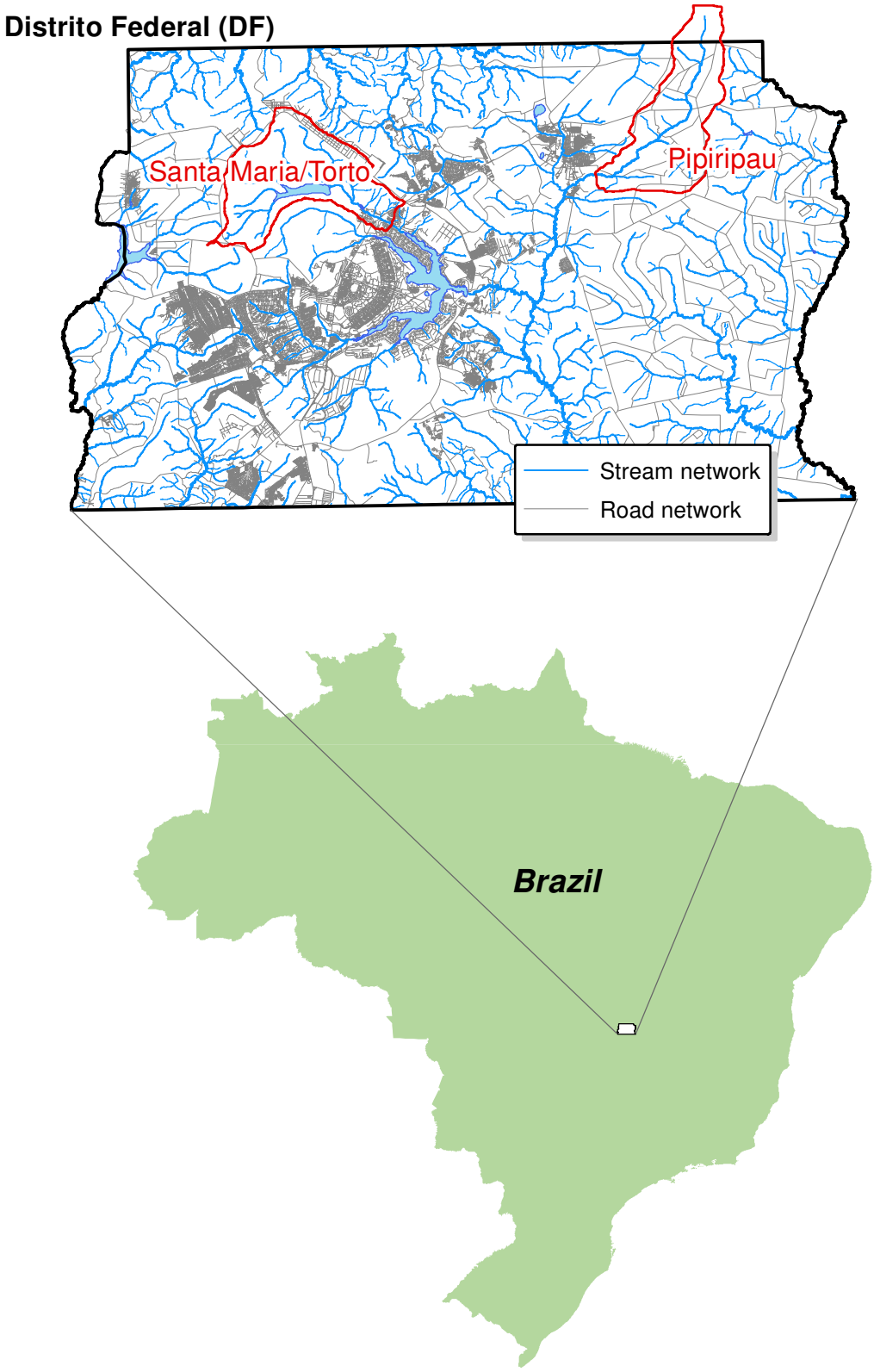

Figure 1.1: The *Distrito Federal* and the two study catchments (Santa Maria/Torto and Pipiripau).

1.2 Watershed modeling and model choice

IWRM and other approaches in land and water resources management, such as the concept of ecosystem services, share an integrative perspective considering both the bio-physical system (including climate, hydrology, topography, soils, land cover) and the socio-economic management system (e.g. human water demand). Given the rapid development of computer technology, complex interactions between and within the two systems can be best captured by mathematical models. Watershed models, for example, are used to simulate bio-physical processes of the flow of water, sediment, chemicals, nutrients, and microbial organisms within watersheds, as well as to quantify the anthropogenic impact on these processes (Singh and Frevert, 2006). Modeling can thus "help to integrate knowledge and data by embedding the best science available" (Liu et al., 2008) and allows for experiments assuming changing conditions, such as changes in land cover, land management, and/or climate (scenario analysis). In fact, watershed models have become a main tool for problems related to water resources assessment and management (Singh and Frevert, 2006; Jajarmizadeh et al., 2012; Daniel et al., 2011).

Today, a large number of watershed models is available (Daniel et al., 2011; Jajarmizadeh et al., 2012; Singh, 1995), varying in the nature of the employed algorithms (empirical, conceptual, or physically based), in the approach used for model input or parameter specification (stochastic or deterministic), and in the way to represent the water resource system spatially (lumped or distributed) and temporally (continuous time, single-event, or steady state). Given the range of available models and software packages, choosing the right model for a particular project can be daunting and should involve questions like whether the model outputs meet the aims of the project, can the assumptions made by the model adequately represent the relevant processes, or can all necessary information be provided within the time and cost constraints of the project (cf. Beven, 2012)?

To study the effects of land management on the water resources in rural and agricultural areas of the DF, the decision was made for the Soil and Water Assessment Tool (SWAT) (Arnold et al., 1998; Arnold and Fohrer, 2005). SWAT has gained international acceptance as an effective tool for assessing water resource and nonpoint source pollution problems for a wide range of scales and environmental conditions across the globe (Gassman et al., 2007). The model is based on well established agricultural models which were linked with simple, efficient, but yet realistic routing components to form a basin-scale model that (1) is computationally efficient, (2) allows spatial details to some extent[5], (3) requires readily available inputs, (4) is continuous-time at a daily time step, and (5) is capable of simulating land-management scenarios (Arnold et al., 1998). In the last decade, the model has undergone continuous revision and upgrading (Arnold et al., 2010; Krysanova and Arnold, 2008). At the time of writing, the SWAT Literature Database[6] listed more than 1,400 peer reviewed journal articles, among which numerous applications have been driven by the needs of various government agencies, particularly in the U.S. and the

[5] SWAT is spatially semi-distributed, a compromise solution between lumped and fully distributed. At the level of sub-basins, spatially distributed data on land use, soils, and slope are combined and aggregated to form Hydrological Response Units (HRUs). Due to the aggregation process, HRUs loose their spatial relationship within the sub-basins.

[6] URL: https://www.card.iastate.edu/swat_articles/, accessed on October 18, 2013.

European Union, for impact assessments as demanded by environmental programs and directives (Volk et al., 2011). SWAT has been used to study water yields and non-point source pollution (nutrients, sediments, pesticides) of surface and groundwater bodies in response to a variety of management aspects (e.g. conservation practices, bioenergy crops, afforestation/deforestation) and climate change (cf. reviews of Memarian et al., 2013 and Gassman et al., 2007). More recently, also economic and ecosystem services assessments were conducted based on SWAT simulations (e.g. Liu et al., 2013; Naramngam and Tong, 2013; Burkart and Jha, 2012; Lautenbach et al., 2013).

Beven (2012) attributes the popularity of SWAT to the wide range of facilities it provides, the ability to freely download the model and its source code, the links to GIS databases which include default parameter values, and the way it can reflect catchment characteristics and land management strategies. In recent reviews on watershed models (e.g. Borah et al., 2006; Daniel et al., 2011), SWAT has been examined as a well-suited model for long-term continuous simulations of a wide variety of conservation practices in predominantly agricultural watersheds.

1.3 Main research questions

The model features mentioned in the previous section favored the choice of SWAT within the project IWAS-Água. The intended use of the model was to assess the impacts of agricultural BMPs in the Pipiripau catchment as proposed and supported by the Water Producer Program. This leads to the overall and applied research question that can be asked as follows:

> *How effective are Best Management Practices supported by PES in reducing sediment loads and what is their impact on streamflow in the Pipiripau River Basin?*

It has to be noted that not all measures proposed by the Water Producer Program can be assessed using SWAT. Riparion buffer strips, for example, play a major role within the program but are impossible to simulate properly due to the simplified, non-spatial routing of water, nutrients, and sediments within the subbasins. The BMPs being evaluated are (1) parallel terraces to different proportions on agricultural areas, (2) small sediment retention basins ("Barraginhas") to different quantities, and (3) a multi-diverse crop rotation including crops during dry season as an alternative to the prevailing monocultures of soybean and corn, likewise to different proportions on cropland. All of these management practices aim at reducing soil losses and, thus, water protection. However, at the time of writing it was still unclear how the final PES scheme will look like in the study catchment, i.e., how much money rural landowners will receive for supporting a single measure. Therefore, the analysis also considers implementation costs to estimate cost-abatement curves, which might be helpful for designing the PES scheme in the Pipiripau catchment.

Since SWAT is, like all watershed models, only an "approximation to the complexity of the perceptual model of catchment processes" (Beven, 2012), the general question arises on how meaningful the model results are. This question can hardly be answered in an unequivocal manner by any modeler since it depends on several more questions that are not

less crucial, i.e., how far can we believe in the algorithms used to represent the complexity, and, assuming the algorithms are adequate, how far can we believe in the values used in the algorithms? The values (often stationary) are reffered to as either model input data or model parameters; and there can be thousands in SWAT given the wide range of processes included and their spatial distribution. In the scientific community there is no doubt that adressing uncertainty is important when models are used to support water management decisions (e.g. Beven, 1993; Uhlenbrook et al., 1999; Jakeman and Letcher, 2003; Refsgaard and Henriksen, 2004). In practice, however, uncertainty analysis is still not standard in many modeling exercises (Pappenberger and Beven, 2006) or it is often done as an 'end of pipe' analysis that is carried out after model setup, calibration and validation have been completed (Refsgaard et al., 2007). The model application presented in this thesis is likewise far from considering all sources of uncertainty in watershed modeling, but it tackles one challenging aspect of uncertainty that is especially important for the region of the DF:

> *Given both, a low density of rain gauges and a high spatial and temporal variability of mostly convective rain events, how can we account for the considerable precipitation uncertainty in SWAT simulations?*

To allow variation within the precipitation input data, the idea was to use an ensemble of four different yet reasonable datasets varying in terms of data source (ground- or satellite-based), spatial distribution (lumped or distributed), and temporal distribution (raw time series or moving average). The study should provide answers on (i) how the different input datasets influence parameter sensitivity, (ii) how the best-fit parameter values defined by auto-calibration and the respective streamflow predictions differ for each rain input model, and (iii) how we can obtain benefits from combining the different simulation results in terms of model performance and predictive uncertainty.

The focus on precipitation uncertainty and its influence on model simulations was a logical consequence of data scarcity in the study area. Other input data, such as information on topography, land use and land management practices as well as soil data could be obtained in overall sufficient quality. However, some data issues certainly deserve more attention than they have received within the modeling procedures presented in this thesis. These concerns, mainly related to soil parameterization and sediment load reference data, will be adressed in the final discussion section.

Questioning the adequacy of input data and parameter values is an integral part of watershed modeling. However, as SWAT was developed for and comprehensively tested in US watersheds, model applications in other regions and, in particular, in other climates have to be critically questioned also for their algorithms to represent processes. One major shortcoming of SWAT when used for tropical watersheds is the representation of vegetation dynamics of perennial plants (e.g. trees, shrubs, grasses) due to the absence of dormancy which is usually (in temperate regions) used to separate growing cycles in each simulation year (Wagner et al., 2011). This fundamental issue is also tackled in the thesis by asking:

> *If there is no cold-induced dormancy in the tropics, which processes should be used instead to automatically trigger growing cycles of perennial plants/land cover within SWAT?*

The idea here was to use the development of soil moisture in the upper two soil layers at the end of the dry season to initiate new growing seasons, which might be plausible because moisture - and not temperature or daylength - is the main driver of plant phenology in tropical regions (e.g. Childes, 1989; Borchert, 1994). Hence, new algorithms were implemented into the SWAT model and tested against satellite-based data on vegetation for the Santa Maria / Torto river basin (Fig. 1.1). The need to adequately model the dynamics and effects of perennials is urgent. Land use types dominated by perennial plants (e.g. savanna, forest, horticultures) are usually as much a part of river basins as crop land and urban areas. They can significantly affect water, sediment, and nutrient fluxes, and are often hot spots of biodiversity (like the Cerrado biome, cf. Klink and Machado (2005) and Silva et al. (2006)). Natural habitats and forests can therefore play a major role in land use planning and management, regardless of the strategy selected (land sharing or land sparing or a combination of both (Phalan et al., 2011)). In addition, even if the model application is only focused on agricultural management, how can we believe in the modeled catchment response (e.g. streamflow at the outlet) to management changes when we know it is biased by improper simulations of other land use classes inherent in the same catchment? In this context, the added value of the plant growth module modification and questions of its transferability to other regions have to be discussed as well.

1.4 Structure of the thesis

The research questions raised above were addressed in three peer reviewed journal articles which make up chapters 2, 3, and 4. In each of the chapters, SWAT model applications are presented. However, they all have a different focus within the modeling workflow illustrated in Fig. 1.2.

Chapter 2 refers to the issue of precipitation uncertainty inherent in model input data which places focus on the first task (model setup). However, since the effects of using an input data ensemble are analyzed in terms of parameter sensitivity, parameter uncertainty, and predictive uncertainty, there is also strong focus on task ii-a (model calibration).

Chapter 3 builds upon this, but model calibration is now extended to include also sediment load. Moreover, the calibrated model is used for scenario simulations (task iii) to study the impact of BMPs in the Pipiripau catchment. It has to be noted that precipitation uncertainty is also considered within the scenario simulations.

Chapter 4 places strong focus on model development which is included in task ii-b (source code adaptation). It presents the modifications of the plant growth module which were made to improve the simulation of perennial tropical vegetation. Model calibration here includes also plant parameters, which are adjusted to fit the model to the observed timeseries of Leaf Area Index (LAI) and evapotranspiration (ET).

Ideally, the workflow in Fig. 1.2 would be only one process capturing each of the different tasks which build upon each other. In fact, each of the tasks was carried out in a different model application. From chapter 2 to 3, there was the need to change the model version (from SWAT2005 to SWAT2009) to make use of the - at that time new - land use update function for running the BMP scenarios in the Pipiripau river basin. Further changes were made due to the inclusion of sediment load in the calibration procedure. The third study

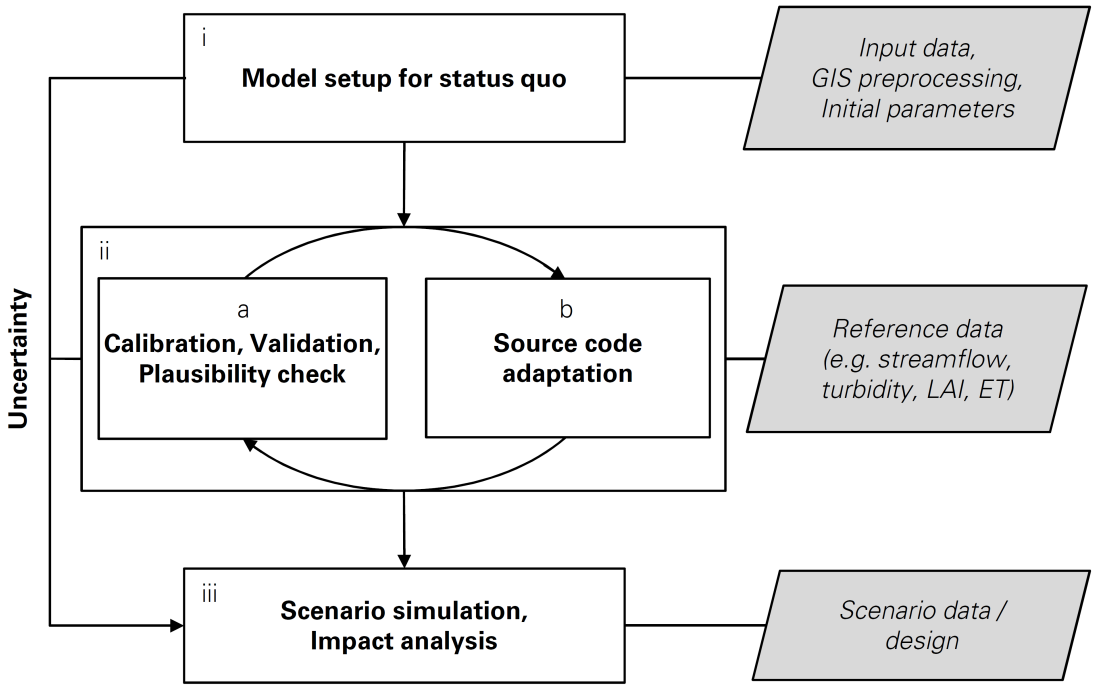

Figure 1.2: General modeling workflow.

(chapter 4) was even carried out for another catchment, the Santa Maria / Torto river basin. This catchment was chosen because it is to large parts covered by native vegetation of the Cerrado biome and thus better suited to derive satellite-based reference data on perennial vegetation. Nonetheless, the different studies still form a unity which is based on the SWAT model and the aim to utilize it for proper simulations that might be useful for water resources management in the region of the DF.

Chapter 5, finally, concludes the thesis with a summarizing discussion of central findings and provides possible directions for future research.

1.5 List of publications

This is a cumulative dissertation including three peer-reviewed publications listed as follows:

1. M. Strauch, C. Bernhofer, S. Koide, M. Volk, C. Lorz, and F. Makeschin (2012): Using precipitation data ensemble for uncertainty analysis in SWAT streamflow simulation. *Journal of Hydrology* 414-415: 413-424

2. M. Strauch, J.E.F.W. Lima, M. Volk, C. Lorz, and F. Makeschin (2013): The impact of Best Management Practices on simulated streamflow and sediment load in a Central Brazilian catchment. *Journal of Environmental Management* 127: S24-S36

3. M. Strauch and M. Volk (2013): SWAT plant growth modification for improved modeling of perennial vegetation in the tropics. *Ecological Modelling* 269: 98-112

2 Using precipitation data ensemble for uncertainty analysis in SWAT streamflow simulation

M. Strauch, C. Bernhofer, S. Koide, M. Volk, C. Lorz, and F. Makeschin
Journal of Hydrology 414-415 (2012): 413-424, available at ScienceDirect
Submitted: 6 September 2011
Accepted: 7 November 2011

Abstract

Precipitation patterns in the tropics are characterized by extremely high spatial and temporal variability that are difficult to adequately represent with rain gauge networks. Since precipitation is commonly the most important input data in hydrological models, model performance and uncertainty will be negatively impacted in areas with sparse rain gauge networks. To investigate the influence of precipitation uncertainty on both model parameters and predictive uncertainty in a data sparse region, the integrated river basin model SWAT was calibrated against measured streamflow of the Pipiripau River in Central Brazil. Calibration was conducted using an ensemble of different precipitation data sources, including: (1) point data from the only available rain gauge within the watershed, (2) a smoothed version of the gauge data derived using a moving average, (3) spatially distributed data using Thiessen Polygons (which includes rain gauges from outside the watershed), and (4) Tropical Rainfall Measuring Mission radar data. For each precipitation input model, the best performing parameter set and their associated uncertainty ranges were determined using the Sequential Uncertainty Fitting Procedure. Although satisfactory streamflow simulations were generated with each precipitation input model, the results of our study clearly illustrate that parameter uncertainty varied significantly depending upon the method used for precipitation data-set generation. Additionally, improved deterministic streamflow predictions and more reliable probabilistic forecasts were generated using different ensemble-based methods, such as the arithmetic ensemble mean, and more advanced Bayesian Model Averaging schemes. This study shows that ensemble modeling with multiple precipitation inputs can significantly increase the level of confidence in simulation results, particularly in data-poor regions.

2.1 Introduction

Hydrological models are useful tools for evaluating the hydrologic effects of factors such as climate change, landscape pattern or land use change resulting from policy decisions, economic incentives or changes in the economic framework (Beven, 2001; Falkenmark and Rockström, 2004). Rainfall data is typically the most important input for hydrological models, and therefore accurate data describing the spatial and temporal variability of precipitation patterns are crucial for sound hydrological modeling and river basin management. Among others, Dawdy and Bergmann (1969), Troutman (1983), Duncan et al. (1993), Faures et al. (1995), Lopes (1996), Andréassian et al. (2001), and Bárdossy and Das (2008) have shown that neglecting spatial variability of rainfall can cause serious errors in model outputs. However, rain gauge networks are usually not able to fully represent the spatial pattern of rainfall, and thus watershed modelers are forced to cope with the uncertainties that arise from limited spatial sampling. This is especially true for the tropics, where rainfall is primarily of convective type and occurs mostly in small cells ranging from 10-20 km^2 to 200-300 km^2 (McGregor and Nieuwolt, 1998).

The Soil and Water Assessment Tool (SWAT) model (Arnold et al., 1998; Arnold and Fohrer, 2005) has been proven to be an effective tool for supporting water resources management for a wide range of scales and environmental conditions across the globe (Gassman et al., 2007). SWAT is a process-based hydrologic model that can simulate most of the key hydrologic processes at the basin scale (Arnold et al., 1998). Uncertainty in SWAT model output due to spatial rainfall variability has been analyzed in several applications. Hernandez et al. (2000) and Chaplot et al. (2005) found that increasing the number of rain gauges used for input data resulted in significantly improved streamflow estimates and sediment predictions. Cho et al. (2009) assessed the hydrologic impact of different methods for incorporating spatially variable precipitation input into SWAT. Because of its robustness to sub-watershed delineation, they recommend the Thiessen polygon approach in watersheds with high spatial variability of rainfall. Another potentially promising approach for improving precipitation data is by using remote sensing methods. Moon et al. (2004) as well as Kalin and Hantush (2006) reported that using Next-Generation Weather Radar (NEXRAD) precipitation resulted in as good or better streamflow estimates in SWAT as using rain gauge data.

An alternative to deterministic prediction methods is the use of probabilistic predictions, which are generated using a range of potential outcomes, and thus allows greater consideration of different sources of uncertainty (Franz et al., 2010). One approach to probabilistic forecasting is through the use of ensemble modeling techniques (Georgakakos et al., 2004; Gourley and Vieux, 2006; Duan et al., 2007; Breuer et al., 2009; Viney et al., 2009). The basis of ensemble modeling is that instead of relying on a single model prediction, it may be advantageous to combine the results of multiple individual models into an aggregate prediction. There are numerous different ensemble methods that can be used to merge the results from the contributing models. The most basic ensemble method is to use the arithmetic mean of the ensemble predictions (ensemble mean). Despite the simplicity of this approach, these ensembles have been shown to exhibit more predictive performance than single model predictions (e.g. Hsu et al., 2009; Viney et al., 2009; Zhang

et al., 2009). Recently, more complex Bayesian model averaging (BMA) methods have been successfully applied to provide improved meteorological and hydrological predictions with corresponding uncertainty measures (Raftery et al., 2005; Duan et al., 2007; Zhang et al., 2009; Franz et al., 2010).

The objective of this study is to account for precipitation uncertainty in streamflow simulations by using an ensemble of precipitation data-sets as input for the SWAT model. By means of the Sequential Uncertainty Fitting (SUFI-2) procedure (Abbaspour et al., 2007) we aim to estimate parameter uncertainty and predictive uncertainty for each of the rain input models. Finally, we try to improve the SWAT streamflow predictions and provide more reliable uncertainty estimates by merging the individual model outputs using simple ensemble combination methods and more advanced Bayesian Model Averaging (BMA) schemes.

The study is part of the IWAS project (International Water Research Alliance Saxony, http://www.iwas-sachsen.ufz.de/) which aims to contribute to an Integrated Water Resources Management in hydrologically sensitive regions by creating system specific solutions. For the Federal District of Brazil, IWAS is addressing the urgent needs for sustainable water supplies in face of rapid population growth, urban sprawl, and intensification of agriculture (Lorz et al., 2011a). Within this context, the current study provides a framework for further model-based scenario analyses in this region.

2.2 Materials and Methods

2.2.1 Study area

This study was conducted on the Pipiripau river basin, located in the north-eastern part of the Federal District, Brazil (Fig.2.1). The 215 km² basin is mainly covered by well drained Ferralsols which are low in nutrients (EMBRAPA, 1978). The Pipiripau river basin is situated within the Brazilian Central Plateau, with an altitude ranging from 920 to 1230 m a.s.l. and primarily moderate slopes ranging from 0.5 and 4°. Approximately 70% of the basin is intensively used for large-scale agriculture producing soybeans, corn and pasture, and to a smaller extent by irrigated horticulture. The remaining 30% is mainly covered by gallery forests and different types of Cerrado vegetation, which varies from very open to closed savannas (Oliveira-Filho and Ratter, 2002). The basin is mostly rural, with only a few small settlements.

The study region is categorized as a semi-humid tropical climate. Most of the precipitation (on average 1,300 mm yr^{-1}) occurs during the summer from November to March. Analysis of time series from 60 rain gauges in the DF region shows a rapidly decreasing correlation with distance between precipitation measurements (Fig. 2.2). This illustrates the high spatial variability of rainfall in this region, which presents a significant challenge for developing accurate precipitation input data.

The Pipiripau River is a perennial river with a long-term average flow rate of 2.9 m^3 s^{-1} for the period 1971-2008 (stream gauge FRINOCAP, Fig. 2.1). Water withdrawal for drinking water supply of nearby cities and for agricultural irrigation demands has increased over this time period, which has exacerbated low-flow conditions during the dry season

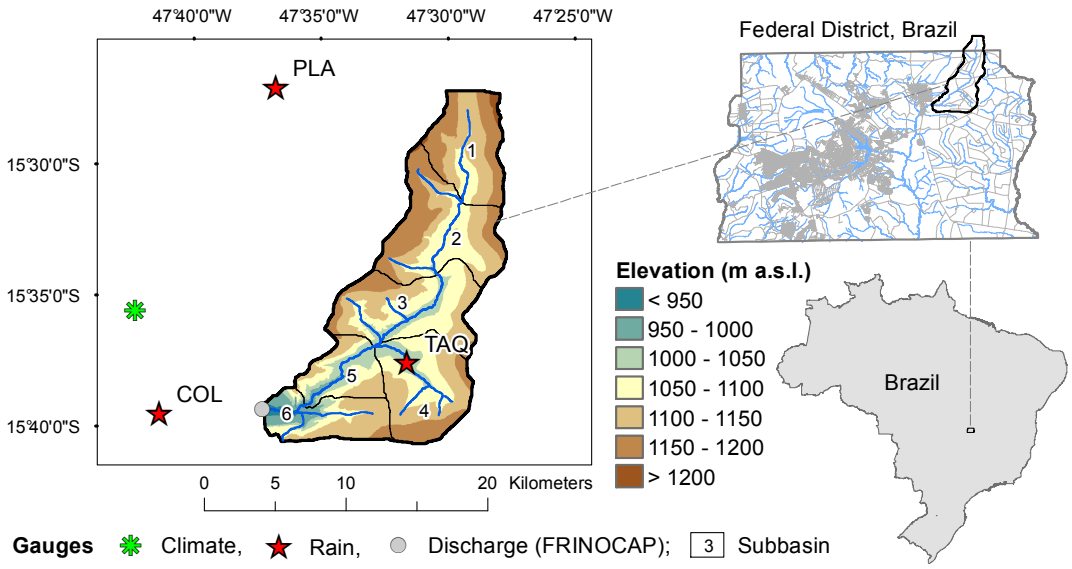

Figure 2.1: Location and topography of the Pipiripau River Basin.

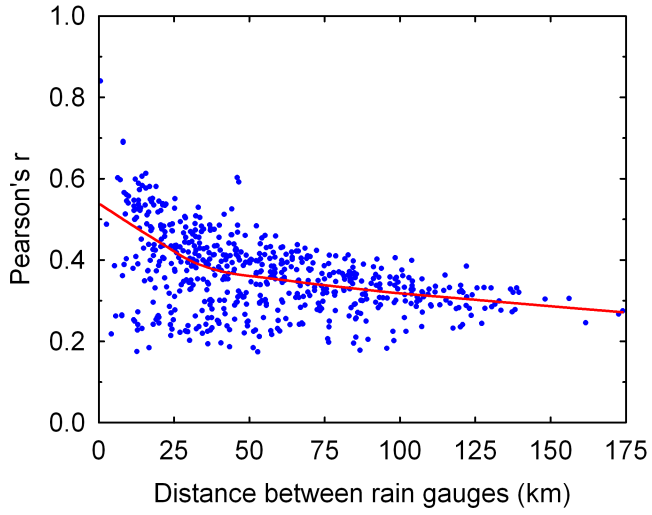

Figure 2.2: Correlation of daily rainfall over distance in the DF and surrounding area. Corresponding daily time series of 60 rain gauges were correlated with each other. The record length of single gauges varies within the time period 1961-2009. For the derivation of Pearson's r between two gauges a minimum corresponding time series of five years was required. The solid line is a Lowess regression with 50% strain (i.e. locally weighted scatterplot smoothing, where each smoothed value is given by a weighted least squares regression using 50% of the data).

(May to October). This effect can be observed by comparing the 5th percentile flow rates over two separate time periods. While the 5th percentile flow in the period 1971-1990 was 1.15 $m^3 s^{-1}$, it dropped to only 0.54 $m^3 s^{-1}$ during the period of 1991-2008. This is despite the similar rainfall totals during the respective periods, with annual averages of 1,334 and 1,269 mm and annual standard deviations of 263 and 230 mm (rain gauge TAQ, Fig. 2.1).

2.2.2 SWAT model description

SWAT is a time-continuous, process-based hydrological model that was developed to assist water resource managers in assessing the impact of management decisions and climate variability on water availability and non point source pollution in meso- to macroscale watersheds (Arnold and Fohrer, 2005). SWAT subdivides a watershed into sub-basins based on topography which are connected by a stream network. Sub-basins are further delineated into Hydrologic Response Units (HRUs), which are defined as land-units with uniform soil, land use, and slope. Model components include weather, hydrology, erosion/sedimentation, plant growth, nutrients, pesticides, and agricultural management. The hydrologic model is based on the water balance equation (Arnold et al., 1998):

$$SW_t = SW_0 + \sum_{i=1}^{t}(R - Q - ET - P - QR), \tag{2.1}$$

where SW_t is the soil water content at time t, SW_0 is the initial soil water content, and R, Q, ET, P, and QR are precipitation, runoff, evapotranspiration, percolation, and return flow respectively; all units are in mm.

The Soil Conservation Service (SCS) Curve Number (CN) method is used to estimate surface runoff from daily precipitation (USDA-SCS, 1972). For evapotranspiration estimation, three methods are available: Penman-Monteith, Priestley-Taylor, and Hargreaves. For this study, Penman-Monteith was utilized to account for different land uses. Water withdrawals for irrigation or urban use can be considered from different sources, such as aquifers or directly from the stream (Neitsch et al., 2005). Channel routing in SWAT is represented by either the variable storage or Muskingum routing methods. For this study, the variable storage method was used. Outflow from a channel is adjusted for transmission losses, evaporation, diversions, and return flow (Arnold et al., 1998). This study was carried out using the 2005 version of SWAT.

2.2.3 Model Inputs

Input data on land use and soils for the SWAT model were derived from maps produced by The Nature Conservancy – TNC (BRASIL, 2010) and the Brazilian Agricultural Research Corporation (EMBRAPA, 1978; Reatto et al., 2004). A digital elevation model (DEM) generated from a 1:10,000 contour line map (Codeplan, 1992) was used to delineate the watershed into six sub-basins varying in size from 20.8 km^2 to 48.7 km^2.

Meteorological input, except rainfall (i.e. temperature, wind, humidity, and solar radiation), was obtained from the EMBRAPA-Cerrados climate station, located 15 km west of the basin (Fig. 2.1). Precipitation data was obtained from three rain gauges: Taquara (TAQ), Colégio Agricola (COL), and Planaltina (PLA). However, only the TAQ gauge is

located within the basin (Fig. 2.1). In addition to the gauge data, gridded estimates of daily precipitation in a 0.25° by 0.25° spatial resolution with the Tropical Rainfall Measuring Mission (TRMM) product 3B42 was obtained. This data is produced using rainfall estimates of microwave and infrared sensors, which are then merged and rescaled to match the monthly estimates of global gridded rain gauge data (Huffman et al., 2007).

Water extraction for urban use was estimated using the average monthly stream water removal from the Captação Pipiripau pumping station over the period 2001 to 2008 (data source: CAESB).

2.2.4 Precipitation data-sets

To account for precipitation uncertainty in the sparsely gauged Pipiripau River basin, we generated four different precipitation inputs for the SWAT model. Each precipitation data-set covers the time period from 1998 to 2008, which provides 3 years for model warm up (1998 to 2000), 4 years for calibration (2001 to 2004), and 4 years for validation (2005 to 2008).

The first precipitation data-set is based on the rain gauge located within the watershed (TAQ), which assumes uniform rainfall across the entire watershed, as measured by this single gauge. Given that this is the only rain gauge located within the basin, it is assumed that TAQ may provide the best rainfall estimates.

The second precipitation data-set (TAQM) is a derivation of TAQ, which attempts to provide a more balanced temporal representation of the rainfall by applying a weighted moving average to the gauge data. TAQM was calculated for every day (i) using:

$$TAQM_i = (2 \cdot TAQ_i + TAQ_{i-1} + TAQ_{i+1})/4. \tag{2.2}$$

The result of TAQM is a smoothed version of TAQ with decreased rainfall intensity and standard deviation, and an increased number of rain days (Tab. 2.1, Fig. 2.3). The potential advantage of this data-set is that it may provide a more realistic representation of rainfall temporal patterns in the whole watershed, by placing less emphasis on the timing at a single point (i.e. TAQ gauge).

The third precipitation data-set includes additional data from rain gauges located outside the watershed, by generating an interpolated rainfall data-set. There are a large number of spatial interpolation methods available; Li and Heap (2008) describe in their comprehensive review over 40 commonly used methods. They found that, in general, kriging methods perform better than non-geostatistical methods, but they also emphasize that the performance of spatial interpolators strongly depends on sampling density and design, as well as variation in the data. In the study region considered here, the sampling size and density is very low. Only four stations (three rain gauges and the climate station shown in Fig.2.1) are located within a 25 km radius of the catchment centroid. Within a radius of 50 km, there are eleven more gauges that cover at least 50% of the simulation period (2001 to 2008). However, nine of these gauges are concentrated in the south-west of the catchment, which would result in a poor spatial representation with respect to sampling design. Due to these limitations, and the low spatial correlation of daily rainfall (compare Fig. 2.3), the application of geostatistical interpolation methods for this study was deemed

Table 2.1: Statistics of all rain input options for period 2001 to 2008 (SUB = subbasin ID cf. Fig.1).

	SUB	MEAN mm/a	MAX mm/d	STD mm/d	Rain[a] %	COR[b]
TAQ	all	1232	90.8	9.14	29.5	1
TAQM	all	1232	50.0	6.40	46.5	0.85
THIE	1	1252	91.3	8.81	32.2	0.79
	2	1233	85.0	8.78	32.3	0.99
	3	1232	90.8	9.14	29.5	1
	4	1232	90.8	9.14	29.5	1
	5	1232	90.8	9.14	29.5	1
	6	1262	78.6	8.60	37.4	0.98
TRMM	1	1344	94.5	7.87	45.7	0.49
	2	1351	83.4	8.24	41.4	0.49
	3	1353	88.0	8.31	41.4	0.49
	4	1354	90.5	8.37	41.4	0.48
	5	1357	96.7	8.59	36.8	0.47
	6	1357	96.7	8.59	36.8	0.47

[a] Percentage of days with rainfall > 0 mm

[b] Pearson's r related to the time series of rain gauge TAQ

inappropriate. Alternatively, the non-geostatistical Thiessen polygon method was used to generate the third precipitation data-set (THIE). The Thiessen polygons were generated using the TAQ, COL, and PLA gauges. For each sub-basin in the watershed, an individual rainfall time series was produced based upon the proportion of each Thiessen polygon within the sub-basin. In the case of missing data, no Thiessen polygon was generated for the respective rain gauge and the shape of the polygons was changed. For rain gauge PLA, 28% of the data record was missing; however, two thirds of this missing data occurred in the warm up period. The resulting THIE data-set is quite similar to the TAQ set, since the Thiessen polygon representing rain gauge TAQ fully covers the sub-basins 3, 4, and 5

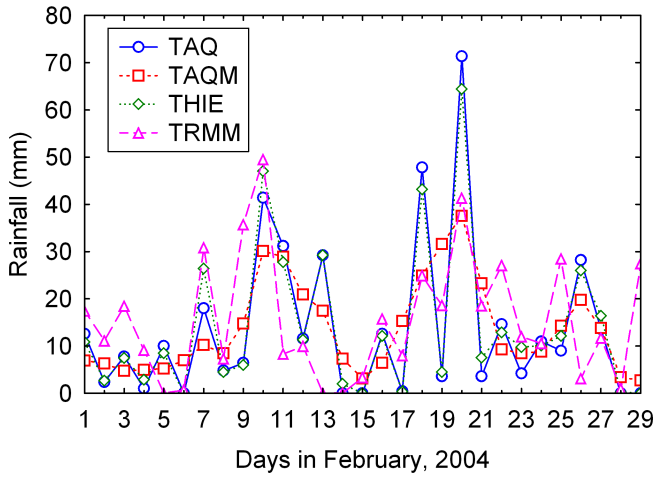

Figure 2.3: Daily catchment rainfall in February 2004 according to TAQ, TAQM, THIE, and TRMM.

(Fig. 2.3 and Fig. 2.4, Tab. 2.1). However, this data-set still may be advantageous, as it does provide additional rainfall information for the sub-basins located on the margins of the watershed, and therefore may provide more reasonable rainfall input in these areas.

The fourth precipitation data-set was derived using the TRMM product 3B42 (TRMM). For this set, sub-basin rainfall was calculated using the proportion of the TRMM grid cells in the respective sub-basin. In comparison to the rain gauge derived results, mean annual precipitation is slightly higher for TRMM. Total maximum and standard deviation of daily rainfall is similar to TAQ, but the number of rain days is significantly higher. TRMM shows a relatively low correlation ($r < 0.5$) to TAQ (Fig. 2.3 and Fig. 2.4, Tab. 2.1). Since TRMM provides spatially distributed areal rainfall estimates, this data-set may be advantageous compared to the rain gauge derived ensemble members.

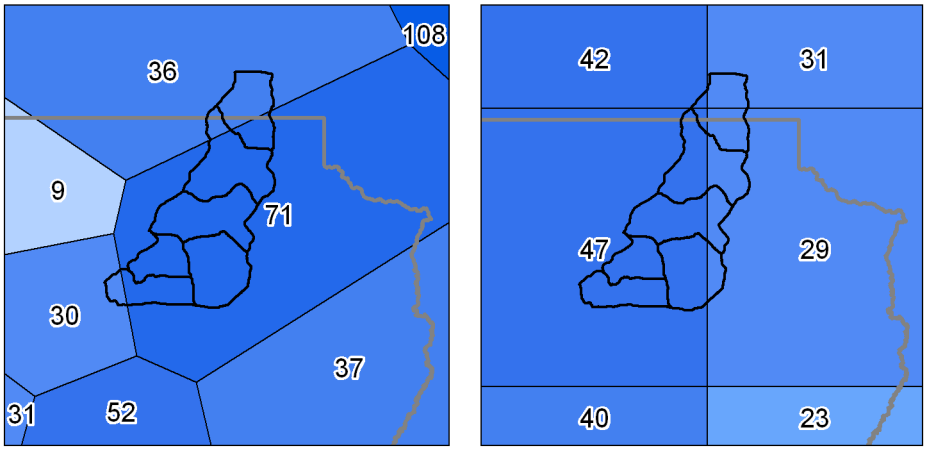

Figure 2.4: Rainfall [mm] on February 20th 2004 according to THIE (left) and TRMM (right).

Figure 2.5 provides an overview of the four individual precipitation data-sets, and the steps used for model calibration and ensemble-based processing, which are described in the following sections.

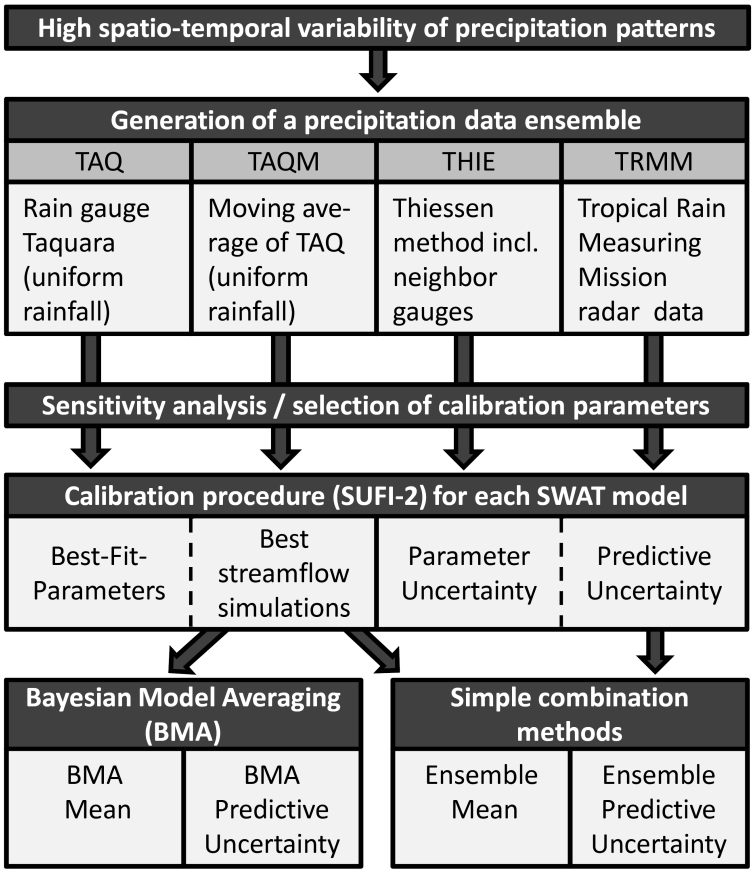

Figure 2.5: Flowchart of the precipitation ensemble appoach.

2.2.5 Model calibration and uncertainty analysis

2.2.5.1 Parameter selection

All four SWAT models, which differ in terms of precipitation input, were calibrated against daily streamflow measured at gauge FRINOCAP (Fig. 2.1). The four models are referred to as M_{TAQ}, M_{TAQM}, M_{THIE}, and M_{TRMM}, according to the precipitation input used. Model calibration was focused on optimizing nine parameters, which were identified using the LH-OAT sensitivity analysis tool (van Griensven et al., 2006). This method combines Latin-Hypercube (LH) and One-Factor-At-A-Time (OAT) sampling. The parameter space was defined by a set of 27 flow parameters with their default bounds (Winchell et al., 2007). Parameter sensitivity changed with the different rainfall inputs, therefore an overall measure to allow selection of a uniform parameter set for all models was generated. To produce this overall measure, a sensitivity analysis (280 simulations) was conducted for each rainfall input data-set, and then the individual sensitivity ranks of each parameter were summed. Table 2.2 lists the nine most sensitive model parameters identified by this procedure.

Table 2.2: Most sensitive model parameters for the Pipiripau catchment considering different rain input models (sorted by sum of individual sensitivity ranks).

Parameter	Description	Sensitivity Rank				
		MTAQ	MTAQM	MTHIE	MTRMM	Sum
CN2	SCS runoff curve number	2	2	1	1	6
ALPHA_B	Baseflow recession constant	1	1	2	3	7
CH_K2	Eff. hydraulic conductivity in main channel alluvium	3	3	3	2	11
ESCO	Soil evaporation compensation factor	4	5	4	4	17
GW_DEL	Groundwater delay time (days)	5	4	5	7	21
CH_N2	Manning's "n" value for the main channel	8	6	9	5	28
GWQMN	Water depth in shallow aquifer for return flow (mm	7	9	6	6	28
CANMX	Maximum canopy storage (mm H2O)	9	7	8	8	32
SURLAG	Surface runoff lag coefficient	6	11	7	9	33

2.2.5.2 The SUFI-2 procedure

Model calibration and estimation of both parameter and predictive uncertainty were performed for each ensemble member using the Sequential Uncertainty Fitting (SUFI-2) routine, which is linked to SWAT under the platform of SWAT-CUP2 (Abbaspour et al., 2004). SUFI-2 is recognized as a robust tool for generating combined calibration and uncertainty analysis of the SWAT model (e.g. Abbaspour et al., 2007; Rostamian et al., 2008; Faramarzi et al., 2009; Setegn et al., 2010). In SUFI-2, parameter uncertainty is described using a multivariate uniform distribution in a parameter hypercube, while model output uncertainty is derived from the cumulative distribution of the output variables (Abbaspour et al., 2007).

The procedure used in SUFI-2 can be briefly described as follows:

(1) In the first step, an objective function is defined. For this study, a summation form of the squared error was selected:

$$g = \frac{1}{\sigma_{low}} \sum_{t=1}^{T} (y_{t_{low}} - f_{t_{low}})^2 + \frac{1}{\sigma_{high}} \sum_{t=1}^{T} (y_{t_{high}} - f_{t_{high}})^2, \tag{2.3}$$

where y_t and f_t are the observed and simulated streamflow on day t, respectively. y_t and f_t are divided into two subsets by the threshold of 2.0 m^3 s^{-1}, which represents the average streamflow during the calibration period. If y_t is lower than or equal to the threshold, y_t and f_t belong to subset $[y_{t_{low}}, f_{t_{low}}]$, otherwise to subset $[y_{t_{high}}, f_{t_{high}}]$. The reciprocal standard deviation of the lower and higher observed flow conditions, σ_{low} and σ_{high}, were used as weights for the respective flow compartments to avoid underrepresentation of base flow during the optimization.

(2) The initial uncertainty ranges $[b_{abs\_min}, b_{abs\_max}]$ are assigned to the calibration parameters (Tables 2.3 and 2.4). Since these ranges play a constraining role, they should be set as wide as possible, while still maintaining physical meaning (Abbaspour et al., 2007). The ranges were established based on the

recommendations of Neitsch et al. (2005) and van Griensven et al. (2006).

Table 2.3: Initial parameter values and ranges for calibration.

		Calibration range	
		Lower	Upper
Parameter	Initial value	(b_{abs_min})	(b_{abs_max})
CN2	Variable (Tab. 2.4)	-30%	30%
ALPHA_BF	0.048	0	1
CH_K2	0	0	150
ESCO	0.95	0.01	1
GW_DELAY	31	0	500
CH_N2	0.014	0.01	0.3
GWQMN	0	0	1000
CANMX	Variable (Tab. 2.4)	-50%	50%
SURLAG	4	0	10

(3) A Latin Hypercube sampling (n = 1000) is carried out in the hypercube $[b_{min}, b_{max}]$ (initially set to $[b_{abs\_min}, b_{abs\_max}]$ and the corresponding objective functions are evaluated. Furthermore, the sensitivity matrix J and the parameter covariance matrix C are calculated according to

$$J_{ij} = \frac{\Delta g_i}{\Delta b_j}, \quad i = 1, ..., C_2^n, \quad j = 1, ..., m, \tag{2.4}$$

$$C = \sigma_g^2 (J^T J)^{-1}, \tag{2.5}$$

where C_2^n is the number of rows in the sensitivity matrix (equal to all possible combinations of two simulations), and m is the number of columns (parameters); σ_g^2 is the variance of the objective function values resulting from n model runs.

(4) The 95% confidence interval of a parameter $b_j$are then computed from the diagonal elements of C as follows:

$$b_{j,lower} = b_j^* - t_{v,0.025}\sqrt{C_{jj}}, \quad b_{j,upper} = b_j^* + t_{v,0.025}\sqrt{C_{jj}}, \tag{2.6}$$

where b_j^* is the parameter b_j for the best simulation according to the objective function, and v is the degrees of freedom $(n - m)$.

(5) The 95% predictive uncertainty interval is calculated at the 2.5% and 97.5% levels of the cumulative distribution of the model output variables (here only streamflow). After that, the *d-factor* (average width of the uncertainty interval divided by the standard deviation of the measured data) is calculated to evaluate the uncertainty interval. Small *d-factors* (<1) are preferred.

(6) Since the parameter uncertainty ranges are initially large, the *d-factor* tends to be quite large during the first iteration. Hence, further iterations are needed

with updated parameter ranges $[b'_{j,min}, b'_{j,max}]$ calculated from:

$$b'_{j,min} = b_{j,lower} - \max(\frac{(b_{j,lower} - b_{j,min})}{2}, \frac{(b_{j,max} - b_{j,upper})}{2}),$$

$$b'_{j,max} = b_{j,lower} + \max(\frac{(b_{j,lower} - b_{j,min})}{2}, \frac{(b_{j,max} - b_{j,upper})}{2}). \quad (2.7)$$

Table 2.4: Initial values of parameters CANMX and CN2.

Land use / land cover	CANMX[a]	CN2[b]		
		Hydrologic Soil Group & Soils		
		A Ferralsols, Arenosols	C Cambisols	D Plinthosols, Gleysols, shallow Cambisols
Coffee	1.5	45	77	-
Tomato	1.5	67	83	-
Large-field crops (soyb., corn, beans)	2	67	-	-
Pasture	1.5	49	-	-
Grass savanna (Campo)	1.5	41	-	81
Tree savanna (Cerrado)	1.5	39	-	79
Gallery forest	4	35	70	77
Low residential urban area	1	56	-	-
Bare soils, unpaved roads	-	77	-	94

[a]rough estimates on the basis of LAI values (Neitsch et al., 2005; Bucci et al., 2008) since reliable data are not available

[b]estimates following Neitsch et al. (2005)

No further SUFI-2 iteration was carried out when a d-factor of lower than 1 was reached (Abbaspour et al., 2007). For each rain input model the SUFI-2 results include a final parameter range, the best model simulation, and the 95% uncertainty interval of simulated streamflow. In addition, simple ensemble based predictions from the individual SUFI-2 outputs were generated, specifically the arithmetic mean of each ensemble member's best prediction and the 95% predictive uncertainty interval for the whole ensemble, calculated at the 2.5th and 97.5th level of the cumulative distribution of the combined SUFI-2 simulation results (ensemble SUFI-2 distribution = ENS).

2.2.5.3 Bayesian Model Averaging

Bayesian Model Averaging (BMA) is a standard approach for post-processing ensemble forecasts from multiple competing models (Hoeting et al., 1999). BMA has been used to infer probabilistic predictions with higher precision and reliability than the original ensemble members generated by several competing models (Duan et al., 2007). The advantage of the BMA predictive mean over the simple model averaging method (ensemble mean) is that better performing models can receive higher weights than poorly performing ones. Following Raftery et al. (2005), the BMA prediction probability can be represented as:

$$p(y \mid f_1, f_2, ..., f_K) = \sum_{k=1}^{K} w_k g(y \mid f_k), \quad (2.8)$$

where K is the number of competing models and k is the index of each model. w_k is the posterior probability of model prediction f_k being the best one and is based on f_k's performance in the training period. w_k can be considered as weight; it is nonnegative and with a sum ($\sum_k^K w_k$) of 1. $g(y \mid f_k)$ represents the probability density function (PDF) of the measurement y conditional on f_k. The PDF $g(y \mid f_k)$ can usually be approximated by a normal distribution with mean $a_k + b_k f_k$ and variance σ^2, where a_k and b_k are regression coefficients obtained through least square linear regression of y on f_k using the training data. The estimation of a_k and b_k can be viewed as a simple bias-correction process (Raftery et al., 2005). However, in several studies BMA analysis has been successfully carried out without bias correction (e.g. Duan et al., 2007; Viney et al., 2009; Franz et al., 2010). In this study, the BMA approach was applied both with and without bias correction.

The weights w_k and variance σ^2 were calculated using the maximum log-likelihood estimation method described in Raftery et al. (2005). After this step, the BMA predictive mean is given by

$$E(y \mid f_1,\ f_2, ..., f_K) = \sum_{k=1}^{K} w_k(a_k + b_k f_k). \tag{2.9}$$

Finally, uncertainty intervals for the BMA prediction were derived from BMA probabilistic ensemble predictions. Here again, the procedure of Raftery et al. (2005) was followed, which involves (i) generating a value of k from the numbers {1,...,K} with the probabilities {w_1,...,w_k}, (ii) drawing a replication of y from the PDF $g(y \mid f_k)$, and (iii) repeating steps (i) and (ii) to obtain 1000 values of y for each time step t. The 95% uncertainty interval is then derived from the cumulative distribution of y_t at the 2.5th and 97.5th levels.

2.2.5.4 Statistical evaluation criteria

The best individual predictions, the ensemble mean, and the BMA mean were evaluated using multiple statistical criteria. The Nash-Sutcliffe Efficiency (NSE), the coefficient of determination (R^2), and the percent bias ($PBIAS$) are frequently used measures in hydrologic modeling studies (Krause et al., 2005; Moriasi et al., 2007) which are calculated as:

$$NSE = 1 - \frac{\sum_{t=1}^{T}(y_t - f_t)^2}{\sum_{t=1}^{T}(y_t - \bar{y})^2}, \tag{2.10}$$

$$R^2 = \frac{(\sum_{t=1}^{T}(y_t - \bar{y})(f_t - \bar{f}))^2}{\sum_{t=1}^{T}(y_t - \bar{y})^2 \sum_{t=1}^{T}(f_t - \bar{f})^2}, \tag{2.11}$$

$$PBIAS = \frac{\sum_{t=1}^{T}(y_t - f_t) \cdot 100}{\sum_{t=1}^{T} y_t}, \tag{2.12}$$

where f_t is the modeled streamflow and y_t is the observed streamflow at time step t, respectively, whereas $\bar{f}$ and $\bar{y}$ represent the mean of the respective streamflow values in time period 1, 2, ..., T.

NSE measures how well model predictions represent the observed data, relative to a prediction made using the average observed value. NSE can range from $-\infty$ to 1, with $NSE = 1$ being the optimal value (Nash and Sutcliffe, 1970). R^2 ranges from 0 to 1 and

represents the proportion of the total variance in the observed data that can be explained by the model, with higher R^2 values indicating better model performance. *PBIAS* measures the average tendency of the simulated data to over- or underpredict the observed data, with positive values indicating a model underestimation bias, and negative values indicating a model overestimation bias (Gupta et al., 1999). Low-magnitude values of *PBIAS* are preferred.

To evaluate the 95% uncertainty intervals obtained by the SUFI-2 procedure and BMA, the percentage of coverage of observations (*POC*) and the *d-factor* were calculated. A significant difference between *POC* and the expected 95% would indicate that the predictive uncertainty is either underestimated or overestimated (Vrugt and Robinson, 2007). However, *POC* should always be related to the average width of the uncertainty band. At the 95% level, *d-factors* of around 1 are preferred, because the average width of the uncertainty interval would then correspond to the standard deviation of the observations.

2.3 Results and Discussion

2.3.1 Parameter uncertainty

The best-fit parameter values for each rainfall input model and the final parameter ranges are shown in Figure 2.6. The CN2 parameter (the most sensitive parameter) was lowered in all models during calibration, which has the effect of reducing the amount of surface runoff generated from rainfall. Since surface runoff also depends on rainfall intensity, the fitted CN2 values reflect the maximum daily rainfall of the rain gauge driven models very well (Tab. 2.1). Higher CN2 values were found for the model based on the smoothed rainfall time series (M_{TAQM},) compared to M_{TAQ} and M_{THIE}. Overall however, the fitted values of CN2 are relatively similar for all rain input models. Similar results were also observed with the parameters GW_DELAY and CH_N2. The best-fit values of GW_DELAY indicate a distinct time delay between water exiting the soil profile and entering the shallow aquifer (around 200 days). However, given that the saprolite zone can be up to decameter thick, this value is considered to be reasonable. The high values of CH_N2 (Manning's "n" for the main channel) characterize natural streams with heavy stands of timber and underbrush. Considering that the riparian zone of the Pipiripau River is covered mainly by dense gallery forests, this high value is assumed to be reasonable. However, it is remarkable that the best-fit values for most parameters vary significantly between input models, particularly for those having a physical meaning (e.g. CANMX and CH_K2). Therefore, using multiple different rainfall inputs reveals that there is a high degree of parameter uncertainty, which would not be apparent if only a single model was used. This is an issue of particular concern related to complex conceptual models, such as SWAT. And an evaluation of best-fit parameter sets on plausibility is difficult to accomplish, since it is usually impractical to define the true parameter values either by field measurements or prior estimation (due to scale problems and model assumptions; Beven, 2001). These results demonstrate that the uncertainty of "goodness of fit" parameterization increases when spatial data on precipitation is limited, which reinforces the rationale for using ensemble modeling approaches instead of relying on individual predictions. The final

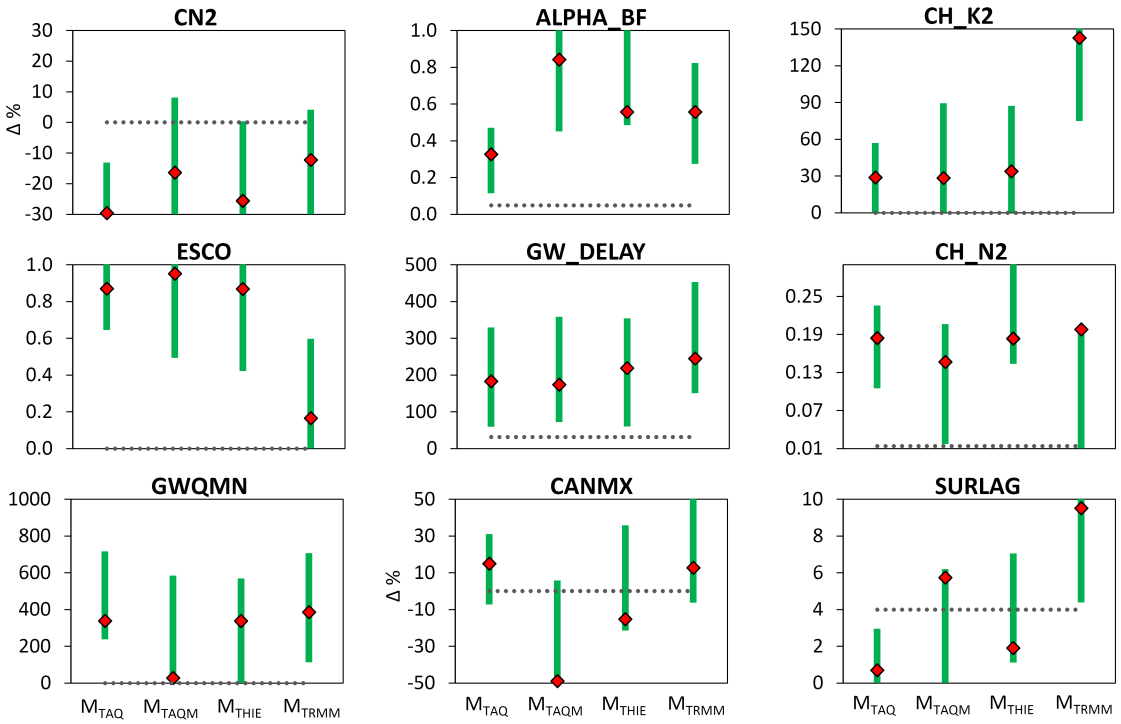

Figure 2.6: Calibrated "best" parameter values (red rhombuses) and updated parameter ranges (green bars) for the four rain input models within the initial parameter range (y-axis domain); the initial parameter values are shown by the dotted line (for parameter descriptions see Tab. 2.2)

parameter ranges obtained through the SUFI-2 procedure can be viewed as uncertainty ranges. However, given the relatively low number of iterations that were carried out, the final parameter uncertainty is still fairly large. SUFI-2 parameter ranges of comparable width were also reported from Yang et al. (2008), who compared different uncertainty analysis techniques for SWAT simulations. Their study reveals that parameter uncertainty ranges can differ significantly depending upon the optimization procedure used which further highlights the challenges inherent in model parameterization.

2.3.2 Model performance

The values of the coefficients used for evaluation of the simulated daily streamflow by the different input models are provided by Table 2.5. According to the performance classification of Moriasi et al. (2007), good model performance (defined as: $0.65 < NSE \leq 0.75$) was achieved for M_{TRMM} and very good model performance (defined as: $NSE > 0.75$) was achieved for the rain gauge driven models in the calibration period. The *NSE* values in validation were significantly lower than in calibration, however, with the exception of the M_{TRMM} model ($NSE = 0.43$), the validation results still meet the 'good performance' threshold. The best individual prediction was achieved by the smoothed time series rain input model (M_{TAQM}). This suggests that in watersheds with high rainfall variability and insufficient data, the temporal rainfall distribution may be better represented by a smoothed or low-pass filtered time series than by the unfiltered measured time series of

point measurements. This seems particularly likely for meso-scale watersheds, such as the Pipiripau catchment, which are large enough to have a significant amount of spatial variability in daily rainfall. In this case, a low-pass filter may be more advantageous since it will reduce the temporal variability of point rainfall, but still retain the signal of the measurements. However, if the size of the modeled watershed is too large, than the use of a single point measurement (even using a low-pass filter) is probably unjustified. It is also important to consider that this approach may results in a loss of rainfall intensity, which can be disadvantageous due to the strongly non-linear relationship between rainfall intensity and runoff generation. Therefore, M_{TAQM} may be a better option than M_{TAQ} for simulating runoff at the meso-/ catchment scale, but for smaller spatial scales (i.e. sub-areas of the catchment) the frequency-intensity relationship of runoff can be significantly affected. The input model using the TRMM data produced the poorest model performance, particularly during the validation period. However, given the fact that TRMM data can be easily generated in areas which may otherwise have limited data available, this data should still be considered valuable to support hydrologic modeling. These results are in accordance with the findings of Tobin and Bennett (2009) and Milewski et al. (2009) who successfully utilized satellite-estimated data (TRMM 3B42) for SWAT simulations. Among all candidate models, calibration with TRMM led to the lowest percent bias (*PBIAS*) in the streamflow simulations. But all in all, *PBIAS* was relatively small for each ensemble member.

The daily streamflow simulated by the different input models and the ensemble predictions are shown in Figures 2.7 and 2.8 for February 2004 and March 2005, which were months with particularly high peak flows during the calibration and validation period, respectively. These figures show that the hydrographs produced by the individual input models are considerably different from each other. Figures 2.7 and 2.8 also show that in contrast to the individual prediction models, the ensemble model predictions are very similar to each other. The reason for this similarity is that the computed weights for the BMA ensemble (Fig. 2.9) differs only slightly from the equitable weights of each model (0.25) that were used to derive the simple arithmetic ensemble mean. However, there is still a distinct ranking among the BMA weights. Duan et al. (2007) found a strong cor-

Table 2.5: Evaluation coefficients for the four SWAT models, the ensemble mean (ENS_M), and the BMA means (biased and unbiased).

	Calibration (2001 - 2004)			Validation (2005 - 2008)		
	NSE	R^2	*PBIAS*	*NSE*	R^2	*PBIAS*
M_{TAQ}	0.79	0.80	+7.7	0.73	0.79	-11.8
M_{TAQM}	0.83	0.83	+3.0	0.76	0.82	-14.0
M_{THIE}	0.81	0.81	+6.4	0.69	0.79	-15.2
M_{TRMM}	0.74	0.74	-1.6	0.43	0.58	-9.5
ENS_M	0.84	0.84	+3.9	0.80	0.84	-12.6
BMA_M_{biased}	0.85	0.85	0.0	0.78	0.84	-15.3
BMA_$M_{unbiased}$	0.84	0.85	+3.0	0.81	0.85	-12.8

relation between BMA weights and model performance. Considering only the rain gauge based models, the BMA weights reflect the relative performance of the different models during the calibration period ($M_{TAQM} > M_{THIE} > M_{TAQ}$). M_{TRMM}, however, received the second-largest weight despite having the lowest *NSE* and R^2 values. The strong dissimilarity of the TRMM data compared to the rain gauge derived precipitation data probably enhances the relative informational content and hence the usefulness of the TRMM data for BMA predictions. This applies to both, bias and unbiased BMA analysis.

In terms of R^2 and *NSE*, the ensemble mean performed better than any individual prediction during both calibration and validation (Tab. 2.5), which is consistent with the findings of Georgakakos et al. (2004) and Viney et al. (2009), and further supports the advantage of predictions made using simple ensemble combination methods. As expected, the BMA predictions provided the best deterministic predictions in calibration period. However, only the unbiased BMA mean outperformed the ensemble mean in validation. This was caused by the trend of the individual model predictions to underestimate streamflow in calibration being reversed in validation, where all models tended to streamflow overestimation. This trend reversal could be partly due to the fact that water extraction from the river for both drinking water supply and irrigation was assumed to be constant for the total simulation period from 2001 to 2008. However, this assumption may not be valid, since it is quite likely that the amount of extracted water has significantly increased during this time period (BRASIL, 2010). Thus, the bias correction based on the calibration data amplified the bias in the validation period. In such cases, BMA without bias

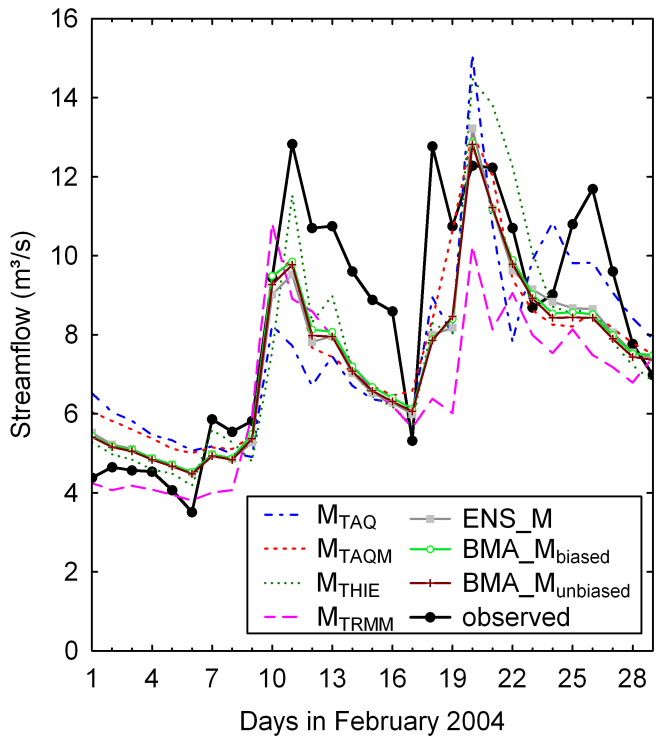

Figure 2.7: Simulated streamflow by different rain input models, the ensemble mean (ENS_M), and the BMA means (biased and unbiased) for a part of the calibration period.

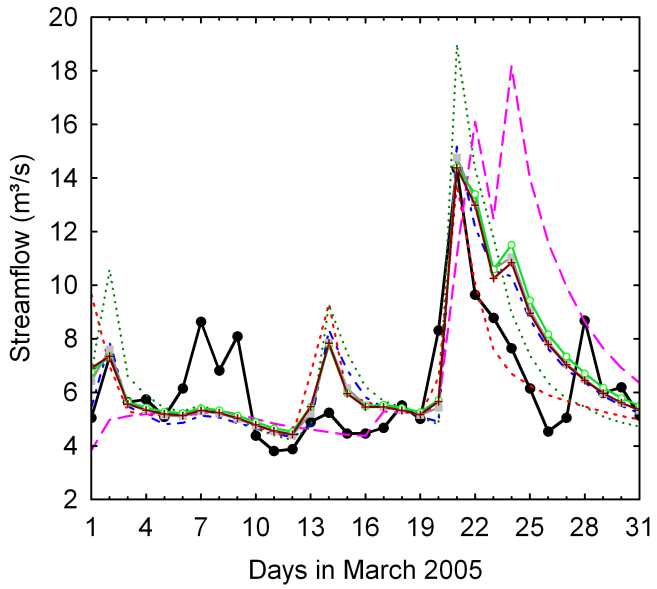

Figure 2.8: Simulated streamflow by different rain input models, the ensemble mean (ENS_M), and the BMA means (biased and unbiased) for a part of the validation period (legend is the same as in Fig. 2.7).

correction seems to be preferable. Nevertheless, the difference between the BMA models' performance is relatively modest, which supports the findings of Viney et al. (2009).

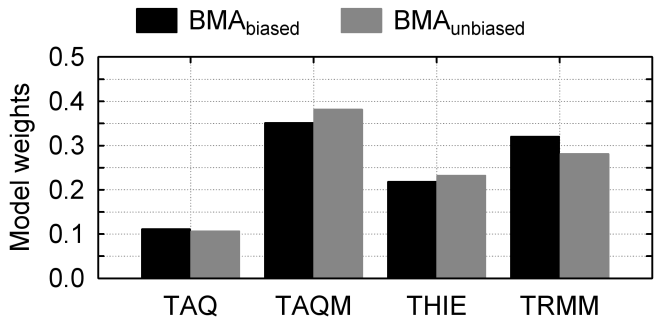

Figure 2.9: BMA weights for the different rain input models.

2.3.3 Predictive uncertainty

Predictive uncertainty was estimated using two different methods. The first method is based on the approach of SUFI-2 which uses the final 1,000 calibration runs of each model. The second method estimates predictive uncertainty using the BMA probabilistic ensemble. Table 2.6 lists the evaluation results for the 95% uncertainty intervals for both the calibration and validation period, as well as for the hydrologic seasons in these periods. During calibration, the uncertainty intervals of the single model predictions have *d-factors* slightly lower than 1, as defined in the SUFI-2 procedure. However, the expected coverage of 95% of observations was not achieved by any of the candidate models. The underestimation of predictive uncertainty ranges from 7% (M_{TAQ}) to 16% (M_{TAQM}).

Similar results were found for the validation period, with the exception of M_{TRMM}. For the M_{TRMM} model, the low *POC* of the uncertainty interval (47%) reflects the relatively low *NSE* of the best deterministic prediction.

Table 2.6: Evaluation of the 95% uncertainty intervals for the hydrologic seasons (rain season = Nov. to Apr., dry season = May to Oct.) and for the whole periods of calibration and validation, respectively.

	Calibration (2001-2004)						Validation (2005-2008)					
	Rain season		Dry season		All		Rain season		Dry season		All	
	POC	*d-factor*	*POC*	*d-factor*	*POC*	*d-factor*	*POC*	*d-factor*	*POC*	*d-factor*	*POC*	*d-factor*
M_{TAQ}	83.4	1.02	92.4	1.19	88.0	0.89	74.9	1.38	86.1	1.43	80.4	1.17
M_{TAQM}	77.7	0.93	79.8	1.04	78.7	0.80	80.7	1.29	89.1	1.32	84.8	1.09
M_{THIE}	85.1	1.16	88.7	1.19	86.9	0.97	81.5	1.73	92.5	1.53	86.9	1.39
M_{TRMM}	74.5	0.93	92.7	1.03	83.6	0.80	48.0	1.13	46.9	0.89	47.3	0.87
ENS	93.2	1.30	97.4	1.31	95.3	1.09	90.6	2.00	96.5	1.63	93.4	1.56
BMA_{biased}	93.1	1.18	99.9	2.43	96.5	1.27	97.0	1.95	100	2.82	98.5	1.90
$BMA_{unbiased}$	92.8	1.17	99.7	2.38	96.3	1.25	96.8	1.92	100	2.75	98.4	1.86

POC: Percentage of coverage of observations

d-factor: Average width of the uncertainty interval divided by the standard deviation of observations

In contrast, the ensemble of the final SUFI-2 distributions (ENS) produced a *POC* that accurately matches the expected 95% in both the calibration and validation period. Ensemble predictions based on combined SUFI-2 outputs have not been previously documented in the literature, but the rationale for utilizing a broader range of reasonable model simulations is consistent with the advantages of ensemble prediction methods. Accurate *POC* values were also achieved by the BMA probabilistic predictions, with only modest overestimations in calibration (+1.5%) and validation (+3.5%). Both versions of BMA, with and without bias correction, provide similar uncertainty bands. The interval of the unbiased BMA prediction in total produced lower d-factors and more concise *POC* values, but these differences were marginal.

The advantages of using a BMA approach to generate probabilistic estimates of streamflow uncertainty has been discussed in numerous studies (e.g. Duan et al., 2007; Vrugt and Robinson, 2007; Zhang et al., 2009; Sexton et al., 2010). However, increasing the precision of *POC* values of the ensemble-based uncertainty intervals has the tradeoff of increasing *d-factors*, which are significantly higher than 1 and thus indicate overestimation of the observed variance in streamflow, especially during the validation period. The *d-factors* are highest for the BMA derived uncertainty intervals, but there are distinct differences between hydrologic seasons. Overdispersion in BMA predictions was mainly observed during the dry season, which is characterized by extremely low variances in streamflow. Here, the BMA predictions led to *d-factors* higher than 2 and *POC* values of nearly 100%. In contrast, during the wet season, the uncertainty intervals derived from BMA perform clearly better than those from the SUFI-2 calibration ensemble.

Figure 2.10 provides an illustration of the relative strengths and weaknesses of the two approaches for estimating predictive uncertainty. Compared to the SUFI ensemble, the BMA uncertainty bands are wider during low flow conditions, but significantly narrower during peak flows. The extreme overestimations of ENS during peak flow conditions can

be are attributed to the relatively small number of SUFI-2 iterations that were utilized during model calibration. The final ranges of parameters, particularly for those controlling surface runoff, were still quite large. Increasing the number of calibration runs may reduce this range, but may also result in lower *POC* values due to a narrowing of the uncertainty bands in general. Thus, neither the SUFI-2 calibration ensemble nor the BMA probabilistic ensemble was able to provide satisfactory uncertainty intervals for all hydrologic conditions. Regardless, these results indicate that the ensemble-based uncertainty predictions are preferable to the underdispersed predictions of the single models. This is consistent with the view that it is advantageous to consider rainfall uncertainty in streamflow predictions by using an ensemble of reasonable rainfall inputs. Among the ensemble predictions, BMA may be preferable to ENS, given its robust theoretical foundation and advantages for scenario applications, since only the participating models with its respective best parameter values have to be run and not the entire ensemble of the final SUFI-2

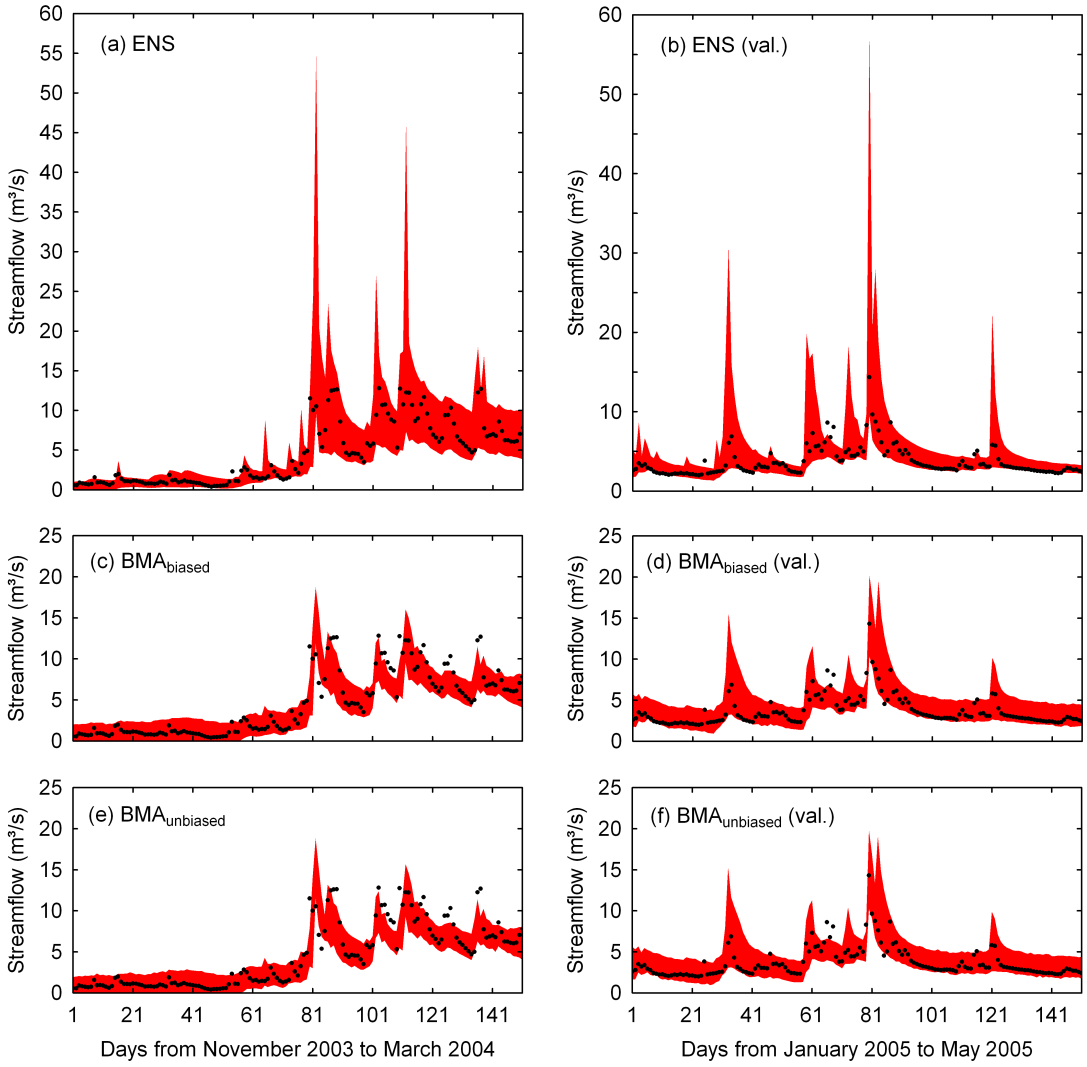

Figure 2.10: 95% uncertainty intervals obtained from SUFI-2 calibration ensemble (ENS) and from BMA probabilistic ensemble predictions for representative parts of the calibration (a, c, e) and validation period (b, d, f), respectively.

parameter hypercubes.

2.3.4 Limitations of the approach

The study shows that a single-model ensemble based on different rain input data-sets can significantly improve hydrologic predictions in terms of model performance and predictive uncertainty estimation. However, there are several limitations to this methodology with regards to model uncertainty that need to be acknowledged. Using this ensemble approach, a range of daily rainfall values can be utilized as model input, however it is important to note that there is a significant amount of correlation between data provided by the contributing ensemble members. These correlations increase during the calibration process, where each rain input model was optimized to match the measured streamflow based on the same objective function. Sharma and Chowdhury (2011) found that dependency across models used to generate an ensemble prediction resulted in reduced performance of the combined output due to less effective stabilization of errors. Due to the problems of input / model overlap, it is preferable to generate ensemble predictions using distinctly different models. In this study, the lack of significantly different data sources led to using precipitation data-sets for the different input models which were quite similar to the rain gauge rainfall of TAQ (with the exception of TRMM; see Tab. 2.1). However, it is important to note that a lack of data is one of the primary motivations for using this ensemble approach. Therefore, the fundamental problem is not the limitations of hydrologic modeling / ensemble methodology, but rather a lack of adequate data to support accurate predictions.

Estimation of parameter uncertainty is furthermore restricted by the limited number of parameters used for model calibration. A sensitivity rank sum across the ensemble was used to select a uniform parameter set for ensemble calibration. While this method is an objective way to identify sensitive parameters with respect to the whole ensemble, it carries the risk that parameters with very different sensitivity across the ensemble (e.g. highly sensitive for one model, but low sensitive for others) might be excluded from model calibration and uncertainty analysis.

With the exception of M_{TAQ}, every rain input model required only two iterations, each with 1,000 model runs, to reach satisfactory *d-factors*. Calibration of M_{TAQ} was complete after an additional iteration, equaling 3,000 model runs in total. A single iteration took approximately four hours on an Intel Core Duo 3.16 GHZ and 3.25 GB RAM computer. Computational efficiency is a major advantage of the SUFI-2 method compared to other optimization procedures, especially more advanced Bayesian techniques, such as Markov Chain Monte Carlo (MCMC) and Importance Sampling (IS). The downside of this approach is that the exploration of parameter space is relatively coarse (Yang et al., 2008). However, for the purpose of this study, the trade-off between computation time and performance was deemed to be acceptable.

To combine the ensemble results, we used traditional methods that assign stationary weights to the ensemble members. Recent studies have found that dynamically adapting weights depending upon the nature of the forecasts and/or catchment states may have advantages for reducing predictive uncertainty (Regonda et al., 2006; Marshall et al.,

2007; Devineni et al., 2008). This approach could be particularly effective when used with an ensemble of different model structures or types. A multi-model ensemble with a large range of inherent model complexity, such as provided by Viney et al. (2009), would also have the benefit of allowing model structural uncertainty to be taken into account. These advances in ensemble methods have the potential to significantly reduce predictive uncertainty in hydrologic modeling.

2.4 Conclusions

This study presented a simple approach to account for precipitation uncertainty in streamflow simulations of a tropical watershed with spatially sparse rainfall information. A range of different input rainfall data-sets was used to examine the uncertainty in parameterization and model output of SWAT. This consisted of two data-sets which assume uniform rainfall based on the only gauge located within the catchment (original gauge data and a weighted moving average) and two spatially distributed data-sets derived using the Thiessen polygon method and TRMM radar data. Acceptable streamflow simulations were possible to achieve for every rain input model, however the best-fit parameter values varied widely across the ensemble. This highlights the advantage of using input ensembles for conceptual hydrological models such as SWAT, precisely because of the difficulty of estimating "true" parameter values. Among the different rainfall-input models, the weighted moving average approach performed best. This may indicate that smoothing operations can provide a reasonable alternative rain input for hydrologic models when only one gauge is available for a mesoscale catchment. However, it is not feasible to infer which method is best for representing rainfall of the Pipiripau catchment. The results show only the suitability of the rainfall data to be transformed to streamflow by the SWAT model given the observed flow rates.

The study also illustrates that hydrologic predictions can achieve higher reliability when different rain input models are combined. Better deterministic predictions were obtained with both the simple ensemble mean and Bayesian Model Averaging (BMA). A further advantage of using a rainfall ensemble is that it provides a more reliable probabilistic forecast. Ensemble predictions generated using both the final auto-calibration iterations and BMA led to uncertainty intervals with accurate coverage of observations. However, these methods also showed considerable limitations with respect to certain flow conditions. Improvement of traditional ensemble combination techniques, such as BMA, was outside the scope of the study, but future efforts are required to achieve more solid performances across a range of different flow conditions.

The demonstrated advantages of using a rainfall input ensemble should be transferable to other catchment models and other regions, but the choice of the rainfall ensemble members must be made with consideration of the gauging situation and availability of alternative observations (e.g. TRMM radar data). Therefore, assuming adequate consideration is given to the feasibility of each contributing rainfall data-set; ensemble modeling can substantially increase the level of confidence in simulation results and support sound hydrological modeling and river basin management, especially in precipitation data sparse regions.

Acknowledgements

This study was funded by the German Federal Ministry of Education and Research (BMBF) within the scope of IWAS (International Water Research Alliance Saxony, FKZ: 02WM1166). The authors sincerely thank Fábio Bakker (CAESB), Henrique Llacer Roig (UnB), Jorge Werneck Lima, Adriana Reatto, Edson Sano, and Éder de Souza Martins (EMBRAPA) as well as the companies ANA, INMET, EMATER, and TNC for providing data. The authors wish to thank Sven Lautenbach (UFZ Leipzig, Germany), Daniel Hawtree (TU Dresden, Germany), and two anonymous reviewers for discussion and helpful comments to improve the quality of this paper.

3 The impact of Best Management Practices on simulated streamflow and sediment load in a Central Brazilian catchment

M. Strauch, J.E.F.W. Lima, M. Volk, C. Lorz, and F. Makeschin
Journal of Environmental Management 127 (2013): S24-S36, available at ScienceDirect
Submitted: 1 July 2012
Accepted: 7 January 2013
With permission by publisher (Elsevier) to be included in a dissertation.

Abstract

The intense use of water for both public supply and agricultural production causes societal conflicts and environmental problems in the Brazilian Federal District. A serious consequence of this is nonpoint source pollution which leads to increasing water treatment costs. Hence, this study investigates in how far agricultural Best Management Practices (BMPs) might contribute to sustainable water resources management and soil protection in the region. The Soil and Water Assessment Tool (SWAT) was used to study the impact of those practices on streamflow and sediment load in the intensively cropped catchment of the Pipiripau River. The model was calibrated and validated against measured streamflow and turbidity-derived sediment loads. By means of scenario simulations, it was found that structural BMPs such as parallel terraces and small sediment basins ('Barraginhas') can lead to sediment load reductions of up to 40%. The implementation of these measures did not adversely affect the water yield. In contrast, multi-diverse crop rotations including irrigated dry season crops were found to be disadvantageous in terms of water availability by significantly reducing streamflow during low flow periods. The study considers rainfall uncertainty by using a precipitation data ensemble, but nevertheless highlights the importance of well established monitoring systems due to related shortcomings in model calibration. Despite the existing uncertainties, the model results are useful for water resource managers to develop water and soil protection strategies for the Pipiripau River Basin and for watersheds with similar characteristics.

3.1 Introduction

Land use and land management practices can adversely affect natural resources and ecosystems. In the fast growing urban area of the Brazilian Federal District (*Distrito Federal* = DF) in Central Brazil, urban sprawl and intensive agriculture have caused severe losses of native savanna vegetation (Cerrado) and an enormous pressure on the region's water resources (Felizola et al., 2001; Fortes et al., 2007; Lorz et al., 2011a). The metropolitan area of the city of Brasília, the federal capital of Brazil, showed the most rapid growth of all the large Brazilian cities and spread beyond the DF region (Martine and Camargo, 1997).

Serious societal conflicts and environmental problems arise in catchments of the DF, where water is used for both public supply and agricultural production. This is also the case for the Pipiripau River Basin (PRB). Recently, DF's water supply company (CAESB) is observing an increase in water treatment costs in the PRB due to soil erosion and nutrient runoff from surrounding agricultural areas (Buric and Gault, 2011).

Best Management Practices (BMPs) can be a useful strategy to mitigate nonpoint source pollution resulting from agricultural activities (Schwab et al., 1995). The PRB is part of the Water Producer Program (Programa Produtor de Água) launched by Brazil's National Water Agency (ANA). This program aims at the implementation of BMPs based on the concept of Payments for Environmental Services (PES). The practices to be supported comprise the restoration and conservation of native vegetation in priority areas such as riparian zones but also BMPs such as terraces, sediment retention basins or sustainable crop management (BRASIL, 2010). The BMPs aim at improving water quality by reducing sediment and nutrient inputs without considerably reducing water quantity. These measures can have a positive effect on water availability during dry seasons, because they improve water infiltration into the soil and thus groundwater recharge.

Watershed models are useful tools to study the impact of various BMP implementations on hydrology and nonpoint source pollution. By effectively capturing site-specific characteristics, i.e. climate, topography, and soil, comprehensive watershed models can limit labor, time, and financial expenses that are associated with intensive field studies (Koch and Grünewald, 2009). The Soil and Water Assessment Tool (SWAT) is such a model and has been used for a wide range of environmental conditions across the globe to predict flow, sediment and nutrient load from watersheds of various sizes (Gassman et al., 2007). Numerous studies have used SWAT to evaluate the impact of BMPs on water quality for watersheds in the US and in Europe, e.g. Vaché et al. (2002), Arabi et al. (2006), Bracmort et al. (2006), Gassman et al. (2006), Secchi et al. (2007), Tuppad et al. (2010b), Lam et al. (2011), and Maringanti et al. (2011). A recent SWAT BMP application for a watershed in Brazil (São Bartolomeu Stream, Minas Gerais) was reported by Rocha et al. (2012). In general, these studies showed that BMPs, such as conservation tillage, no-till, contouring, filter strips, terraces, or grassed waterways, can lead to significant reductions of sediment and nutrient loads depending on catchment properties and the type and extent of the BMPs considered.

Several studies included sensitivity analysis of BMP implementation parameters (Arabi et al., 2008, 2007a; Ullrich and Volk, 2009; Woznicki and Nejadhashemi, 2012), and very

few studies incorporated probabilistic uncertainty analysis of BMP effectiveness (Arabi et al., 2007b; Sohrabi et al., 2003). Uncertainty considerations are particularly important when model results are supposed to support decisions regarding water resource policy, regulation, and program evaluation (Shirmohammadi et al., 2006).

In this study, the SWAT model is utilized to evaluate the impact of BMPs on streamflow and sediment loads in the PRB. Among the catalogue of possible BMPs supported by the Water Producer Program, we selected (i) terraces, (ii) small sediment retention basins ('Barraginhas'), and (iii) a multi-diverse crop rotation system for impact analysis. SWAT is capable of accounting for these types of BMPs (Arabi et al., 2008; Waidler et al., 2011). The analysis is based on a previous SWAT case study conducted for the PRB by Strauch et al. (2012), where it was shown that using an ensemble of precipitation input data can lead to improved streamflow predictions in this region. They also found that uncertainty in 'goodness of fit' parameterization of the SWAT model increases when spatial data on precipitation is limited. Therefore, the evaluation of BMP effectiveness presented in this study follows this approach by considering that precipitation data ensemble.

The study is part of the IWAS-ÁGUA-DF project (`http://www.iwas-sachsen.ufz.de/`) which supports the development of an integrated water resources management for the DF (Lorz et al., 2011a). IWAS-ÁGUA-DF includes three major complexes: (1) catchments and water bodies, (2) waste water (Aster et al., 2010), and (3) drinking water (Vasyukova et al., 2012). This paper is addressing complex (1) by investigating to what extend BMPs might contribute to sustainable water resources management in this region.

3.2 Materials and Methods

3.2.1 Study area

The PRB is located in the Brazilian Central Plateau. From the headwaters in the state of Goiás to its mouth into the São Bartolomeu River (DF), the Pipiripau River drains an area of about 235 km². This study focuses on the part up to stream gauge Montante Captação which covers an area of 188 km² (Fig. 3.1). The terrain is gently undulating with predominantly nutrient-poor and well-drained Ferralsols (EMBRAPA, 1978). Characterized by semi-humid tropical climate, rainfall is unevenly distributed throughout the year. Over the period 1978-2007, nearly 85% of the catchment's annual rainfall (1350 mm) occurred during the rainy season from November to April. The temperature varies slightly around 20.5 °C throughout the year.

During the rainy season, more than 50% of the study area is intensively cropped with soybean and corn, mainly in monoculture (cf. "large-scale cropping" in Fig. 3.1). Brachiaria pasture covers 23%, while irrigated horticulture (4%) is usually limited to areas close to the river network where stream water and groundwater can be easily accessed. Native vegetation of the Cerrado Biome, i.e. fairly dense woody savanna of shrubs and small trees as well as treeless subtypes (Campo) and gallery forests along the watercourses (Mata) (Oliveira-Filho and Ratter, 2002), has been reduced in the last 50 years from nearly 100% to 20% of the area.

In addition to water abstractions for irrigation, the perennial Pipiripau River is also

used for the drinking water supply of nearby cities outside the watershed (Sobradinho and Planaltina, satellite cities northeast of Brasília). More than 180,000 of DF's 2.6 million residents depend on the Pipiripau River for water (Buric and Gault, 2011), which is withdrawn at the outlet of the study area.

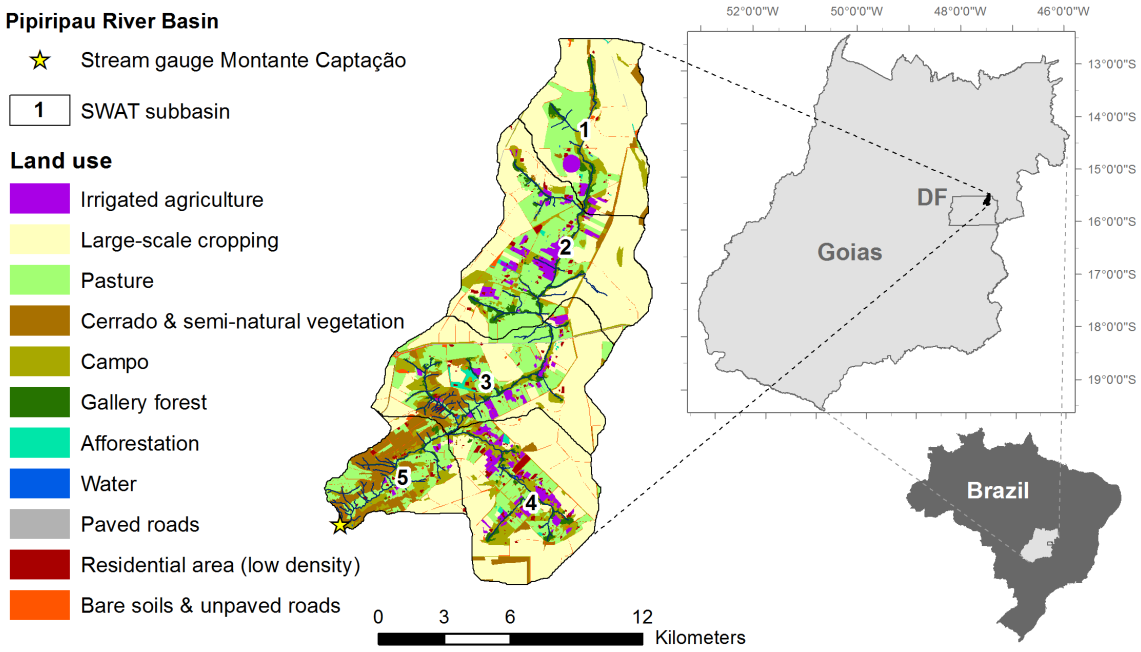

Figure 3.1: Land use map of the Pipiripau River Basin.

3.2.2 SWAT model description

SWAT is a process-based, continuous-time model that operates on a daily time step to predict the impact of management practices on water, sediment and agricultural chemical yields at the catchment scale (Arnold et al., 1998). In SWAT, a watershed is divided spatially into subbasins, which are further subdivided into lumped hydrologic response units (HRUs) consisting of homogeneous landscape, soil, and land use characteristics that are not spatially identified in a given subbasin.

The hydrologic cycle as simulated by the model can be separated into two major divisions, the land phase and the routing phase. The land phase simulates runoff and erosion processes, soil water movement, evapotranspiration, crop growth and yield, soil nutrient and carbon cycling, pesticide and bacteria degradation, and thus controls the amount of water, sediment, nutrient and pesticide loadings entering the main channel in each subbasin. SWAT accounts for a wide array of agricultural structures and practices including tillage, fertilizer and manure application, subsurface drainage, irrigation, ponds and wetlands (Douglas-Mankin et al., 2010) that can impact flow and pollutant movement to channels. The routing phase can be defined as the movement of water, sediments, etc. through the channel network to the watershed outlet. Streamflow routing includes channel transmission losses of water, settling and entrainment of sediments and degradation of nutrients, pesticides, and bacteria during transport.

Over the last two decades, the SWAT model has undergone continuous development

(Arnold et al., 2010; Bosch et al., 2010; Gassman et al., 2007). In its current version, SWAT2009 (Neitsch et al., 2011), several watershed processes can be represented by alternative methods. Table 3.1 gives an overview of the relevant methods used in this study.

Table 3.1: SWAT process representation as used in the study.

Process	Method (cf. Neitsch et al., 2011)
Evapotranspiration	Penman-Monteith[a]
Surface runoff	SCS curve number equation[a]
Erosion	Modified Universal Soil Loss Equation
Lateral flow	Kinematic storage model
Groundwater flow	Steady-state response[a] from shallow aquifer
Streamflow routing	Variable storage routing[a]
Sediment routing	Physics based approach for channel erosion using the simplified version of Bagnold's streampower equation[a]

[a] alternative methods available in SWAT2009

3.2.3 Model setup

The SWAT model was previously set up for the PRB including a comprehensive streamflow calibration and uncertainty analysis with regard to precipitation input uncertainty (Strauch et al., 2012). However, for this study we rebuilt and recalibrated the model for the following reasons: (i) the model version was changed from SWAT2005 to SWAT2009 to make use of the 'land use update' function (explained in section 3.2.5) in the BMP scenario simulations, (ii) additional HRUs with an initial area of zero were introduced for later use in the BMP scenarios, (iii) model calibration and validation now includes daily sediment load (since some parameters are effective for both streamflow and sediment load, it was reasonable to calibrate the model simultaneously for both outputs), and (iv) based on available sediment reference data, model calibration and validation was carried out for a stream gage and a time period that differ from the previous PRB study. Compared to the previous model, however, all input data (Tab. 3.2) remained the same including the ensemble of precipitation data-sets.

Within the model, large-scale cropping sums up to an area of 95.9 km², which equals 50.8% of the study area. All large-scale cropping HRUs were divided into eleven crop rotation or placeholder HRUs using the HRU split method (Winchell et al., 2010), which resulted in (i) a soybean (SOYB) monoculture (Tab. 3.3) with a share of 44%, (ii) a soybean-corn (SOYB-CORN) rotation (Tab. 3.4) with a share of 30%, (iii) a corn (CORN) monoculture (Tab. 3.5) with a share of 26%, and (iv-xi) placeholder HRUs (PH_1 to PH_8) for later BMP scenario runs with an initial share of 0%. Due to their initial area of zero, HRUs PH_1 to PH_8 are not effective on the status quo simulation representing the current land management in the PRB. However, since they were defined as HRUs during model setup, one can easily consider them in scenario runs by increasing their areal contribution to respective subbasins using the land use update function as described in section 3.2.5.

Table 3.2: SWAT input data for the PRB.

Type	Source (date)	Description
DEM	Codeplan (1992)	20m resolution grid derived from contour line map 1:10,000
Climate	EMBRAPA (2001-09)	Daily temperature (min., max.), solar radiation, humidity, wind speed of EMBRAPA CPAC station
Rainfall M_{TAQ}	CAESB (2001-09)	Daily rainfall of gauge Taquara (TAQ)[b]
Rainfall M_{TAQM}	CAESB (2001-09, modified)	Weighted moving average of TAQ[b]
Rainfall M_{THIE}	CAESB; ANA (2001-09)	Thiessen polygons using TAQ and gauges outside Pipiripau basin (Planaltina and Colégio Agricola)[b]
Rainfall M_{TRMM}	TRMM product 3B42 (2001-09)	Daily TRMM radar estimates for a 0.25° grid[b]
Land use	BRASIL (2010)	Land use map of the PRB generated for program „Produtor de Água" (Fig.3.1)
Soil	EMBRAPA (1978), Reatto et al. (2004), and PTFs[a]	Soil map 1:100,000 and horizon specific soil properties for each soil type
Management	EMATER (2009, interview), FAO (2004)	Crop management schedules (cf. tab. 3.3, 3.4, 3.5)
Water use	CAESB (2001-2009)	Monthly stream water extraction for human supply (Captação Pipiripau), averaged for period 2004-2006 (used in calibration) and 2007-2009 (used in validation

[a]PTFs = Pedotransfer functions to derive bulk density (Benites et al., 2007), available water capacity (Tomasella and Hodnett, 2004), and saturated hydraulic conductivity (Schaap et al., 2001) from available soil data (EMBRAPA, 1978).

[b]for detailed information, see Strauch et al. (2012)

The proportions of the different crops and the respective management settings presented in Tables 3.3 to 3.5 are based on information of EMATER DF – Taquara (C. Bianci, personal communication, 2009) and FAO (2004).

Table 3.3: SOYB monoculture operations schedule.

Year	Crop*	Operation	kg/ha	Date
1	SOYB	Harvest and kill		Apr 5
1	SOYB	No-Till Mixing		Nov 1
1	SOYB	Elemental Phosphorus fertilizer application	33	Nov 9
1	SOYB	Elemental Nitrogen fertilizer application	7	Nov 9
1	SOYB	Planting		Nov 10

* SOYB = soybean

Table 3.4: SOYB-CORN operations schedule.

Year	Crop*	Operation	kg/ha	Date
1	SOYB	Harvest and kill		Feb 15
1	CORN	No-Till Mixing		Feb 17
1	CORN	Elemental Phosphorus fertilizer application	20	Feb 19
1	CORN	Elemental Nitrogen fertilizer application	40	Feb 19
1	CORN	Planting		Feb 20
1	CORN	Harvest and kill		Jun 15
1	SOYB	No-Till Mixing		Nov 1
1	SOYB	Elemental Phosphorus fertilizer application	33	Nov 9
1	SOYB	Elemental Nitrogen fertilizer application	7	Nov 9
1	SOYB	Planting		Nov 10

* SOYB = soybean, CORN = corn

Table 3.5: CORN operations schedule.

Year	Crop*	Operation	kg/ha	Date
1	CORN	Harvest and kill		Apr 5
1	CORN	No-Till Mixing		Nov 1
1	CORN	Elemental Phosphorus fertilizer application	20	Nov 9
1	CORN	Elemental Nitrogen fertilizer application	40	Nov 9
1	CORN	Planting		Nov 10

* CORN = corn

3.2.4 Model calibration

Daily streamflow data and bimonthly turbidity data from gauge Montante Captação (cf. fig. 3.1) were available for the period 2004 to 2009 (CAESB). These time series were split into two sub-sets for model calibration (2004 to 2006) and model validation (2007 to 2009). For model calibration, we generated daily suspended-sediment loads (LSS, t/d) using the correlation between measured turbidity (TU, NTU) and suspended-sediment concentration (CSS, mg/l) which was found by Lima et al. (2011) for the Jardim River Basin. This catchment is located 10 km south of the PRB and consists of comparable size, soil, relief and land use characteristics relative to the study area. The relationship between CSS and TU was best estimated ($R^2 = 0.958$) with the following linear function:

$$CSS = 1.114 \cdot TU + 1.4731. \tag{3.1}$$

To generate a daily time series for calibration, we performed a regression analysis between corresponding measurements of streamflow (F) and TU. Suspended-sediment rating curves are usually expressed as power functions, $LSS = aFb$, where a and b are rating curve parameters (Crawford, 1991). Considering all measurements, the power function TU_I shown in Figure 3.2 was found to be the best fit. However, the relatively small value for parameter b bears the risk of underestimating peak loads. Therefore, we applied a combined power function (TU_{II}) where two power functions were derived from two different subsets, one using all corresponding measurements for F lower than 5 m^3s^{-1} (TU_{IIa}) and another one using the data for F greater than 2 m^3/s (TU_{IIb}). The two power functions are then combined at $F = 3$ m^3s^{-1} (cf. Fig. 3.3). We used TU_{II} to compute the daily loads based on eq. 3.1 and the following expression:

$$LSS = 0.0864 \cdot CSS \cdot F\,. \tag{3.2}$$

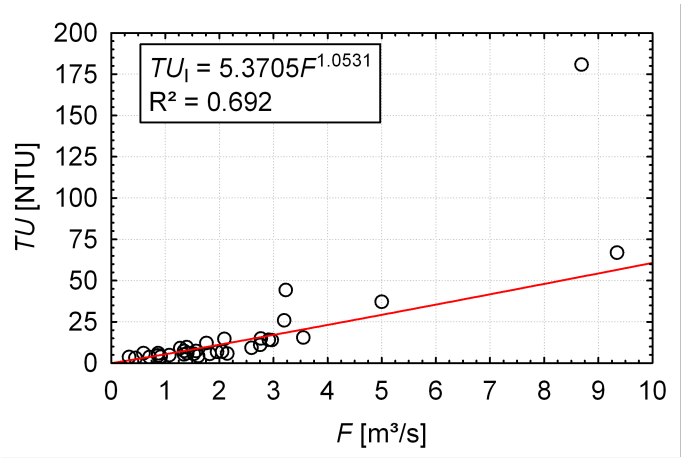

Figure 3.2: Power regression between streamflow (F) and turbidity (TU).

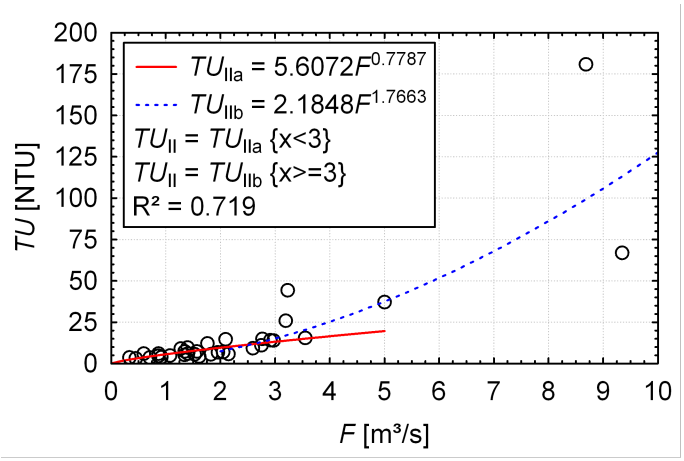

Figure 3.3: Combined power regression between streamflow (F) and turbidity (TU) using subsets.

Model calibration was conducted following the procedure reported in Strauch et al. (2012). This included sensitivity analysis using the LH-OAT sensitivity analysis tool (van Griensven et al., 2006) and auto-calibration using the Sequential Uncertainty Fitting (SUFI-2) routine (Abbaspour et al., 2004). In contrast to the previous study of Strauch et al. (2012), the procedure of this study considered both streamflow and sediment loads. For model calibration, we used the most sensitive streamflow and sediment parameters that could be found for the PRB (Tab. 3.6). It is noteworthy that the parameters CH_N2 and CN2 are strongly effective for both model outputs. Therefore, model optimization was carried out based on a multi-objective formulation of the sum of squared error including the errors in streamflow and sediment load estimation. The objective function g can be expressed as:

$$g = \frac{1}{\sigma_{F_{low}}} \sum_{t=1}^{T} (F_{t_{low}} - SF_{t_{low}})^2 + \frac{1}{\sigma_{F_{high}}} \sum_{t=1}^{T} (F_{t_{high}} - SF_{t_{high}})^2 + \frac{1}{\sigma_{LSS_{low}}} \sum_{t=1}^{T} (LSS_{t_{low}} - SLSS_{t_{low}})^2 +$$

Table 3.6: Description of streamflow and sediment parameters used in calibration.

Parameter	Description
Flow & Sediment	
CH_N2	Manning's "n" value for main channel
CN2	Initial SCS runoff curve number for moisture condition II
Flow	
ALPHA_BF	Baseflow recession constant
CANMX	Maximum canopy storage (mm H2O)
CH_K2	Eff. hydraulic conductivity in main channel alluvium (mm/h)
EPCO	Plant uptake compensation factor
ESCO	Soil evaporation compensation factor
GW_DELAY	Groundwater delay time (days)
GWQMN	Water depth in shallow aquifer for return flow (mm H2O)
SURLAG	Surface runoff lag coefficient
Sediment	
ADJ_PKR	Peak rate adjustment factor for sediment routing in subbasins (tributary channels)
CH_COV1	Channel erodibility factor
CH_COV2	Channel cover factor
PRF	Peak rate adjustment factor for sediment routing in the main channel
SPCON	Linear parameter for sediment that can be reentrained during channel sediment routing
SPEXP	Exponent parameter for sediment reentrained in channel sediment routing

$$\frac{1}{\sigma_{LSS_{high}}} \sum_{t=1}^{T} (LSS_{t_{high}} - SLSS_{t_{high}})^2, \tag{3.3}$$

where F and SF are the observed and simulated streamflow and LSS and $SLSS$ are the rating curve derived and simulated sediment loads on day t in period 2004 to 2006, respectively. The subscript *low* indicates subsets for low flow and low sediment load conditions; i.e., values lower than or equal to the mean of F and LSS, respectively. Subscript *high* is used for the complement subsets. The reciprocal standard deviations of F and LSS are used as weights to avoid underrepresentation of low flow and low sediment load conditions during optimization. As in Strauch et al. (2012), the SUFI-2 auto-calibration routine was conducted for each of the rain input models M_{TAQ}, M_{TAQM}, M_{THIE}, and M_{TRMM}, which differ solely in the type of precipitation input data (cf. tab. 3.2). To evaluate model performance, we used standard statistical criteria suggested by Moriasi et al. (2007), i.e. coefficient of determination (R^2), Nash-Sutcliff Efficiency (NSE), and percentage bias ($PBIAS$). All of these criteria are based on the difference between observation and prediction using absolute values. As a result, predicted deviations from higher values have, in general, a greater influence than those from lower values. Therefore, we used the NSE based on relative deviations (NSE_{rel}), introduced by Krause et al. (2005), as an additional measure. NSE_{rel} can be calculated as:

$$NSE_{rel} = 1 - \frac{\sum_{t=1}^{T} (\frac{O_t - P_t}{O_t})^2}{\sum_{t=1}^{T} (\frac{O_t - \overline{O}}{\overline{O}})^2}, \tag{3.4}$$

where O and P are the observed and predicted values at time t, respectively, and $\overline{O}$ is the arithmetic mean of the observed data. Being nearly insensitive for model enhancement during peak flow, NSE_{rel} was found to be an appropriate measure for evaluating model realizations during low flow conditions (Krause et al., 2005).

3.2.5 BMP representation in SWAT

All BMPs evaluated in this study were simulated by straightforward parameter changes in each of the calibrated rain input models. The impact analysis was carried out for period 2004 to 2009 by comparing the scenario simulations with the respective baseline scenario (BASE); i.e., the calibrated model without any BMP implementation. A key method for running the BMP scenarios was the use of the land use update function. This new function of SWAT2009 allows an HRU fraction updating during a simulation (Neitsch et al., 2010). With this method, it was possible to assign the BMP parameter changes to different extents of the agricultural area in the PRB. The representation of the single BMPs within SWAT is described in the following sections.

3.2.5.1 Terraces

Terraces are broad earthen embankments constructed across the slope to intercept runoff water and control erosion (Schwab et al., 1995). Terracing in SWAT is simulated by adjustment of parameters CN2 and USLE_P (Waidler et al., 2011). CN2 affects the amount of modeled surface runoff, while USLE_P is the support practice factor of the

USLE equation, and thus effective for soil loss at the level of HRUs. For the terraces scenario (TER), the values of CN2 were reduced by 5 from the calibration values and USLE_P was set to 0.12 (Arabi et al., 2008; Tuppad et al., 2010b). Several SWAT applications also considered parameter SLSUBBSN (i.e. the average slope length) for representing parallel terraces (e.g. Arabi et al. (2008), Bracmort et al. (2006)). However, reducing SLSUBBSN according to the horizontal terraces intervals would also lead to a reduced flow concentration time of the subbasin and thus to increased peak runoff rates, which would counteract with the desired effect of terraces (increase of infiltration, reduction of soil erosion). Therefore, we decided to simulate terraces without considering slope length in accordance to the studies of Gassman et al. (2006), Tuppad et al. (2010b), Rocha et al. (2012), and Secchi et al. (2007).

It has to be noted that at present terraces occur on 8,500 ha of the watershed. But most of these terraces have not been maintained for more than 20 years with a consequent loss of effectiveness (BRASIL, 2010). To consider existing terraces in poor condition, the baseline value of USLE_P was set to 0.5. This value can be used to represent contouring (Wischmeier and Smith, 1978) and might therefore be more reasonable than a practice factor of 1, which assumes that no terraces are existing. For the TER scenarios (TER25, TER50, TER75, and TER100), terraces were re-established on 25%, 50%, 75%, and 100% of the agricultural area, respectively. Therefore, the large-scale cropping HRUs representing SOYB, SOYB-CORN, and CORN as well as the pasture HRU of each subbasin have been emulated by placeholder HRUs PH1 to PH4, but with the scenario values for CN2 and USLE_P. Using the land use update method, the area of PH1 to PH4 increased in the TER scenarios to the amount SOYB, SOYB-CORN, CORN, and PAST decreased. For example, in TER25, large-scale cropping and pasture HRUs are represented by the same management, but now include terraces on 25% of the HRU area.

3.2.5.2 Sediment retention basins

Like in many areas of Brazil, unpaved rural roads in the PRB lack efficient drainage systems and are predestined for sediment transport. Therefore, the Water Producer Program supports the implementation of 'Barraginhas' (BAR), which are small sediment retention basins with a size of approximately 50 m^2 and an average effective depth of 0.7 m. The 'Barraginhas' might be constructed in regular intervals along roads (up to 10 BAR per road km) to collect and store surface runoff and sediment (BRASIL, 2010). In practice, the goal of erosion / sediment control is to avoid erosion in the first instance through implementation of on-site measures, e.g. terraces, while sediment controls (e.g. sediment basins) provide a back up where erosion cannot be avoided.

Sediment basins can be simulated in SWAT as ponds (Waidler et al., 2011). Ponds are incorporated at the level of subbasins to represent impoundments that receive loadings only from the land area. For this study, however, we modified the routing of water through the ponds. Because of the small size of BAR and their topographic position along roads, the SWAT code was changed so that only surface runoff was allowed to flow into ponds (code available at `http://iwas.tu-dresden.de/Downloads/swatcode_brazil_strauch.zip`). This was done because in the original SWAT version the total amount of water that

leaves the HRUs (including lateral and groundwater flow) flows into the ponds. The parameterization of ponds used to represent BAR is shown in Table 3.7.

Table 3.7: Pond parameter used for representing the BAR scenarios.

		Subbasin				
Parameter	Description *{assumption to derive values}*	1	2	3	4	5
PND_FR*	Fraction of subbasin area that drains into ponds *{GIS analysis assuming the drainage area shown in figure 4}*	0.645	0.679	0.606	0.708	0.489
PND_ESA*	Surface area of ponds [ha] when filled to emergency spillway *{10 BAR per road km with an area of 50 m² each}*	3.310	7.565	5.755	5.140	2.865
PND_EVOL*	Volume [10^4 m³] when filled to the emergency spillway *{PND_ESA multiplied by average depth of 0.7 m}*	2.317	5.296	4.029	3.598	2.006
PND_NSED	Normal sediment concentration in pond water [mg/l] *{typical dry season concentration in streamflow}*	20	20	20	20	20
PND_K	Hydraulic conductivity through bottom of ponds [mm/hr] *{assuming total seepage time of 3-4 days after heavy rainfall}*	10	10	10	10	10
IFLOD1	Beginning month of non-flood season *{begin of dry season}*	5	5	5	5	5
IFLOD2	Ending month of non-flood season *{end of dry season}*	9	9	9	9	9

*Values represent BAR100. For BAR75, BAR50, and BAR25 the values are multiplied by 0.75, 0.5, and 0.25, respectively

It is extremely difficult to define the drainage area of ponds for the targeted design of 10 BAR per road km. Therefore, we assumed in an extreme scenario (BAR100) that the pond drainage area equals the area that would drain into the whole road network excluding the intersections between roads and streams by a buffer of 100 m (GIS analysis, cf. Fig 3.4).

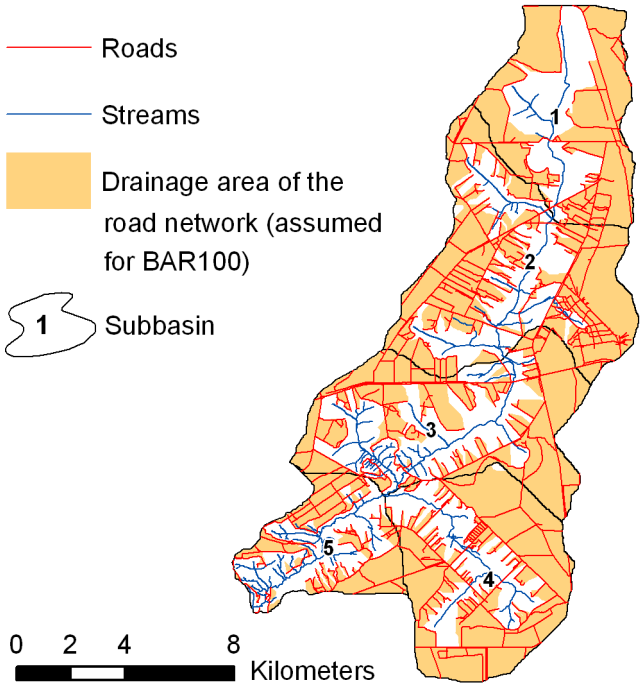

Figure 3.4: Drainage area of the road network in the PRB.

Since roads in the PRB can channel the surface runoff in case of heavy rainfall events, a dense design of BAR along roads might catch most of the runoff produced in this area. For reasons of simplicity, we assumed that BAR100 might be an adequate representation for a design of 10 BAR per road km. Based on these assumptions, we derived three further scenarios of decreasing intensity, BAR75, BAR50, and BAR25, by simply multiplying the pond dimension parameters (signed with an asterisk in Tab. 3.7) by 0.75, 0.5, and 0.25, respectively.

3.2.5.3 Multi-diverse crop rotation

A further conservation management practice discussed by the project management unit of the water producer program is the implementation of diversified crop rotations. As an alternative to the currently dominant monocultures of soybean and corn, diversified crop rotations including cover crops during the dry season could improve soil properties (e.g. soil structure, fertility, soil organic matter) and reduce soil erosion, as well as suppress pests and weeds (Carvalho, 2009, 2010).

In this study, we tested a multi-diverse crop rotation (ROT) including the following regionally common crops besides soybean and corn (cf. Tab. 3.8): green beans (GRBN), spring wheat (SWHT), grain sorghum (GRSG), bell pepper (PEPR), upland cotton (COTP), sunflower (SUNF), sweet corn (SCRN), spring canola (CANA), and potato (POTA). With a 50% share of SOYB, it still meets the market demands. While the rainy season is used for the cultivation of two subsequent crops - which is similar to the SOYB-CORN schedule (Tab. 3.4) - one further crop is grown during the dry season.

Thus, ROT provides a longer ground cover period, but this comes at the cost of a considerable irrigation effort. In the ROT scenario, irrigation of the dry season crop was triggered by plant water demand (auto-irrigation operation, cf. Neitsch et al. (2010)) with a maximum application rate of 5 mm d^{-1} diverted from the shallow aquifer and assuming an irrigation efficiency of 80%. This is still a moderate application rate, as center pivot irrigation in this region might require application rates of more than 6 mm d^{-1} (Lima, 2010). In order to rotate the crops not only temporally but also spatially, we used all placeholder HRUs (PH_1 to PH_8) of each subbasin to represent ROT. In each HRU, the crop rotation was shifted by one year to reach a full spatial rotation. Using the land use update function, large scale cropping of the BASE scenario was converted to ROT by 5%, 10%, 25%, and 50% in the scenarios ROT5, ROT10, ROT25, and ROT50, respectively.

The extents of implementation were chosen smaller than for TER and BAR because this scenario is expected to be very water intensive due to irrigation. Table 3.9 summarizes the BMPs and their level of implementation.

Table 3.8: Crop rotation scenario schedule for PH_1 (for PH_2 to PH_8 the schedule is shifted, each by one year).

					Application rate (kg/ha)[c]	
Year	[a]	Crop[b]	Planting	Harvest	Elemental N	Elemental P
1	a	SOYB	Oct 3	Jan 10	7	33.2
1	b	CORN	Jan 15	May 13	40	20.1
1	c	GRBN	May 19	Aug 16	11	8.7
2	a	CORN	Oct 2	Jan 29	40	20.1
2	b	GRBN	Feb 4	May 4	11	8.7
2	c	SWHT	May 10	Sep 6	9	27.9
3	a	SOYB	Oct 7	Jan 14	7	33.2
3	b	GRSG	Jan 20	Apr 18	8+40	26.2
3	c	PEPR	Apr 25	Jul 23	150	141.9
4	a	COTP	Oct 5	Feb 1	90	64.2
4	b	SUNF	Feb 5	May 14	35+50	24.0
4	c	SCRN	May 20	Aug 12	40	20.1
5	a	SOYB	Oct 15	Jan 22	7	33.2
5	b	CANA	Jan 29	May 7	20+40	48.0
5	c	GRBN	May 13	Aug 10	11	8.7
6	a	CORN	Oct 4	Jan 31	40	20.1
6	b	CANA	Feb 9	May 20	20+40	48.0
6	c	SWHT	May 29	Sep 25	9	27.9
7	a	SOYB	Nov 1	Feb 8	7	33.2
7	b	GRSG	Feb 14	May 13	8	26.2
7	c	POTA	May 24	Aug 31	100	189.1
8	a	COTP	Oct 1	Jan 27	90	64.2
8	b	SWHT	Jan 31	May 27	9	27.9
8	c	GRBN	May 31	Aug 28	11	8.7

[a] a = first crop ('safra'), b = second crop ('safrinha'), c = irrigated dry season crop ('inverno')
[b] SOYB = soybean, CORN = corn, GRBN = green beans, SWHT = spring wheat, GRSG = grain sorghum, PEPR = bell pepper, COTP = upland cotton, SUNF = sunflower, SCRN = sweet corn, CANA = spring canola, POTA = potato.
[c] average crop specific values for the Centre West region of Brazil (FAO, 2004)

Table 3.9: Overview of BMPs and their level of implementation in the PRB.

BMP	Code	Assumed extent	[% PRB]	[ha]
Terracing	TER25	25 % of LCS & PAST	18.5	3,487
	TER50	50 % of LCS & PAST	36.9	6,975
	TER75	75 % of LCS & PAST	55.4	10,462
	TER100	100 % of LCS & PAST	73.9	13,950
Barraginhas (small retention basins)	BAR25	2.5 BAR per road km		
	BAR50	5 BAR per road km		
	BAR75	7.5 BAR per road km		
	BAR100	10 BAR per road km		
Multi-diverse crop rotation including dry season crop	ROT5	5 % of LCS	2.5	479
	ROT10	10 % of LCS	5.1	959
	ROT25	25 % of LCS	12.7	2,397
	ROT50	50 % of LCS	25.4	4,795

LCS = large scale cropping, PAST = pasture

3.3 Results and Discussion

3.3.1 Model performance and parameter uncertainty

Model performance results achieved through the calibration procedure are shown in Table 3.10. In terms of streamflow, each of the models was capable of performing reasonable daily predictions in both calibration and validation period. Compared to the previous PRB study (Strauch et al., 2012), however, R^2 and *NSE* values decreased. This is probably due to the changed frame conditions for the calibration procedure, i.e. different period and stream gauge, while considering at the same time predictions for sediment load. The performance ranking between the different rain input models was found to be similar to the previous study, with best predictions for M_{TAQM} and poorest predictions for M_{TRMM}. Averaging over the ensemble (ENS_M) led to performance values similar or even higher than the best performing individual model. A visual comparison between ENS_M and the observed streamflow for both calibration and validation period is given in Figure 3.5. From this, it can be seen that the observed peak flows are significantly higher in calibration period than those in validation period. However, several of these peak flow events, such as the observed maximum in December 2005, can hardly be explained by any of the rain input data-sets and thus were underestimated by all of the models. This is might be related to local (convective) rainfall events which were not detected by observation – neither by the

Table 3.10: Model performance of different rain input models and ensemble mean in calibration (cal., 1/2004-12/2006), validation (val., 1/2007-6/2009) and the combined period (total, 1/2004-6/2009) for predicting daily streamflow and sediment loads.

		Streamflow			Sediment load		
Statistic	Model	Cal.	Val.	Total	Cal.	Val.	Total
R^2	M_{TAQ}	0.59	0.69	0.63	0.31	0.42	0.31
	M_{TAQM}	0.67	0.73	0.69	0.42	0.43	0.34
	M_{THIE}	0.66	0.74	0.70	0.35	0.47	0.31
	M_{TRMM}	0.43	0.62	0.49	0.09	0.07	0.10
	ENS_M	0.68	0.79	0.72	0.37	0.52	0.35
NSE	M_{TAQ}	0.56	0.30	0.56	0.29	-4.68	0.27
	M_{TAQM}	0.67	0.58	0.68	0.42	-4.53	0.33
	M_{THIE}	0.57	0.37	0.58	0.28	-9.16	0.11
	M_{TRMM}	0.39	0.15	0.41	-0.10	-0.67	-0.09
	ENS_M	0.67	0.57	0.68	0.37	-2.10	0.34
NSE_{rel}	M_{TAQ}	0.83	0.35	0.71	0.62	-1.23	0.60
	M_{TAQM}	0.88	0.68	0.84	0.85	-0.47	0.62
	M_{THIE}	0.83	0.67	0.81	0.50	-0.62	0.56
	M_{TRMM}	0.73	0.00	0.54	0.42	-1.00	0.47
	ENS_M	0.86	0.57	0.79	0.74	-0.08	0.73
PBIAS	M_{TAQ}	-5	-26	-12	-12	-159	-35
	M_{TAQM}	-2	-15	-6	8	-106	-20
	M_{THIE}	-11	-18	-13	0	-104	-17
	M_{TRMM}	-8	-37	-17	-4	-70	-15
	ENS_M	-6	-24	-12	-2	-110	-22

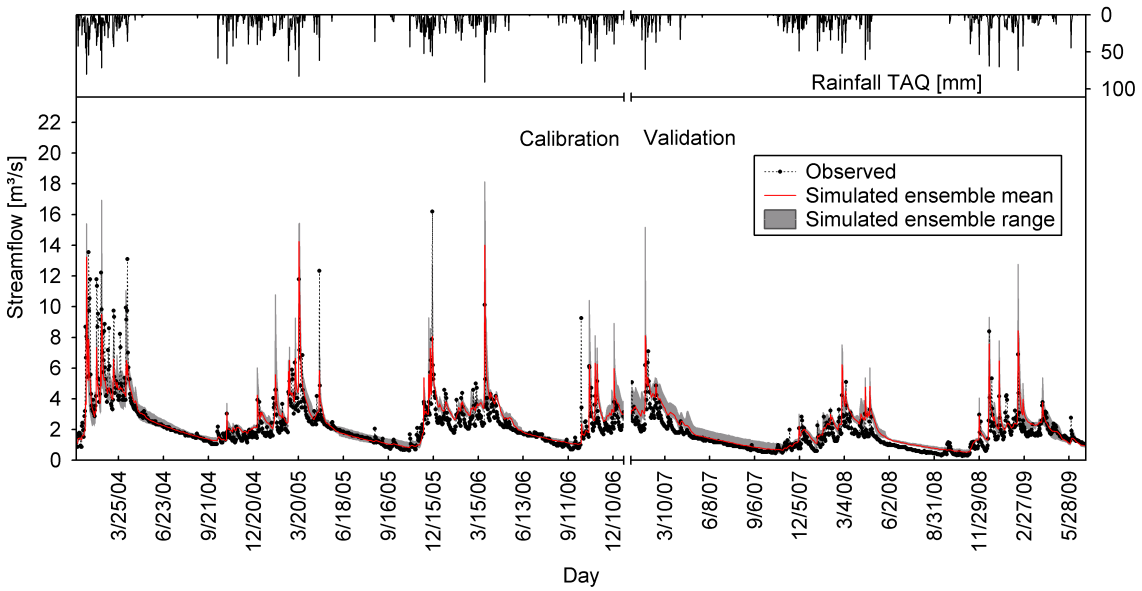

Figure 3.5: Simulated (ensemble mean and range) vs. observed streamflow in calibration and validation period.

sparse network of gages nor by remote-sensing technique (TRMM). The difficulty of using representative rainfall input data for this watershed is discussed in Strauch et al. (2012). Low flow during the dry season, on the contrary, was predicted very well as indicated by relatively high NSE_{rel} values.

In contrast to streamflow, model calibration failed to adequately predict daily sediment loads. While R^2 of ENS_M improved from 0.37 to 0.52 comparing calibration and validation period, *NSE* decreased in validation to inacceptable negative values (from 0.37 to -2.10 for ENS_M, cf. tab. 3.10). This failure is probably due to the fact that the magnitudes of observed streamflow peaks are barely correlating with corresponding rainfall amounts, which consequently led to improper peak flow simulations as described above. However, for the reference sediment loads the differences between single peak load events become considerably larger due to applying a power function (sediment rating curve) on the observed streamflow. For this reason, reference sediment peaks are excessively large in calibration, while remaining on a relatively low level in validation period. Consequently, the model underestimated peak loads during calibration period and overestimated those in the validation period (cf. Fig. 3.6).

The performance ranking between the rain input models is similar as for streamflow, with model M_{TAQM} being the best performer and the TRMM based model being the worst. This is plausible because the sediment reference data is a derivative of the observed streamflow. It has to be noted, however, that the daily loads used for model calibration are surrounded by large uncertainties. Walling (1977) found for British rivers that rating curve estimates of sediment load may be associated with errors of 50% or more. The subject is even more delicate due to the fact that only bimonthly measurements on turbidity could be used in this study in combination with a $TU - CSS$ correlation found for a different, albeit neighboring, catchment. Several studies have shown that water quality monitoring with

Figure 3.6: Simulated sediment loads (ensemble mean and range) vs. sediment loads derived from measured turbidity in calibration and validation period.

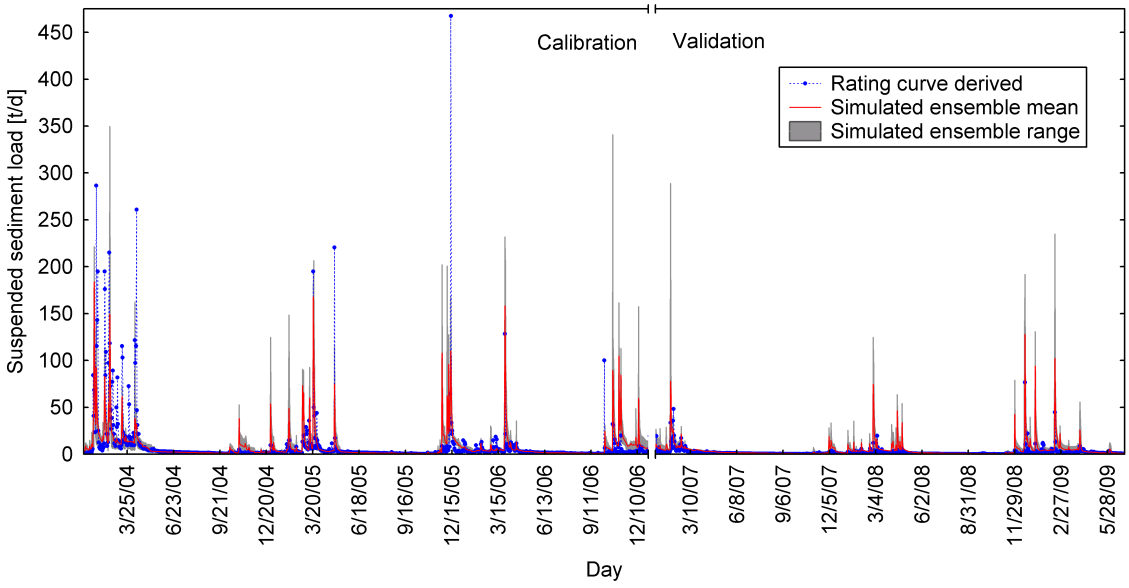

monthly sampling frequency (or lower) is insufficient and associated with high uncertainty of resulting load estimates (Johnes, 2007; Ullrich and Volk, 2010; Vandenberghe et al., 2005). However, due to logistic and financial constraints, it was not possible within this study to conduct continuous or event-based measurements on our own.

Although single peak loads were clearly underestimated, the simulated annual yield was in average 20% higher than the rating curve derived reference yield of 10.05 tons km^{-2} yr^{-1}. This is a considerably low yield. Vanmaercke et al. (2011) presented a large database of sediment yields for 1,794 European catchments which are widely ranging in size. They found that median sediment yields ranged over climatic zones from 6 tons km^{-2} yr^{-1} (boreal) to 218 tons km^{-2} yr^{-1} (mediterranean). Similar to our results, Bicalho et al. (2006) estimated comparably low sediment yields for subbasins of the Descoberto lake, which is also located in the DF (cf. Tab. 3.11). From this perspective, the average yield estimate for the PRB is reasonable.

The advantage of using an ensemble of different input models becomes apparent when considering uncertainty in model parameterization. This study accounts for a rainfall data induced parameter uncertainty. For several parameters, best fit values vary significantly over the ensemble of rain input models as shown in Table 3.12. If these ranges are related to the initial ranges used in auto-calibration, one can infer a parameter specific degree of uncertainty. Some ranges of best fit parameter values, such as for CH_N2, ALPHA_BF, CANMX, or CH_COV1 cover the initial range by around 50% or more. The overall degree of parameter uncertainty is 37%. Hence, it is reasonable to consider parameter uncertainty also in the BMP impact analysis by running scenarios with each of the calibrated rain input models instead of relying on only one single set of best-fit parameters. Similar for all rain input models is a considerably large reduction of CN2 values due to calibration, ranging from -17 to -30%. This might indicate that our reference values initially assumed for CN2 (cf. Strauch et al., 2012) were too high. It might be possible that soil physical properties

Table 3.11: Average sediment yield of the PRB compared to yields of several subbasins of Lake Descoberto.

Method	Catchment	Area [km²]	Sediment yield [t km^{-2} yr^{-1}]
Simulated	PRB[a]	188.68	12.03
	PRB[a]	188.68	10.05
Rating curve derived	Ribeirão Capão Comprido[b]	15.69	26.25
	Ribeirão Chapadinha[b]	18.14	13.77
	Rio Descoberto - montante barragem[b]	104.61	13.45
	Ribeirão das Pedras[b]	82.63	20.11

[a]period 2004-2009, whereas the simulated value refers to the ensemble mean
[b]period 1995-2005 (Bicalho et al., 2006)

(good to very good infiltration capacity of most of the soils, EMBRAPA, 1978; Reatto et al., 2004) and soil management (no-till practice) were not properly reflected in our initial CN2 values. The calibrated values of GW_DELAY are relatively high - indicating a distinct time delay between water exiting the soil profile and entering the shallow aquifer (more than 200 days). However, high values were necessary to maintain simulated baseflow during dry season. A more extended discussion on model parameterization and parameter uncertainty for the PRB is given in Strauch et al. (2012).

Table 3.12: Calibration ranges and best fit parameter values for streamflow and sediment parameters. The uncertainty range is the ratio of the best fit range to the initial range multiplied by 100.

			Initial range		Fitted value for rain input model				Degree (%) of
Parameter	Change	Initial value	Min	Max	MTAQ	MTAQM	MTHIE	MTRMM	Uncertainty
Flow & Sediment									
CH_N2	absolute	0.014	0.01	0.3	0.19	0.24	0.10	0.16	48
CN2	relative (%)	variable[a]	-30	30	-29.86	-17.29	-28.39	-26.62	21
Flow									
ALPHA_BF	absolute	0.048	0	1	0.40	0.68	0.80	0.95	55
CANMX	relative (%)	variable[a]	-50	50	-14.21	33.85	48.93	32.71	63
CH_K2	absolute	0	0	150	31.84	19.65	46.12	86.80	45
EPCO	absolute	0	0	1	0.37	0.74	0.41	0.57	37
ESCO	absolute	0	0	1	0.07	0.05	0.11	0.49	45
GW_DELAY	absolute	31	0	500	347.56	285.88	240.95	355.87	23
GWQMN	absolute	0	0	1000	111.66	79.30	73.38	447.15	37
SURLAG	absolute	4	0	10	1.34	2.36	0.25	1.00	21
Sediment									
ADJ_PKR	absolute	1	0.5	2	0.56	0.90	0.61	0.54	24
CH_COV1	absolute	0	0	1	0.99	0.46	0.63	0.44	54
CH_COV2	absolute	0	0	1	0.18	0.32	0.07	0.40	33
PRF	absolute	1	0.1	2	0.58	0.92	0.10	0.71	43
SPCON	absolute	0.0001	0.0001	0.1	0.0014	0.0010	0.0083	0.0006	8
SPEXP	absolute	1	1	1.5	1.48	1.49	1.30	1.43	38

[a]values reported in Strauch et al. (2012)

3.3.2 Impact of BMPs

The BMPs evaluated in this study aim primarily at the reduction of nonpoint source pollution. At the same time, it is important to maintain streamflow in the PRB for drinking water supply. Hence, we evaluated the BMP impact on both streamflow and suspended sediment load for the 6-year period from 2004 to 2009. The BMP scenario results of each rain input model were compared to the respective base line results and expressed as average percentage changes.

Table 3.13 shows the average percentage changes of streamflow and sediment load for the different rain input models and ENS_M. Some values vary considerably over the model ensemble, which shows that BMP scenario results can be very sensitive to both the considered rain input dataset and the respective calibrated parameter set. The ensemble range of the results can thus be viewed as an indicator of output uncertainty induced by different assumptions for rainfall input. For each of the BMPs, it was found that the ensemble range and thus output uncertainty increased with increasing level of BMP implementation. ENS_M, in contrast, shows the average scenario effect. Unless stated otherwise, all percentage changes given in this section refer to ENS_M, since this might be a more robust measure to quantify the BMP impact. In average, both streamflow and sediment loads were reduced by each of the BMPs, and all the more so, the higher their level of implementation. However, there are remarkable differences between the tested BMPs as described below.

Substantial changes for streamflow resulted only from the multi-diverse crop rotation scenario. Depending on the area of implementation, average streamflow reductions ranged from 4.8% (ROT5) to 42.6% (ROT50), whereas at the same time respective sediment loads were reduced by only half of that. This effect would be disproportionate to the intended objective of maintaining water provisioning services in the PRB. In contrast to ROT, scenario TER affected the average water yield only slightly but led to sediment load re-

Table 3.13: Average change of simulated streamflow and sediment load (%) for each rain input model and the ensemble mean under scenario conditions compared to the respective baseline scenarios.

	Percentage change of streamflow					Percentage change of suspended sediment load				
Scenario	MTAQ	MTAQM	MTHIE	MTRMM	ENS_M	MTAQ	MTAQM	MTHIE	MTRMM	ENS_M
TER25	-0.17	-0.16	-0.18	-0.05	-0.14	-8.16	-8.57	-10.50	-7.15	-8.59
TER50	-0.35	-0.33	-0.35	-0.10	-0.28	-16.31	-16.97	-20.35	-14.09	-16.93
TER75	-0.52	-0.50	-0.53	-0.15	-0.42	-23.60	-24.70	-28.82	-20.93	-24.50
TER100	-0.69	-0.66	-0.71	-0.19	-0.57	-30.16	-30.96	-36.35	-26.54	-31.00
BAR25	-0.02	-0.01	-0.02	0.00	-0.01	-4.82	-5.33	-7.12	-4.96	-5.54
BAR50	-0.04	-0.03	-0.04	-0.01	-0.03	-9.72	-10.63	-14.26	-9.83	-11.07
BAR75	-0.06	-0.05	-0.06	-0.01	-0.04	-14.62	-16.01	-20.96	-14.81	-16.54
BAR100	-0.08	-0.06	-0.08	-0.02	-0.06	-19.21	-21.30	-27.00	-19.79	-21.74
ROT5	-4.84	-4.26	-4.44	-5.40	-4.75	-2.68	-1.10	-0.57	-3.40	-1.97
ROT10	-9.51	-8.62	-8.99	-11.02	-9.56	-5.42	-2.62	-1.27	-7.24	-4.19
ROT25	-23.73	-21.72	-22.18	-28.08	-24.00	-13.44	-8.63	-5.12	-18.67	-11.53
ROT50	-42.17	-38.08	-38.37	-51.31	-42.64	-23.90	-15.98	-10.25	-32.39	-20.73

ductions of up to 31.0% (TER100). However, considering the extent of implementation (up to 74% of the watershed area, Tab. 3.9), terracing had a comparably low impact on the modeled sediment loads. SWAT simulations for a watershed in northeast Iowa, carried out by Gassman et al. (2006), predicted reductions of 63.9% when terraces would be implemented on all cropland (80% of total area); and Tuppad et al. (2010b) simulated sediment reductions of 17.2% for the outlet of the Bosque River watershed (Texas) considering terracing on only 10% of the catchment area. The moderate reduction predicted for the PRB is probably due to the baseline value for parameter USLE_P, which was set to 0.5 to represent existing terraces in poor condition. The studies mentioned above assumed no terraces existing in the baseline scenario (USLE_P = 1). Terracing led to average streamflow reductions of up to 0.6% (TER100). This reduction was expected to be more intensive, since terraces might significantly increase infiltration and thus plant available water, which in turn might increase evapotranspiration.

The simulated effectiveness of small sediment retention basins (BAR scenarios) in reducing sediment load was smaller than compared to terraces, but with a maximum reduction of 21.7% (BAR100) still considerable. Similar to terracing, sediment basins should reduce the total water yield, since surface runoff is collected for infiltration as long as the maximum storage volume is not exceeded. However, the predicted water loss due to evaporation from the temporarily filled basins was negligible and with a range from 0.01% (BAR25) to 0.06% (BAR100) 10 times smaller than the predicted water loss caused by terracing. To the authors' best knowledge, no previous studies have been conducted so far to predict the effectiveness of a large quantity of rather small sediment basins. Hence, this scenario might inherit a larger structural uncertainty than the others.

To further illustrate model behavior, we compared the cumulative distributions of daily streamflow and sediment load predictions of each BMP extreme scenario with the baseline distributions (Fig. 3.7). With this, it was possible to study the effects for different hydrologic conditions. Terraces and 'Barraginhas' significantly reduced streamflow only within the top five percent of the distribution (Fig. 3.7a). This is plausible, because it shows that mainly surface runoff was reduced, while during periods of low-to-moderate flow conditions streamflow tended to increase, albeit marginally. The opposite effect was found for the crop rotation scenario, where the lowest 25% of the distribution collapsed to near zero. Thus, baseflow decreased dramatically due to irrigation during dry season, while on the contrary peak flow was far less reduced. Irrigation of large areas during dry season might therefore represent a huge risk for the drinking water supply function of the watershed and the ecological health of the Pipiripau River.

The sediment load distribution shown in Fig. 3.7b underlines the disadvantage of the crop rotation scenario. At the HRU level; i.e., without considering channel deposition and channel erosion, predicted sediment load could not be reduced with the crop rotation. This is because considerable soil erosion occurs only in about five percent of the modeled distribution. These are events associated with heavy rainfalls during the rainy season, in which the ground is generally covered by crops, independent from the scenario considered. The three highest erosion events of the simulation period were even higher with the ROT50 scenario. This is probably due to the changed management schedule including harvest and planting dates, where heavy rainfalls might coincide with a temporarily barren ground due

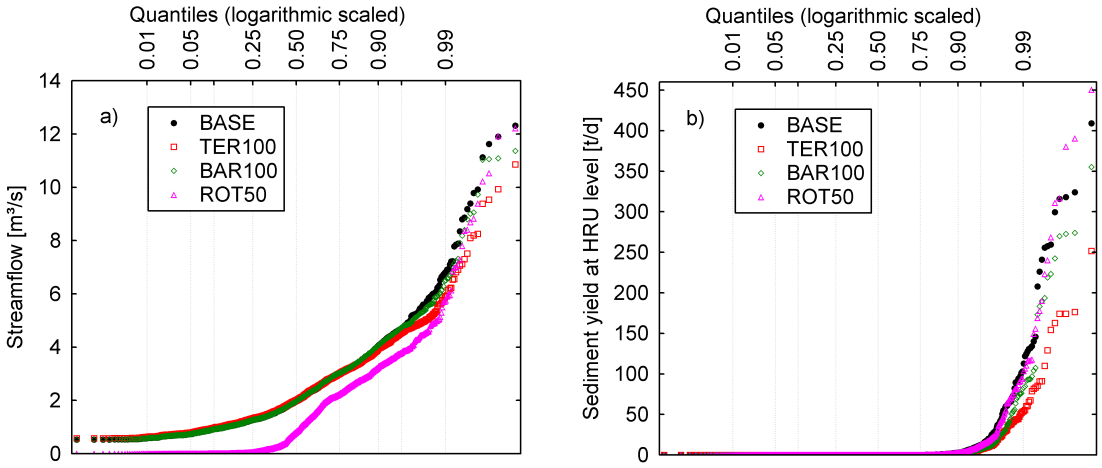

Figure 3.7: Quantile plots of a) simulated daily streamflow at watershed outlet (ensemble mean, period 2004-2009) for the baseline scenario and conservation management scenarios, each with maximum intensity and b) quantile plots of simulated daily sediment load (ensemble mean, period 2004-2009) at HRU level for the baseline scenario and conservation management scenarios, each with maximum intensity. Here, the daily sediment yield of all HRUs (in t ha-1 d-1) was averaged weighted according to the HRU area and multiplied with the total watershed area (ha).

to the change from main crop to secondary crop. It thus becomes clear that the average sediment load reduction of 20.7% (Tab. 3.13) can only be attributed to the reduction of streamflow and its capacity to transport sediments.

In contrast, terraces and 'Barraginhas' led to significant reductions of sediment load by effectively reducing surface runoff. The predicted effectiveness was lower for the sediment basins probably due to the limited storage volume, which is likely to be exceeded during heavy storm events.

Since both BMPs substantially reduced sediment loads at the watershed outlet while not adversely affecting streamflow, we tested a further scenario which considered TER and BAR at the same time. Sediment load reductions predicted with the combined scenarios are shown in Figure 3.8. The simultaneous simulation of extreme scenarios TER100 and BAR100 led to the highest possible load reductions (40%). However, the effectiveness of 'Barraginhas' decreased when they are installed in combination with terraces. This seems reasonable, since both BMPs act as barrier for sediment transport – terraces at first within the agricultural areas (HRUs) and 'Barraginhas' subsequently by routing the HRU sediment loads through ponds (i.e., sediment retained by terraces cannot be retained by 'Barraginhas'). This reduced effect can easily be recognized in Figure 3.8, as well as the increased uncertainty with increasing BMP implementation indicated by the ensemble range.

For the total area of the PRB (235 km²) it is assumed that the implementation and re-establishment of terraces on all cropland and pasture (in total 148 km²) would cost about USD 1.77 million, while the catchment-wide installation of 8,760 'Barraginhas', which equals ten per road kilometer would amount to USD 1.04 million (BRASIL, 2010).

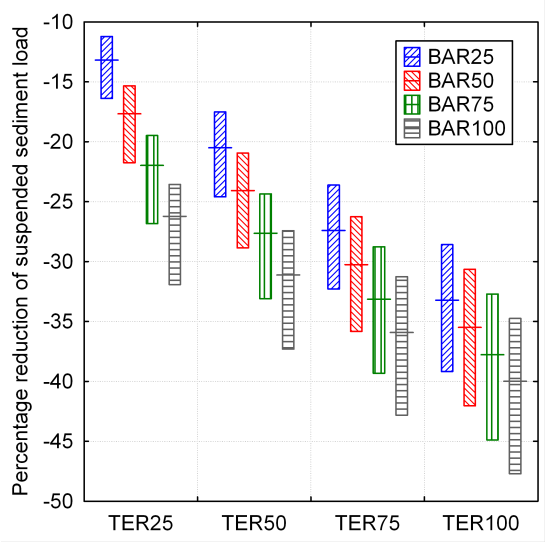

Figure 3.8: Average percentage change of suspended sediment loads for combined scenario simulations (TER and BAR), where the ensemble mean is displayed as crossing line within the range of the different rain input models.

Figure 3.9 relates the average sediment load reductions predicted for TER, BAR, and the combined scenarios (TER+BAR) to the costs of implementation. This calculation is based on the assumption that the percentage load reductions can be extrapolated for the whole PRB watershed. The catchment-wide costs for terraces and 'Barraginhas' were simply multiplied by 0.25, 0.5, 0.75, and 1, depending on the degree of BMP implementation in the respective scenarios. It is shown that sediment load reduction in the single BMP scenarios (TER, BAR) increases linearly with the level / costs of implementation. The BAR scenarios had a slightly higher cost effectiveness than the TER scenarios. However,

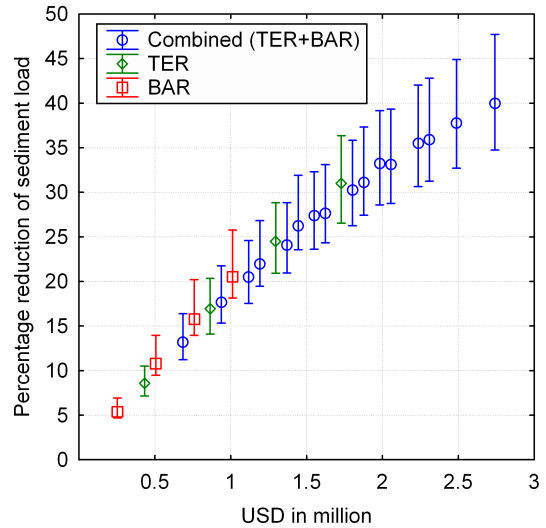

Figure 3.9: Average percentage reduction of sediment load (ensemble mean as dots and ensemble range as whisker) due to different BMP strategies related to the costs of implementation.

in view of the huge uncertainties associated with the simplified process and BMP representation within SWAT, these differences are negligibly small. In contrast to the single BMP scenarios, the predicted cost-benefit relationship for the combined scenarios (TER+BAR) approaches the shape of a saturation curve, which again describes the reduced efficiency in a combined implementation.

3.4 Conclusions

The SWAT model was utilized to evaluate different BMPs regarding their effects on streamflow and sediment load in the Pipiripau River Basin. By allowing different calibrated parameter sets for the scenario simulations (depending on the used rain input data-set), the study provides ranges for BMP effectiveness. We assume that in a watershed with spatially sparse rainfall information the arithmetic ensemble mean of model outputs can be used as a robust measure to study the impact of BMPs.

It was found that structural BMPs, such as terraces and small sediment basins along roads, are promising and recommendable measures to ensure and improve the water provisioning service of the catchment. Terracing might reduce sediment loads by up to 31% in the Pipiripau River Basin, but the highest load reduction was found for the combined implementation of terraces and 'Barraginhas' (40%). These measures might significantly reduce damages due to soil erosion and sediment transport, on-site by reducing the loss of fertile top soil and off-site by lowering water treatment costs. However, the cost effectiveness of a combined implementation is likely to decrease with increasing level of implementation. This should be considered in the BMP selection process. The simulated impact of an economically attractive multi-diverse crop rotation with irrigation was disadvantageous in terms of water availability during dry season. Future efforts to diversify large scale cropping systems in the Cerrado region might only be reasonable if there is no need for additional irrigation. This could be achieved by more extensive crop rotations without dry season crops, but also without repeating soybean or corn every year. Such an option, however, would not be based on the market demand and might thus be hard to implement on a wider scale.

Even though the scenario results seem plausible, the model (ensemble) lacks a solid proof for accurate predictions of daily sediment load. This is mainly because of the insufficient data availability in the study area. Since the Pipiripau River Basin is dedicated as a pilot catchment for testing the effectiveness of BMPs within the water producer program, there is an urgent need for an improved and more comprehensive monitoring, spatially (rainfall) and temporally (water quality including sediment). With this, it might be not only possible to evaluate watershed models such as SWAT more reasonably in terms of process representation and applicability for the Cerrado region. In the long-term, it would also be possible to assess the BMP representation within SWAT by comparing modeled and observed BMP effects. This is of particular relevance for region-specific BMPs such as 'Barraginhas', which have not yet been modeled at the catchment scale.

Despite of shortcomings in the available data and uncertainties due to model assumptions, the study provides first insights into a process based analysis of BMP effectiveness for a watershed that shows representative topographic and soil characteristics for large

parts of the Central Brazilian Cerrado region. It may therefore be concluded that the effectiveness of BMPs evaluated in this study is similar also for other intensively cropped areas of that region including several watersheds of the *Distrito Federal* which drain into reservoirs and where silting is a major concern.

Resource-saving land use is a key element on the agenda of the IWAS-Água DF project. The study shows that conservation practices, such as terraces and 'Barraginhas', can substantially contribute to the development towards more sustainable water resources management in the Pipiripau River Basin as well as in watersheds with similar characteristics.

Acknowledgements

The study is part of the project IWAS-ÁGUA DF, which is funded by the German Ministry of Education and Science (BMBF) in scope of the initiative 'Excellent research and innovation in the New Länder'(FKZ: 02WM1166 and 02WM1070). Many thanks to UnB, EMATER DF, TNC, EMBRAPA Cerrados, and CAESB for technical support and providing data.

4 SWAT plant growth modification for improved modeling of perennial vegetation in the tropics

M. Strauch and M. Volk
Ecological Modelling 269 (2013): 98-112, available at ScienceDirect
Submitted: 2 July 2013
Accepted: 23 August 2013
With permission by publisher (Elsevier) to be included in a dissertation.

Abstract

The Soil and Water Assessment Tool (SWAT) has been used for assessing the impact of land cover and land management changes on water resources for a wide range of scales and environmental conditions across the globe. However, originally designed for temperate regions, SWAT must be critically examined for its appropriate use in tropical watersheds. One major concern is the simulation of perennial tropical vegetation due to the absence of dormancy. While for temperate regions SWAT uses dormancy to terminate growing seasons of trees and perennials, seasonality in the tropics (wet and dry season) can only be represented by defining date or heat unit specific "plant" and "kill" operations which are fixed for every year of simulation. In this paper, we discuss these shortcomings and present an alternative approach to automatically initiate annual growing cycles based on changes in soil moisture. Furthermore, we propose a logistic Leaf Area Index (LAI) decline function which approaches a user-defined minimum LAI instead of using the default function, which is not considering the minimum LAI. The modified SWAT model was tested based on MODIS LAI and evapotranspiration data for the Santa Maria / Torto watershed in Central Brazil, covered mostly by Cerrado (savanna) vegetation. Our model results show that the modified model can reasonably represent seasonal dynamics of the Cerrado biome. However, since the proposed changes are process-based but also allow flexible model settings (e.g. the beginning of growing cycles based on a soil moisture threshold adjustable for plant / land cover types), the modified plant growth module should be useful for large parts of the model community.

4.1 Introduction

Vegetation is a key component of terrestrial ecosystems and thus mandatory to be considered in integrated models simulating biophysical and hydrological processes. The Soil and Water Assessment Tool (SWAT) (Arnold et al., 1998) is such a model that utilizes – in contrast to numerous other comparable tools – a plant growth module to simulate many types of land cover. Over the last two decades, SWAT has been used to assess water resource and nonpoint-source pollution problems in many parts of the world, extensively in the US, in Europe, China, India, Iran, and South Korea (Gassman et al., 2007). Recently, the number of SWAT applications is rapidly increasing also in tropical regions of Africa (e.g. Bossa et al., 2012; Easton et al., 2010; Schuol et al., 2008), Asia (e.g. Phomcha et al., 2011; Thampi et al., 2010; Wagner et al., 2011), and Latin America (e.g. Plesca et al., 2012; Strauch et al., 2012, 2013).

Wagner et al. (2011) pointed out that the methods to model plant growth in SWAT were developed for temperate regions and that they are not suitable for monsoon-driven or tropical climates. However, the vast majority of SWAT studies for tropical regions did not critically reflect the model's suitability to simulate vegetation dynamics (e.g. with regard to the absence of a daylength-driven dormancy, which is in temperate regions used to separate annual vegetation cycles), probably because model calibration and validation is usually based only on discharge and/or water quality outputs. However, successfully matching those outputs does not mean that internal catchment processes are simulated correctly.

This paper aims at overcoming this shortcoming by explicitly focusing on vegetation growth within a SWAT case study for the Santa Maria/Torto watershed (SMTW) in Central Brazil, which is covered mostly by Cerrado vegetation. The Cerrado landscape typically consists of savanna of very variable structure on well-drained interfluves, with gallery forests or other moist vegetation following the watercourses. After Amazonia, the Cerrado is the second largest of Brazil's major biomes and one of the world's biodiversity hotspots. Over the past four decades, however, more than 50% of its approximately two million km² have been transformed into pasture and agricultural lands producing cash crops. This change of land cover is threatening numerous animal and plant species with extinction and might significantly affect water resources and carbon stocks and fluxes (Klink and Machado, 2005). Modeling those effects on larger scales (e.g. river basins) is therefore a major challenge for current research, e.g. in projects contributing to integrated water resources management such as the IWAS-ÁguaDF project (Lorz et al., 2011a), which provided the framework for this study.

On the basis of the identified shortcomings of SWAT to represent seasonal vegetation dynamics, we modified the source code of the plant growth module. One major innovation is the consideration of soil moisture. We hypothesize that soil moisture can be used to indicate the transition from dry to wet seasons and, thus, is suitable to initiate tropical perennial plant growth in SWAT. Furthermore, we modified the decline rate of the leaf area index (LAI) by implementing a logistic function which approaches a minimum value for LAI instead of zero. Model plausibility was then tested by using remote-sensing based estimates for LAI and evapotranspiration (ET) derived from NASA's MODerate Resolu-

tion Imaging Spectroradiometer (MODIS). Few studies provide ground measurements for the Cerrado biome on LAI (e.g. Bucci et al., 2008; Hoffmann et al., 2005b) or ET (e.g. Giambelluca et al., 2009; Lima et al., 1990, 2001; Santana et al., 2010). While ground measurement campaigns require huge efforts, the results are often limited to time and location of measurement. Remote sensing, in contrast, is increasingly being considered as a useful technique for cyclical vegetation monitoring at relatively low cost (Rizzi et al., 2006), providing temporally and spatially continuous information regarding vegetation and surface energy (Justice et al., 2002).

The paper is organized as follows. Section 4.2 describes the study area, provides information related to SWAT (including an introduction of our modified plant growth module), and briefly describes the methods to derive LAI and ET control data from MODIS. Section 4.3 presents and discusses the results, starting with the MODIS estimations for different land cover types and followed by the results of the performance of the modified SWAT model for predicting LAI, ET, and streamflow. In the conclusions section, our modification is finally discussed in a broader context, e.g. in terms of its applicability to other tropical regions.

4.2 Materials and Methods

4.2.1 Study area

The SMTW is located in the Federal District (DF) in Central Brazil (Figure 4.1), close to the city of Brasília, at an altitude ranging from 1,006 to 1,302 m above sea level. With seven to eight humid months, an average annual precipitation of 1420 mm (period 1971 – 2000) and a pronounced dry season, the climate can be classified as Aw (tropical wet and dry), which is the predominant Köppen climate group in the tropics. While average monthly temperature varies only slightly around 20 °C throughout the year, the wettest months (November, December, January) have about 30 to 40 times higher precipitation sums than the driest (June, July, August, Fig. 4.2).

The SMTW covers an area of approximately 234 km², from which large parts (200 km²) are protected as national park comprising natural Cerrado vegetation. The land use classification presented in Figure 4.1 cannot reflect the remarkable physiognomic variation of the Cerrado vegetation as described in the literature (e.g. Oliveira-Filho and Ratter, 2002; Scholz et al., 2008), but distinguishes at least three broad categories: (1) Campo, referring to pure grassland or savanna with a sparse presence of shrubs, (2) Cerrado, referring to savanna with a dominance of either shrubs or stunted trees and a grass understorey, and (3) Mata, referring to evergreen gallery forest in permanently wet riparian zones or deciduous to semideciduous valley forests in topographic depressions which are moist for most of the year. Both Campo and Cerrado are strongly linked to infertile soils with deep groundwater table and seasonal water deficit at the top soil level. While Cerrado physiognomies are usually found on well drained soils, Campo predominates where periods of strong water deficit follow periods of waterlogging, e.g. due to laterite crusts which impede drainage and may also limit root penetration into deeper horizons. Mata, in contrast, is favored by higher soil fertility and continuous water availability throughout the year (cf.

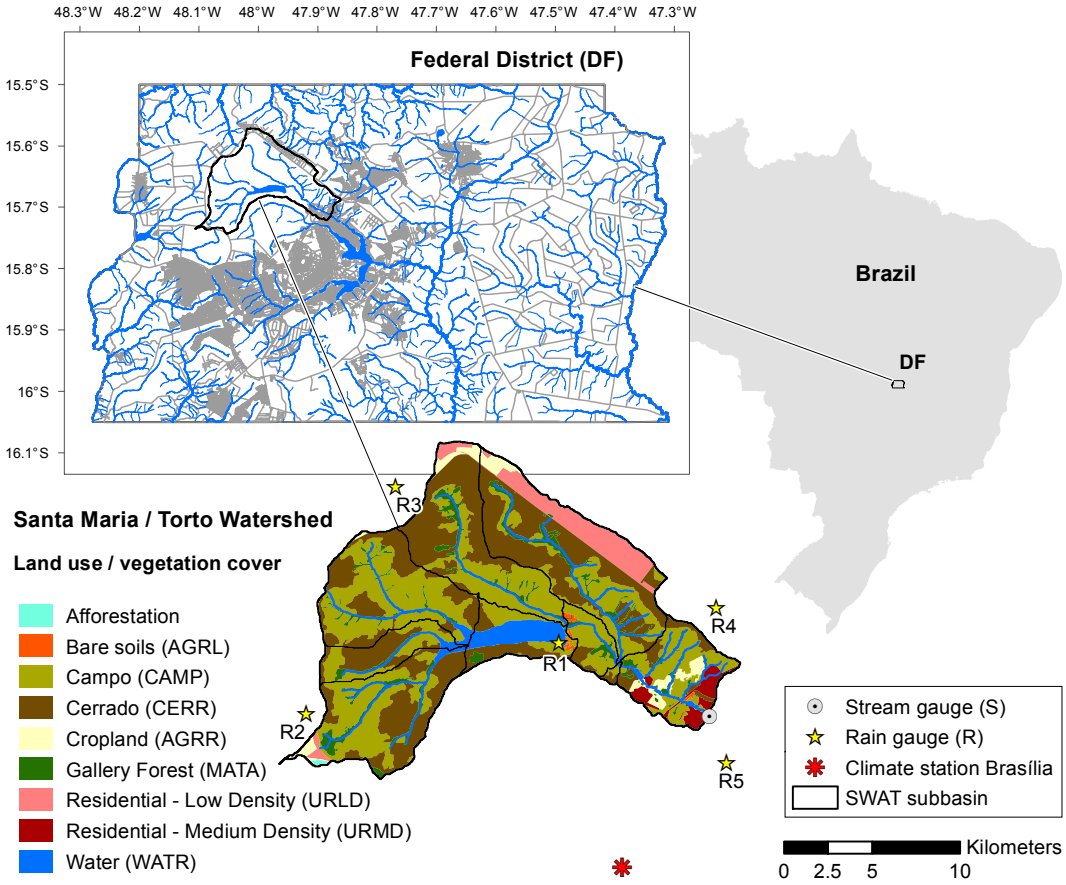

Figure 4.1: Location map, land use, and hydro-meteorological stations for the SMTW. The land use classification is provided by Fortes et al. (2007), whereby the SWAT terminology is shown in brackets.

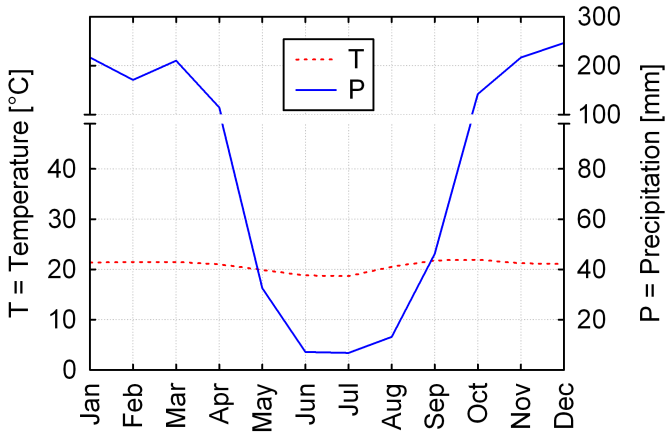

Figure 4.2: Average monthly temperature (climate station Brasília) and precipitation (average of gauges R1 to R5 (cf. Figure 4.1) weighted by Thiessen polygon proportion on watershed area) for period 1971 – 2000. Note the change of scale for precipitation higher than 100 mm.

Oliveira-Filho and Ratter, 2002; Scholz et al., 2008). Urban and agricultural use is restricted to marginal areas of the SMTW and accounts for only 11% of the watershed area. A considerable part of DF's water supply (17%) is provided by the Santa Maria / Torto system. The system, mainly consisting of the Santa Maria reservoir, is producing drinking water at a rate of approximately 1.6 m^3 s^{-1} (CAESB, 2002, 2004), while on average 1.9 m^3 s^{-1} leave the watershed as streamflow of the Torto River (period 1998 – 2006, gauge Torto – Lago / Montante Paranoá, cf. Fig. 4.1). The Torto River is one of four tributaries of Lake Paranoá, which was constructed in 1959 for recreation and energy production. Current plans involve the use for human water supply.

4.2.2 The SWAT model

4.2.2.1 Model description

SWAT (Arnold et al., 1998) is a semi-distributed, partly physically-based watershed model for continuous time simulations of daily discharge as well as nutrient, pesticide, and sediment loads. Spatial heterogeneity is considered by delineating the watershed into multiple topologically connected sub-basins. Within each sub-basin, Hydrologic Response Units (HRUs) are formed by overlaying maps on land use, soil, and topography (Neitsch et al., 2010). Most of the land phase processes, including water flow, nutrient transformation and transport, and vegetation growth are simulated at the HRU level. HRU outputs are aggregated and summed for each sub-basin. At the sub-basin level, SWAT integrates land phase and channel processes. Channel processes include for example streamflow, channel erosion and deposition, or in-stream transformation and transport of nutrients, pesticides, and bacteria (Neitsch et al., 2011). In this study, we primarily focus on vegetation growth and evapotranspiration (ET) at the level of HRUs. The water balance calculation for each HRU considers five storages: snow, canopy storage, the soil profile with up to ten layers, a shallow aquifer, and a deep aquifer. Water pathways at HRU level include evaporation, surface runoff, infiltration, plant uptake, lateral flow and percolation to lower layers (Neitsch et al., 2011).

Surface runoff and infiltration is estimated from daily precipitation using the Soil Conservation Service (SCS) Curve Number (CN) method (USDA-SCS, 1972). For estimating ET, three methods are available: Penman-Monteith, Priestley-Taylor, and Hargreaves. We used Penman-Monteith (Monteith, 1965), which is also the underlying method for ET estimations provided by MODIS. The Penman-Monteith equation used in SWAT can be simplified written as (cf. Neitsch et al., 2011):

$$\mathrm{ET} = \frac{\Delta \cdot R_{net} + \gamma \cdot \rho \cdot VPD/r_a}{\lambda \cdot (\Delta + \gamma \cdot (1 + r_c/r_a))}, \tag{4.1}$$

where ET is the maximum transpiration rate [mm d^{-1}], Δ is the slope of the saturation vapor pressure-temperature curve [kPa $°C^{-1}$], R_{net} is the net radiation [MJ m^{-2} d^{-1}], γ is the psychrometric constant [kPa $°C^{-1}$], ρ is a coefficient derived from latent heat of vaporization, λ [MJ kg^{-1}], air density [kg m^{-3}], atmospheric pressure [kPa], and a dimension coefficient [m s^{-1}]. VPD is the vapor pressure deficit [kPa], r_a is the atmospheric resistance [s m^{-1}], and r_c is the canopy resistance [s m^{-1}]. Plant growth is considered in r_c, which

is estimated by dividing the minimum effective stomatal resistance for a single leaf, r_l, [s m^{-1}] by one-half of the leaf area index (LAI):

$$r_c = \frac{r_l}{0.5 \cdot \mathrm{LAI}}. \tag{4.2}$$

The LAI, defined as one sided green leaf area per unit ground area [m^2 m^{-2}], gives an account of the structural properties of the plant canopy and influences the exchange of energy and mass fluxes between the surface and the atmospheric boundary layer (Schaffrath et al., 2010). It is a key parameter for numerous large-scale models used in climatology, hydrology, biogeochemistry, and ecology (Myneni et al., 2002). Within SWAT, the LAI is modeled itself (section 4.2.2.3).

4.2.2.2 Model setup and calibration

SWAT2009 (revision 477) was set up for the SMTW based on the input data listed in Table 4.1. The model includes 10 sub-basins, one reservoir, and 91 HRUs. Most of the HRUs represent native vegetation types. As initial plant parameter settings for Campo, Cerrado, and Mata we used the SWAT default values for "Range-grasses" (RNGE), "Range-brush" (RNGB), and "Forest-evergreen" (FRSE), respectively. Observed daily streamflow for model calibration and validation was provided by the regional water supplier and sewage company (CAESB) for the watershed outlet (gauge Torto – Lago) covering the time period from 1991 to 2006. Reference data for LAI and ET were obtained from MODIS as described in section 4.2.3. For model calibration, we used the time period from 2000 to 2006 since there the entire set of reference data was available. While validation for LAI and ET was conducted for period 2007 -2009, the model was validated for streamflow using period 1991-

Table 4.1: SWAT input data for the SMTW.

Type	Source (date)	Description
DEM	Codeplan (1992)	20m resolution grid derived from contour line map 1:10,000
Climate	INMET	Daily temperature (min., max.), solar radiation, humidity, wind speed of climate station Brasília (cf. fig. 4.1)
Rainfall	CAESB	Sub-basin rainfall derived from sub-basin proportion on Thiessen polygons generated using 5 rain gauges (cf. fig. 4.1)
Land use	Fortes et al. (2007)	Land use map based on LANDSAT ETM-7 (2002)
Soil	EMBRAPA (1978), Reatto et al. (2004) and PTFs[a]	Soil map 1:100,000 and horizon specific soil properties for each soil type
Water use	CAESB (2004)	Average daily water extraction for human supply from Santa Maria reservoir (8,900 m^3) and from Torto reservoir (4,000 m^3)
Reservoir	Campana et al. (1998)	Average daily controlled outflow from Santa Maria reservoir (0.13 m^3 s^{-1})

[a]PTFs = Pedotransfer functions to derive bulk density (Benites et al., 2007), available water capacity (Tomasella and Hodnett, 2004), and saturated hydraulic conductivity (Schaap et al., 2001) from available soil data (EMBRAPA, 1978).

1999. Model performance was evaluated by visual assessment and statistical analysis. For the latter we used measures that are commonly applied in hydrologic modeling (Moriasi et al., 2007): the coefficient of determination (R^2), the Nash-Sutcliff-Efficiency (NSE), and the percentage bias ($PBIAS$). Since both LAI and ET are HRU-related outputs, we derived the area-weighted HRU mean for comparison with the median of the MODIS data.

Since our study investigates whether process-based structural changes of the plant growth module can lead to reasonable simulations of tropical vegetation dynamics, it was considered appropriate to limit the effort of model calibration. Therefore, the modified SWAT version was calibrated only manually (trial and error) for LAI, ET, and streamflow using process-relevant parameters, shown in Table 4.4 within the results section.

4.2.2.3 SWAT vegetation dynamics and limitations for the tropics

The SWAT plant growth module (Neitsch et al., 2011) is a simplification of the "Environmental Policy Impact Climate" (EPIC) crop growth module (Williams et al., 1984, 1989), which was developed to support assessments of soil erosion impacts on soil productivity for soil, climate, and cropping conditions representative of for a broad spectrum of U.S. agricultural production regions (Gassman et al., 2005). SWAT uses EPIC concepts of phenological plant development based on daily cumulative heat units, harvest index for partitioning grain yield, Monteith's approach (Monteith, 1977) for potential biomass production, and water, nutrient and temperature stress adjustments (Arnold et al., 1998).

The heat unit approach assumes that plants have heat requirements that can be quantified and linked to the time to maturity (Neitsch et al., 2011). Heat units (HU) are calculated using the following equation (cf. Arnold et al., 1998):

$$HU_i = (\frac{T_{mx,i} + T_{mn,i}}{2}) - T_{b,j} \text{ when } (\frac{T_{mx,i} + T_{mn,i}}{2}) > T_{b,j}, \tag{4.3}$$

where HU, T_{mx}, and T_{mn} are the values of heat units, maximum temperature, and minimum temperature in °C on day i, and T_b is the plant-specific base temperature [°C] of crop j. No growth occurs for average temperatures at or below T_b, i.e. heat units can only have positive values. For each plant or land cover, the user has to define the potential heat units (PHU) required for maturity. PHU can be calculated for crops using typical plant and harvest dates. For trees and perennials, however, PHU refers to the number of days between budding and leaf senescence. During simulation, a day (i) and plant (j) specific fraction of potential heat units (FR_{PHU}) ranging from 0 at planting to 1 at maturity is computed as follows:

$$FR_{PHU,i,j} = \frac{\sum_{k=1}^{i} HU_k}{PHU_j}. \tag{4.4}$$

FR_{PHU} is a basic variable for calculating the optimal plant growth. The optimal leaf area development in SWAT is computed by:

$$FR_{LAImax} = \frac{FR_{PHU}}{FR_{PHU} + \exp(l_1 - l_2 \cdot FR_{PHU})}, \tag{4.5}$$

where FR_{LAImax} is the fraction of the plant's maximum leaf area index corresponding to a given fraction of potential heat units for the plant and l_1 and l_2 are shape coefficients.

For annuals and perennials, the leaf area added on day i is calculated as follows:

$$\Delta LAI_i = (FR_{LAImax,i} - FR_{LAImax,i-1}) \cdot LAI_{max} \cdot (1 - \exp(5 \cdot (LAI_{i-1} - LAI_{max}))), \quad (4.6)$$

which is then used to derive the total leaf area index:

$$LAI_i = LAI_{i-1} + \Delta LAI_i, \quad (4.7)$$

where ΔLAI_i is the leaf area added on day i, LAI_i and LAI_{i-1} are the leaf area indices and $FR_{LAImax,i}$ and $FR_{LAImax,i-1}$ are the fraction of the plant's maximum leaf area for day i and *i-1*, respectively. LAI_{max} is the maximum leaf area index of the plant defined by the user. For trees, LAI_{max} is adjusted by considering the current age of the trees and the number of years for the tree species to reach full development (Neitsch et al., 2011). However, the actual plant growth computed for each day may vary from optimal growth due to temperature, water, and/or nutrient stress.

One fundamental feature of trees and perennials in SWAT is dormancy, during which plants do not grow. Dormancy occurs when the day length approaches its minimum for the year. Then, a fraction of biomass is converted to residue and the LAI is set to a plant specific minimum value. Dormancy also resets FR_{PHU} to zero, which allows the beginning of a new growing cycle once the daylength exceeds a latitude-specific threshold. Dormancy is the only approach in SWAT to repeat growing cycles for perennials and trees each year. However, in the tropics (in SWAT defined as regions within latitudes between 20° S to 20° N) plants do not undergo dormancy. In that case, heat units and thus FR_{PHU} are accumulated continuously throughout the whole simulation period. However, the model will only simulate plant growth until the plant reaches maturity (at $FR_{PHU} = 1$), i.e. from that point on, plants will not transpire or take up nutrients and water (Neitsch et al., 2011). Without dormancy, the model requires management operation "kill" for stopping a growing season and thus enabling a new one (by resetting FR_{PHU} to zero). Management operations such as the "kill" operation can be scheduled by FR_{PHU} or by date.

Figure 4.3 shows the LAI of Cerrado simulated in test runs (period 2000 – 2006) using different management settings (a-c). Case a) refers to the setting typically used for simulations of permanent vegetation cover (e.g. range brush, forest). Here, only initial plant growth parameters were defined, i.e. *IGRO* was set to 1, which considers land cover growing from the beginning of the simulation. This setting resulted in only one growing cycle (cf. Figure 4.3) because plant growth in SWAT is simulated as long as $FR_{PHU} < 1$ and this was given only for the first year of the 6-year simulation period. In the remaining five years, FR_{PHU} continued to increase since there is no reset mechanism without dormancy (tropics). Graphs b) and c) represent LAI simulations based on scheduled management operations. Case b) considers a "plant" operation at $FR_{PHU} = 0.1$ and a "kill" operation at $FR_{PHU} = 0.925$ to allow plant grow every year. However, the seasonality is represented insufficiently since LAI reaches its maximum in August/September, i.e. in the driest months of the year, and drops to zero during wet season. To improve the temporal pattern, one can use the date modus for scheduling management operations. In case c), Cerrado is "planted" at September 1st and "killed" at August 31th. With this, it was pos-

sible to shift the simulated LAI maximum to the end of the rainy season in March/April. However, there are still two severe shortcomings. First, the start of a growing season is assumed to be static, i.e. plant growth begins at the same date each year and, second, the LAI drops down towards zero with FR_{PHU} approaching the value of one. For trees and perennials, SWAT considers a plant-specific minimum LAI to ensure that the LAI is not falling below that value (parameter *ALAI_MIN*, here also referred as LAI_{MIN}). However, LAI_{MIN} is only effective in the dormant period and, thus, not effective for the tropics.

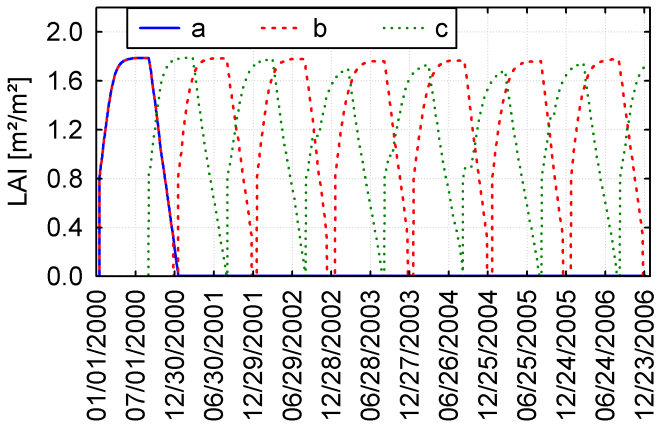

Figure 4.3: LAI simulation for Cerrado using the default version of SWAT with different settings: a) initial plant growth setting with $IGRO = 1$ (vegetation is growing); b) scheduled management using *PHU* fractions: "plant" operation at 0.1 and "kill" operation at 0.925; c) scheduled management using the date modus: "plant" operation at September 1st and "kill" operation at August 31st. In all cases, *PHU* is set to 4300.

4.2.2.4 SWAT plant growth modification

Our main objective was to couple the growing seasons of tropical perennial vegetation to plant available water. Several studies have shown that moisture – and not temperature – is the primary control for plant phenology in tropical regions, especially in those having distinct dry and wet seasons (Borchert, 1994; Bullock and Solis-Magallanes, 1990; Childes, 1989; Monasterio and Sarmiento, 1976; Seghieri et al., 1995).

Moreover, growing cycles should be initiated automatically without requiring management operations ("plant" and "kill") defined for specific dates or fractions of *PHU* which remain fixed for each simulation year. Jolly and Running (2004) have successfully used significant precipitation events, i.e. days where precipitation exceeds potential evapotranspiration, to trigger leaf flush in tropical savannas within the BIOME-BGC model, which simulates forest stand development through a life cycle. Our approach is even more straightforward by using simulated plant available water in the upper soil layers as a trigger for new growing cycles. During dry season, soils or at least their upper horizons usually dry to wilting point (Young, 1976). New growing seasons in SWAT should therefore start once simulated soil moisture is effectively increasing after dry season. However, to ensure that short dry periods during wet season or single rainfall events at the beginning of a dry season do not initiate the end / start of a growing season by mistake, we had to implement

two new parameters, $TRAMO_1$ and $TRAMO_2$, which define the first and the last month of a region-specific 'transition period' from dry to wet season. According to the equinoxes, the default values of $TRAMO_1$ and $TRAMO_2$ were set to 3 (March) and 4 (April) for the northern hemisphere and 8 (August) and 9 (September) for the southern hemisphere. If appropriate, the user may adjust the transition period in the sub-basin input files. The algorithm for initiating new growing seasons can then be described as follows (cf. Fig. 4.4): If (i) the HRU being simulated belongs to a sub-basin, whose centroid has a latitude (LAT_{SUB}) between -20 and 20°, and if (ii) the simulation day is within the transition period, and if (iii) there has not yet occurred a transition from one growing cycle to the next in the current year of simulation (indicated by value zero for variable I_{SEASON}), then the actual soil water content of the upper two layers (SW_{UPPER2} in mm) is compared with a threshold fraction (FR_{AWC}) of the available water capacity of the upper two layers (AWC_{UPPER2} in mm). FR_{AWC} is a new non-dimensional parameter between 0 and 1, which can be defined in database "crop.dat". In case SW_{UPPER2} equals or is greater than this threshold fraction, the fraction of PHU (FR_{PHU}) is reset to zero, the LAI is set

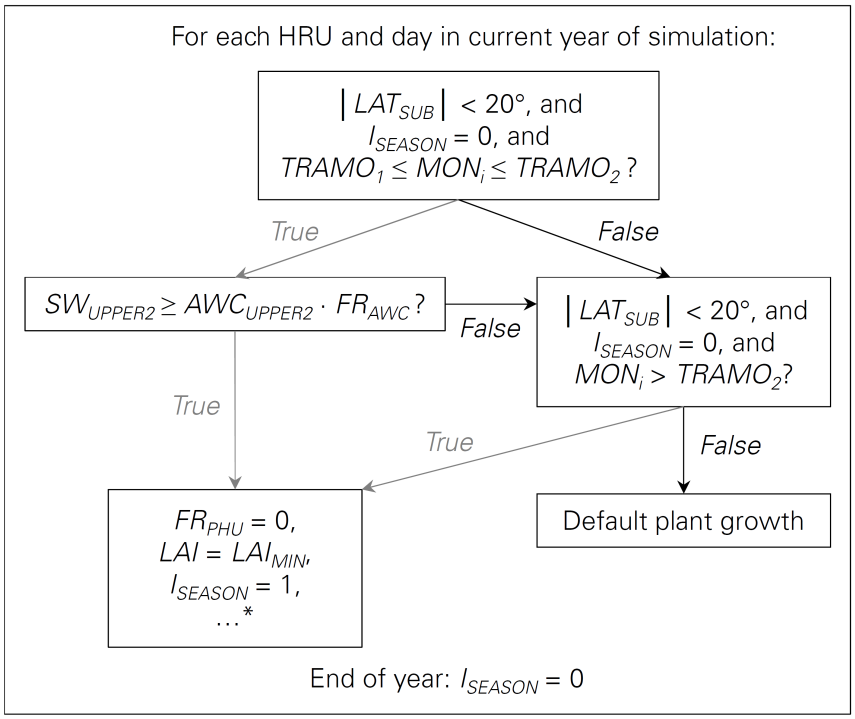

Figure 4.4: Flowchart showing the implementation of soil moisture into the SWAT plant growth module: LAT_{SUB} is the subbasin latitude, MON_i is the current simulation month, $TRAMO_1$ is the beginning and $TRAMO_2$ is the ending month of the transition period (defined in *.sub input files), I_{SEASON} is a switch variable indicating whether or not a season change has occurred in the current simulation year, SW_{UPPER2} is the simulated actual soil water content of the upper two layers in mm, AWC_{UPPER2} is the simulated available water capacity of the upper two layers, FR_{AWC} is a user-defined fraction (between 0 and 1) of available water capacity (defined in database "crop.dat"). FR_{PHU} is the simulated fraction of potential heat units, and LAI_{MIN} is the minimum LAI (defined in database "crop.dat").

to its minimum (LAI_{MIN}), and plant residue decomposition and nutrient release (*) is calculated exactly as if dormancy would occur. Resetting FR_{PHU} to zero initiates a new growing cycle from the next simulation day; and variable I_{SEASON} is set to 1 indicating that a transition has occurred in the current year. If, however, soil moisture remains below the threshold, the transition is initiated latest on the first day of the subsequent month of $TRAMO_2$. At the end of a simulation year, I_{SEASON} switches back to zero to allow a new transition in the next year. Outside the tropics ($LAT_{SUB} \geq 20°$), growing seasons are not affected by soil moisture, since there dormancy is used to initiate growing cycles of perennials and trees (default mode).

With this, growing seasons can be triggered dynamically based on a physical premise. The actual plant growth follows then the normal heat units based LAI cycle (Eqs. (4.3)-(4.7)) until a new growing season is initiated in the subsequent year. While these modifications affect only simulations within the tropics (latitude $< 20°$ N/S), further changes have been done referring to LAI simulations in general. The default LAI decline rate was substituted by a logistic decline rate approaching LAI_{MIN} instead of zero. In the default version, the LAI of trees and perennials can temporarily drop to zero before entering the stage of dormancy. The LAI begins to decline once a user-defined fraction of FR_{PHU} (model parameter $DLAI$) is reached. From then, LAI at day i is simulated as follows:

$$LAI_i = LAI_{OPT} \cdot r, \quad r = \frac{(1 - FR_{PHU,i})}{(1 - DLAI)}, \quad FR_{PHU,i} \geq DLAI, \tag{4.8}$$

where LAI_{OPT} is the optimum LAI of the current year, i.e. the LAI simulated for the day at which FRPHU equaled $DLAI$. With increasing fraction of potential heat units ($FR_{PHU,i}$), LAI_i declines using r as a decline rate. During senescence (period in which $FR_{PHU,i}$ increases from $DLAI$ to the value of 1), r declines from 1 to 0 linearly proportional to the increase of FR_{PHU}. We modified this decline rate using a simple logistic function as expressed in the following:

$$LAI_i = \frac{LAI_{OPT} - LAI_{MIN}}{1 + \exp(t)}, \quad t = (r - 0.5) \cdot (-12), \quad FR_{PHU,i} \geq DLAI, \tag{4.9}$$

where the term used as exponent is a function of time (t). To obtain a standard declining S-curve, values for t range from $+\infty$ to $-\infty$. However, it is sufficient to compute t over a small range of real numbers. By using the values -0.5 and -12 in Eq. (4.9), t ranges from 6 to -6.

Logistic models have been extensively used to depict vegetation growth curves as a function of time or cumulative heat units (Atkinson et al., 2012; Beck et al., 2006; Darroch and Baker, 1990; Thornley and France, 2005; Zhang et al., 2003). Hence, it might be more reasonable to combine the sigmoidal rise of the optimal LAI curve (Eqs. (4.5) and (4.6)) with a likewise sigmoidal decline (Eq. (4.9)), which is at the same time considering LAI_{MIN}. The logistic LAI decline is exemplarily shown in Figure 4.5. The inflection point (IP) of the logistic function is always at the point where the LAI has declined to half the difference of LAI_{OPT} and LAI_{MIN}. In case no value is set for LAI_{MIN} ($LAI_{MIN} = 0$), the logistic curve intersects at that point with the default LAI curve. Assuming constant daily temperature during senescence, as approximately given in tropical regions, the IP

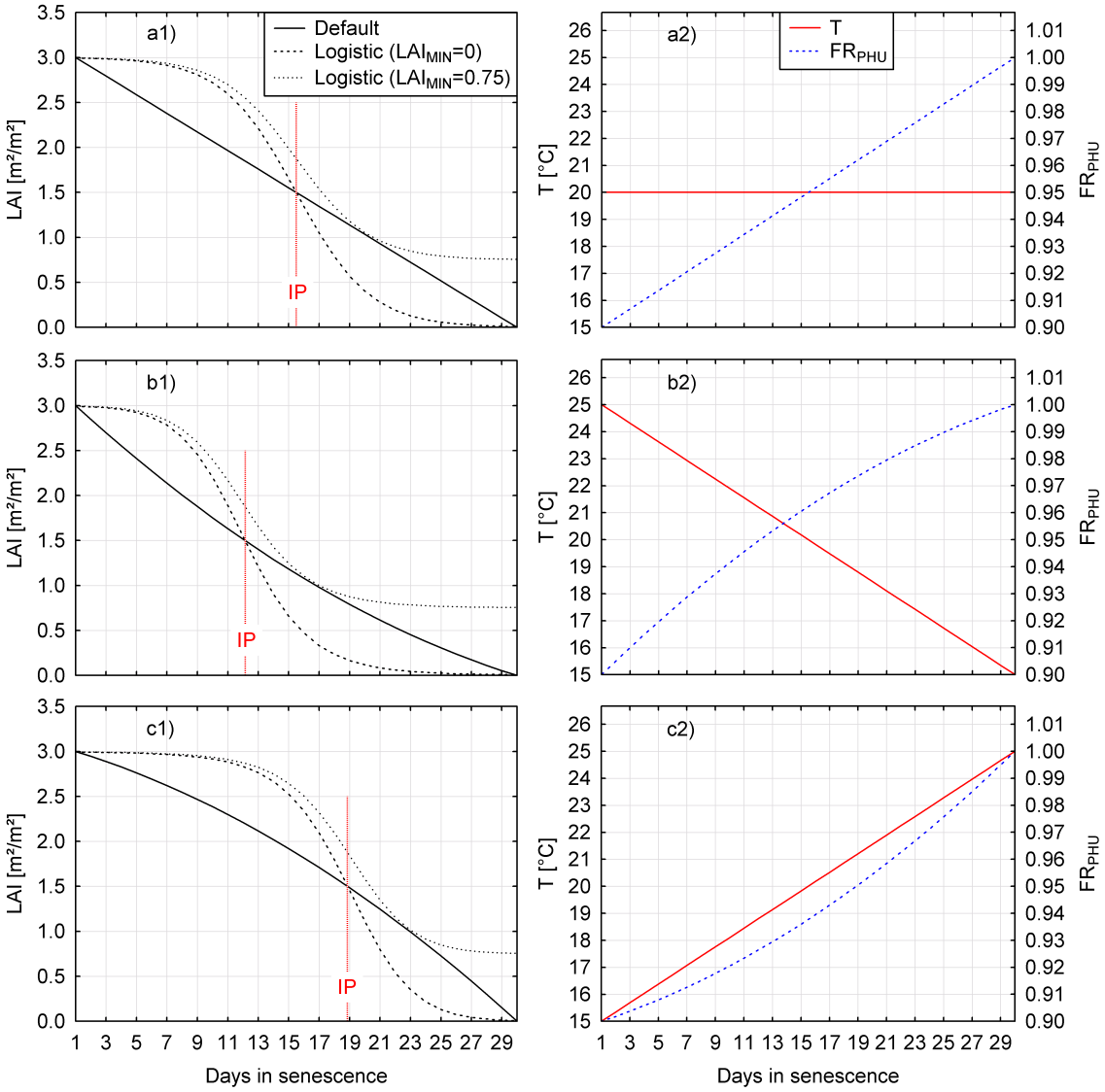

Figure 4.5: LAI decline to represent vegetation senescence calculated using both the default (linear) and the modified (logistic) decline rate (Eqs. (4.8) and (4.9)). In this example, LAI begins to decline from an optimum LAI value of 3 at a fraction of potential heat units (FR_{PHU}) of 0.9. A user-defined minimum LAI (e.g. $LAI_{MIN} = 0.75$) can be considered in the logistic decline rate while the default decline rate does not consider LAI_{MIN}. Seasonal temperature (T) trends (a = constant temperature, b = decreasing temperature, c = increasing temperature) during senescence modify the overall shape of the LAI decline. While the shape of the default decline curve can become either concave or convex, the logistic curve reacts with a shift of its inflection point (IP).

is located in the centre of the senescence period (Fig. 4.5a). Any declining or increasing trend of daily temperature during senescence results in a shift of the IP towards the start or the end of that period, respectively (Figs. 4.5b and 4.5c); and this shift is the stronger, the stronger the trend. Thus, the logistic function is still in accordance with the heat unit approach of SWAT, assuming that decreasing temperature during senescence, like in temperate climates, accelerates the LAI decline.

The modified SWAT version (as executable) as well as the changed model code (Fortran files) and example input files are available at http://iwas.tu-dresden.de/Downloads/swat_tropics_strauch.zip.

4.2.3 MODIS LAI and ET data

We hypothesize that the modified SWAT plant growth module is able to represent the seasonal dynamics of savanna vegetation as given in the study area. In order to evaluate the modified SWAT model, we utilized remote sensing based MODIS products (cf. Tab. 4.2) for LAI and ET. Both products were obtained for the time period from 2000 to 2009 for the area of the DF. They are available at a 1 km by 1 km spatial and an eight days temporal resolution. For the theoretical basis of the algorithms underlying the LAI and ET estimations the reader is referred to the references given in Table 4.2.

We extracted all LAI and ET estimates with a corresponding 'best quality' flag (LAI_QC = 0). Moreover, we focused solely on estimates for the land cover classes Campo, Cerrado, and Mata given in the land use classification of Fortes et al. (2007). Land use polygons where only considered if (i) their location is within the SMTW, (ii) their area is at least 5 km², and (iii) their shape is rather compact, indicated by an area/perimeter ratio higher than 90. Constraints (ii) and (iii) were chosen due to the coarse resolution of MODIS (1 km², cf. Figure 4.6a) to reduce the risk of including pixels that cover different land cover classes. However, these constraints made it impossible to include polygons for Mata within the SMTW; the polygons were either too small or too long and narrow. Hence, for Mata we had to consider areas outside the SMTW (cf. Figure 4.6b).

By overlaying pixel centroids and land cover polygons, 75 pixel could be selected for Campo, 73 for Cerrado, and 20 for Mata. From these subsets we derived for each 8-day time step of period 2000 to 2009 the median (Q0.5) and the lower and upper quartile (Q0.25 and Q0.75, respectively) for MODIS LAI and MODIS ET (exemplarily shown for Cerrado in Figs. 4.7a and b).

Both, LAI and ET, vary seasonally with higher values in the wet season from October to April and lower values in the dry season from May to September. Almost systematically, however, MODIS LAI values collapse to near zero within the period where plant growth is expected to steadily increase (from November to January). This period corresponds well with the period of highest convective activity found for the Mato Grosso state (Brazil, comparable latitude) by Funatsu et al. (2012) using satellite-based microwave observations. It therefore appears reasonable to consider these drops as undetected cloud contamination. Despite of advances in sensor techniques and signal processing algorithms, noise in satellite-based temporal vegetation data remains the rule rather than the excep-

Table 4.2: MODIS products used for model evaluation.

	Product	References	Provided by
LAI	Collect. 5 MOD15A2	Knyazikhin et al. (1998); Myneni et al. (2002); Tian et al. (2000)	Land Processes Distrib. Active Archive Ctr., NASA/EOS (https://lpdaac.usgs.gov/)
ET	Collect. 5 MOD16A2	Mu et al. (2007, 2011)	Numerical Terradynamic Simulation Group, NASA/EOS (http://www.ntsg.umt.edu/)

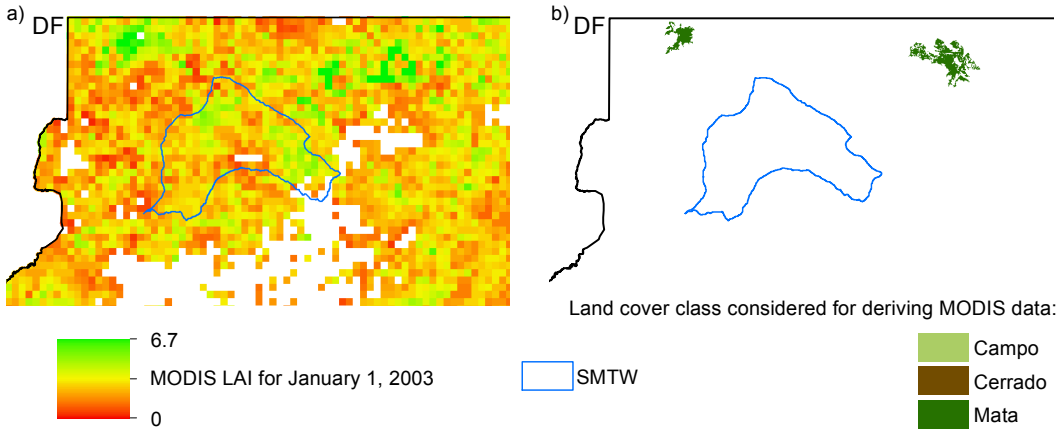

Figure 4.6: a) MODIS LAI with 'best quality' (LAI_QC = 0) exemplarily for time step January 1, 2003 and b) areas covered by native vegetation (Campo, Cerrado, and Mata) for which the MODIS data were analyzed.

tion. Hence, smoothing or filtering methods are commonly applied to vegetation time series in a first step(Atkinson et al., 2012).

We used the 'Best Index Slope Extraction' (BISE) algorithm (Viovy et al., 1992) which was developed to isolate 'true' NDVI values from noise. The algorithm, provided within R-package 'phenex' (Lange and Doktor, 2013), searches forward and accepts decreasing values only if no higher value is found within a moving window of pre-defined length ('sliding period'). Viovy et al. (1992) reported that a sliding period of 30 days was most efficient for NDVI data of tropical West Africa. However, for the data used in this study a value of 40 days, which equals five MODIS time steps, was necessary to sufficiently eliminate high frequency 'noise' while still allowing genuine drops and seasonal variations in LAI to be represented (cf. Figure 4.7a, where the red squares represent BISE-filtered LAI values). In contrast to MODIS LAI, the MODIS ET data for the study region are less affected by high fluctuations and have therefore been used as reference data without filtering (Figure 4.7b).

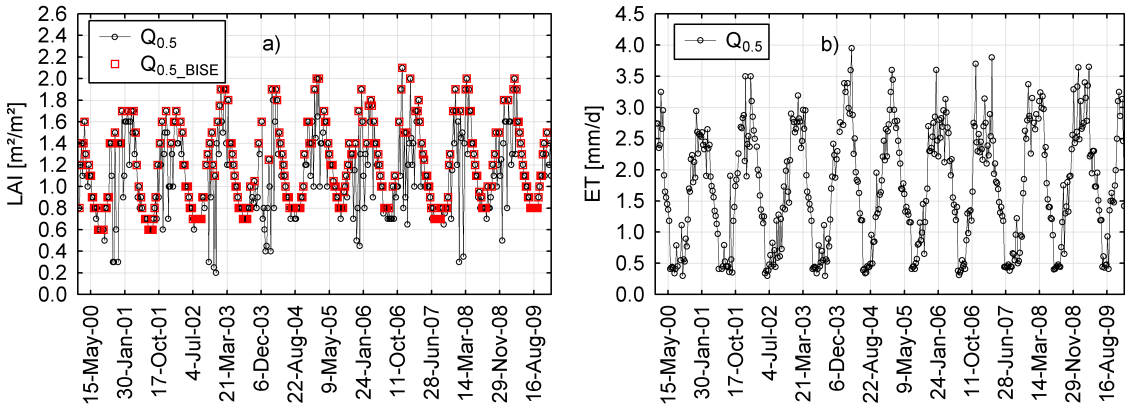

Figure 4.7: a) median (Q0.5) and BISE-filtered median (Q0.5_BISE) of MODIS LAI and b) median of MODIS ET estimates for Cerrado.

4.3 Results and Discussion

4.3.1 MODIS LAI and ET

For each land cover type, the MODIS LAI and ET data reflect a plausible seasonal pattern with highest values at the end of the wet season and lowest values at the end of the dry season (Figs. 4.8 and 4.9) . Across the seasons, median values of MODIS LAI range from 1.4 to 3.2 for Mata and from 0.7 to 1.7 for both, Campo and Cerrado. Higher LAI and ET for Mata may result from greater water and nutrient availability within the river valleys, leading to a species composition strongly different from Campo and Cerrado (Hoffmann et al., 2005b). Hoffmann et al. (2005a) studied seasonal leaf area dynamics across a tree density gradient in the Ecological Reserve of IBGE (Instituto Brasileiro de Geografia e Estatística) located near Brasília. According to their measurements, mean wet season LAI of Mata was found to be 4.2, while for Campo Sujo (open shrub savanna) and Cerrado sensu strictu (typical "Cerrado", i.e. tree savanna) wet season LAI values averaged to 2.3 and 2.8, respectively. In this context, the MODIS LAI estimations appear too low. Moreover, Hoffmann et al. (2005a) report that grasses exhibit much greater seasonality than woody plants. For trees and shrubs, late dry season LAI (September) was on average 68% of the wet season values (February and April), whereas for grasses, late dry season LAI was only 28% of wet season values. These marked differences are not reflected within the MODIS data. Here, the percentages are quite similar, decreasing only slightly along the gradient towards lower tree density from 60% for Mata to 58% for Cerrado and 56% for Campo.

Average monthly MODIS ET varies over a range from 151.2 mm, 84.1 mm, and 82.7 mm for Mata, Cerrado, and Campo in wet season to 47.4 mm, 14.8 mm, and 14.7 mm,

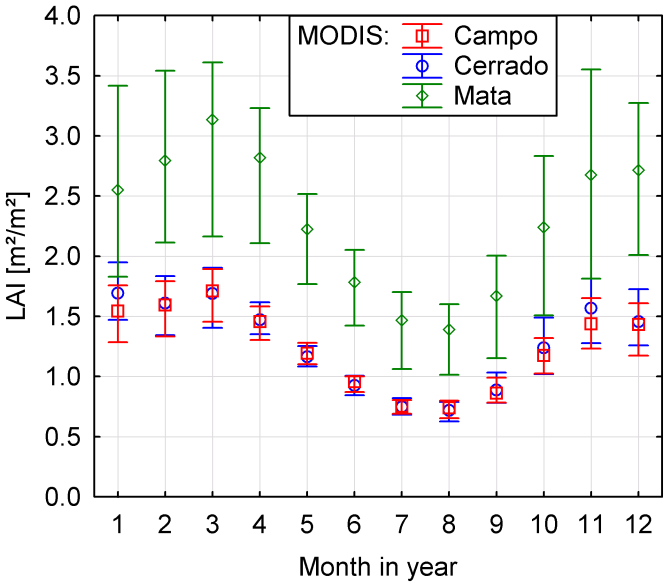

Figure 4.8: Average annual cycle of the median (dots) and the lower and upper quartile (whiskers) of the BISE-filtered MODIS LAI for different land cover types (period 2000-2009).

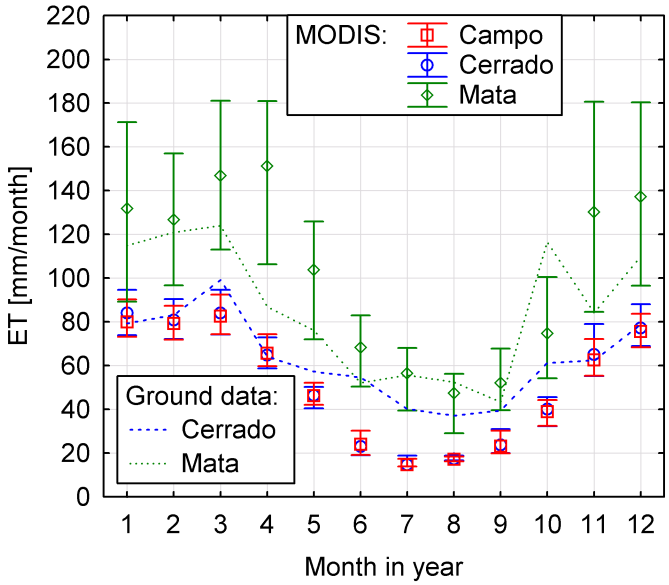

Figure 4.9: Average annual cycle of the median (dots) and the lower and upper quartile (whiskers) of MODIS ET for different land cover types (period 2000-2009) and reference ET graphs averaged to monthly values from ground measurements of different studies, sites, and time periods (for Cerrado: 1 - Giambelluca et al. (2009), 2 - Lima et al. (1990), 3 - Lima et al. (2001), and 4 - Santana et al. (2010); for Mata: 4 - Santana et al. (2010)).[1] IBGE ecological reserve (15°56´S, 47°53´W), DF, 7/2001 – 6/2003; [2] Grão Mogol, Minas Gerais (16°34´S,-42°54´W), 7/1981 – 7/1983; [3] Bacia do Córrego Capetinga (15°57´S, 47°56´W), DF, 8/1998 – 7/1999; [4] IBGE ecological reserve (15°56´S, 47°53´W), DF, 1/2006 – 12/2007.

respectively, in late dry season (Fig. 4.9). Ground measurements provided in the literature (also shown in Fig. 4.9) might indicate that MODIS is overestimating ET for Mata during wet season; while ET for Cerrado might be underestimated during dry season. However,seasonal patterns were reflected well.

For Campo, we found no representative measurements that could be included in Figure 4.9. While many trees of the Cerrado have deep roots allowing them to maintain transpiration during dry season, Campo is dominated by shallow-rooted grasses (Oliveira et al., 2005). Therefore, it can be assumed that Campo uses less water than Cerrado, especially during dry season. Oliveira et al. (2005) found that wet season ET of Campo Sujo was 17% lower than that of a dense tree savanna (Cerrado Denso); this difference was even larger during dry season (41%). Similar results were reported in the study of Giambelluca et al. (2009), where the difference in ET between an open tree and shrub savanna (Campo Cerrado) and Cerrado Denso was measured to be 13% during wet season and 27% during dry season. Similar to LAI, however, the difference between average annual ET cycles of Cerrado and Campo derived from MODIS are negligibly small.

The fact that the MODIS estimates in some cases deviate significantly from ground measurements might indicate that global MODIS data-sets are not appropriate to estimate exact LAI and ET for the vegetation types considered. However, one might also argue that

in larger scales point measurements may lose representativeness and that aerial surveys and remote sensing techniques may be more useful for deriving spatially continuous data. In any case, the advantage of MODIS is its high temporal resolution, which is of utmost relevance for this study. The seasonal patterns derived from MODIS are plausible and by no means contradictory to literature. It therefore can be concluded that the MODIS data are appropriate to evaluate the SWAT model predictions with regard to vegetation dynamics.

4.3.2 SWAT model performance

For Campo and Cerrado, which were both reflected very similar by MODIS, the modified SWAT model performed reasonably well for LAI and ET, with *NSE* values greater than 0.6 in calibration period and values greater than 0.7 in validation. For Mata, in contrast, calibration performance was significantly poorer indicated by *NSE* values around 0.4. Model validation attested a better performance for Mata in case of LAI (*NSE* around 0.7), but for ET the rather poor performance was confirmed ($NSE \approx 0.4$). However, values for R^2 were slightly higher than those for *NSE*, ranging from 0.5 to 0.8, and *PBIAS* was always within reasonable limits (± 15%), indicating an overall good model performance (Tab. 4.3).

For further discussion of model performance and calibrated parameter values, it is useful to visually compare model simulation and reference data. The seasonal LAI development is represented very well by the modified SWAT model (Fig. 4.10). However, this required the adjustment of process-relevant parameters (Neitsch et al., 2010) listed in Table 4.4.

LAI relevant parameters are managed in the model's plant parameter database (crop.dat). Considering a minimum temperature (*T_BASE*) of 10 °C for all land cover types and long-term temperature statistics of climate station Brasília, a *PHU_PLT* of 4300 was calculated (Eq. (4.3)) to ensure that a single heat unit cycle covers approximately one full year. Parameters *BLAI* and *ALAI_MIN* control the upper and lower limit of the possible LAI magnitude. According to the MODIS curves, larger values were assigned to Mata, while values for Campo and Cerrado were defined to be rather small with only slight differences among each other. Starting from the default plant parameter settings (RNGE for Campo, RNGB for Cerrado, and FRSE for Mata), eight further parameters had to be calibrated to adjust the shape of the LAI curve. However, here the calibrated values were similar for each of the land cover types since there were no considerable differences in the seasonality estimated by MODIS.

Table 4.3: SWAT model performance for predicting LAI and ET for different types of land cover.

	LAI (8- to 40-day resolution)						ET (8-day resolution)					
	Calibration (00-06)			Validation (07-09)			Calibration (00-06)			Validation (07-09)		
	Campo	Cerrado	Mata	Campo	Cerrado	Mata	Campo	Cerrado	Mata	Campo	Cerrado	Mata
NSE	0.72	0.68	0.42	0.80	0.72	0.71	0.65	0.62	0.43	0.69	0.71	0.36
R^2	0.79	0.73	0.47	0.82	0.79	0.72	0.75	0.75	0.54	0.74	0.75	0.51
PBIAS	-1.9	-4.3	-3	-4.5	-6.6	-3.8	-8.8	-14.0	7.4	3.2	-1.7	14.2

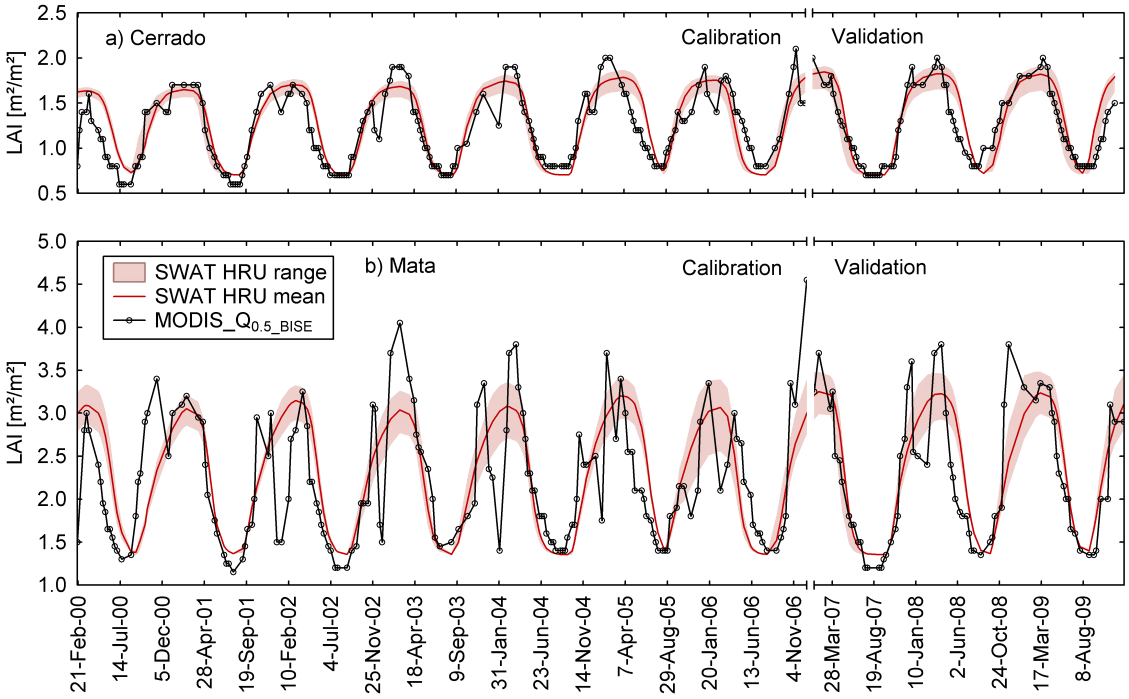

Figure 4.10: Simulated LAI (range over HRUs and area weighted HRU mean) for (a) Cerrado and (b) Mata compared to the corresponding BISE-filtered MODIS median.

Parameter FR_{AWC}, which was introduced in this study, defines the start of new growing seasons after dry season senescence as response to increasing soil moisture in the upper two soil layers. We found that a value of 0.1 (equals 10% of simulated available water capacity) is a suitable threshold for initiating new growing cycles each year. This is reasonable since the upper soils in the study area dry to wilting point during dry season. However, it has to be noted that parameter FR_{AWC} can strongly depend on the tropical region under study and possibly also on the type of land cover. In regions with shorter or less distinct dry seasons, it might be appropriate to set FR_{AWC} to a higher value. Furthermore, the transition period from dry to wet season, which is also introduced in this study and which represents the only time during a simulation year where FR_{AWC} is effective, might be adapted according to regional conditions.

The months August ($TRAMO_1$) and September ($TRAMO_2$), chosen in this study, are based on the spring equinox in the Southern hemisphere (around 22nd September). However, if desired, the transition period can be adjusted on the level of sub-basins (*.sub-files). Figure 4.10 depicts that the model matches the timing of transition as estimated by MODIS reasonably well, although the transition time may vary from year to year. In most of the years, MODIS LAI for Cerrado begins to increase end of August. However, in several years LAI increased not before mid of September (e.g. 2002, 2009) or even not before beginning of October (2004). The model tends to reflect the varying dry season lengths (e.g. longer dry season in 2004, shorter dry season in 2005), which indicates that soil moisture is a suitable trigger within SWAT to initiate plant grow cycles. Due to the modification of the LAI decline rate, it was possible not only to simulate a more realistic

Table 4.4: SWAT parameters used for LAI, ET, and streamflow (Q) calibration.

Parameter (model file)	Calibrated output	Parameter description	Calibrated values *(initial values)* Campo	Cerrado	Mata
ALAI_MIN (crop.dat)	LAI	Minimum leaf area index for plant (LAI_{MIN}, m^2/m^2)	0.7 *(-)*	0.7 *(-)*	1.35 *(0.75)*
BIO_E (crop.dat)	LAI	Radiation-use efficiency ((kg/ha)/(MJ/m^2))	20 *(34)*	20 *(34)*	20 *(15)*
BLAI (crop.dat)	LAI	Maximum potential leaf area index (m^2/m^2)	2.1 *(2.5)*	2.3 *(2)*	3.5 *(5)*
DLAI (crop.dat)	LAI	Fraction of PHU when LAI begins to decline	0.58 *(0.35)*	0.54 *(0.35)*	0.53 *(0.99)*
FRAWC (crop.dat)	LAI	Fraction of available water capacity when plants begin growing season in tropics	0.1 *(-)*	0.1 *(-)*	0.1 *(-)*
FRGRW1 (crop.dat)	LAI	Fraction of PHU corresponding to the 1st point on the optimal leaf area development curve	0.07 *(0.05)*	0.07 *(0.05)*	0.07 *(0.15)*
FRGRW2 (crop.dat)	LAI	Fraction of PHU corresponding to the 2nd point on the optimal leaf area development curve	0.4 *(0.25)*	0.4 *(0.25)*	0.5 *(0.25)*
GSI (crop.dat)	ET	Maximum stomatal conductance at high solar radiation and low vapor pressure deficit (m/s)	0.0008 *(0.005)*	0.0010 *(0.005)*	0.003 *(0.002)*
LAIMX1 (crop.dat)	LAI	Fraction of BLAI corresponding to the 1st point on the optimal leaf area development curve	0.15 *(0.1)*	0.15 *(0.1)*	0.15 *(0.7)*
LAIMX2 (crop.dat)	LAI	Fraction of BLAI corresponding to the 1st point on the optimal leaf area development curve	0.95 *(0.7)*	0.95 *(0.7)*	0.95 *(0.99)*
T_BASE (crop.dat)	LAI	Minimum temperature for plant growth (°C)	10 *(12)*	10 *(12)*	10 *(0)*
VPDFR (crop.dat)	ET	Vapor pressure deficit (kPa) corresponding to the second point on the stomatal conductance curve	1 *(4)*	1 *(4)*	1.6 *(4)*
EPCO (*.hru)	ET	Plant uptake compensation factor	0.25 *(0)*	0.25 *(0)*	1 *(0)*
ESCO (*.hru)	ET	Soil evaporation compensation factor	0.9 *(0.95)*	0.9 *(0.95)*	0.01 *(0.95)*
GW_DELAY (*.gw)	Q	Groundwater delay time (days)	120 *(31)*	120 *(31)*	10 *(31)*
GWQMN (*.gw)	Q	Threshold depth of water in the shallow aquifer required for return flow to occur (mm H2O)	100 *(0)*	100 *(0)*	100 *(0)*
GWREVAP (*.gw)	ET	Groundwater "revap" coefficient	0.2 *(0.02)*	0.2 *(0.02)*	0.8 *(0.02)*
REVAPMN (*.gw)	ET	Threshold depth of water in the shallow aquifer for "revap" to occur (mm H2O)	101 *(1)*	101 *(1)*	1 *(1)*
CN2[a] (*.mgt)	Q	Initial SCS runoff curve number for moisture condition II	46 [86] *(41 [81])*	44 [84] *(39 [79])*	35 [82] *(30 [77])*
PHU_PLT (*.mgt)	LAI	Total number of heat units or growing degree days needed to bring plant to maturity	4300 *(1800)*	4300 *(1800)*	4300 *(1800)*
CH_K2[b] (*.rte)	Q	Effective hydraulic conductivity in main channel alluvium (mm/hr)		105 *(0)*	
CH_N2[b] (*.rte)	Q	Manning's "n" value for the main channel		0.1 *(0.014)*	

[a] *CN2* values for Hydrologic Soil Group A [and D], both Soil Groups are occurring in the study area.

[b] Non-specific for land cover type.

sigmoidal LAI decline, but also to account for a vegetation type specific minimum LAI (Fig. 4.10), since this value is at the same time the minimum of the logistic function proposed in Eq. (4.9). Although in reality the minimum LAI can vary from one year to the next, considering a certain minimum value is crucial for model applications in tropical watersheds. This is thus a significant improvement over the default model, which only accounts for a minimum LAI in case of dormancy (Neitsch et al., 2011).

Figure 4.10 also reveals that there is a slight annual variation in maximum LAI derived from MODIS. This variation is not reproduced well by the simulated LAI, which might indicate that the plant parameter setting can still be improved, especially in terms of sensitivity to stress factors (nutrient and water stress). Furthermore, it has to be noted that although a filtering technique was applied for MODIS LAI, several large drops during wet season remained in the reference data. This is especially true for Mata (Fig. 4.10b). Ignoring these unrealistic drops might probably lead to improved performance values similar to those derived for Campo and Cerrado, which are less affected by wet season drops after BISE-filtering. In general, the model results for LAI are convincing.

The same applies to the simulation of ET shown in Figure 4.11. Although LAI is affecting ET (Eqs. (4.1) and (4.2)), the model had to be calibrated using further ET relevant parameters (Table 4.4) to account for variations among the considered vegetation types and, thus, to represent differences in the plant-specific water use described in section 4.3.1.

Water use of gallery forests (Mata) is considerably higher than that of savanna (Campo and Cerrado). Beside of considering higher LAI values for Mata, this could be achieved by adjusting the parameters controlling the transpirative demand (higher *GSI* and *VPDFR*), the water use from the soil profile (higher *EPCO*, lower *ESCO*), and the access to groundwater (higher *GW_REVAP*, lower *REVAPMN*). However, despite of these adjustments, SWAT still underestimates ET of Mata in several parts of the simulation period as shown in Figure 4.11b. This might be a failure of the model, but the reference data (MODIS) might likewise overestimate ET (cf. ground measurements of Santana et al. (2010) in Fig. 4.9). A lower ET during wet season, and in particular at the end of the wet season (March,

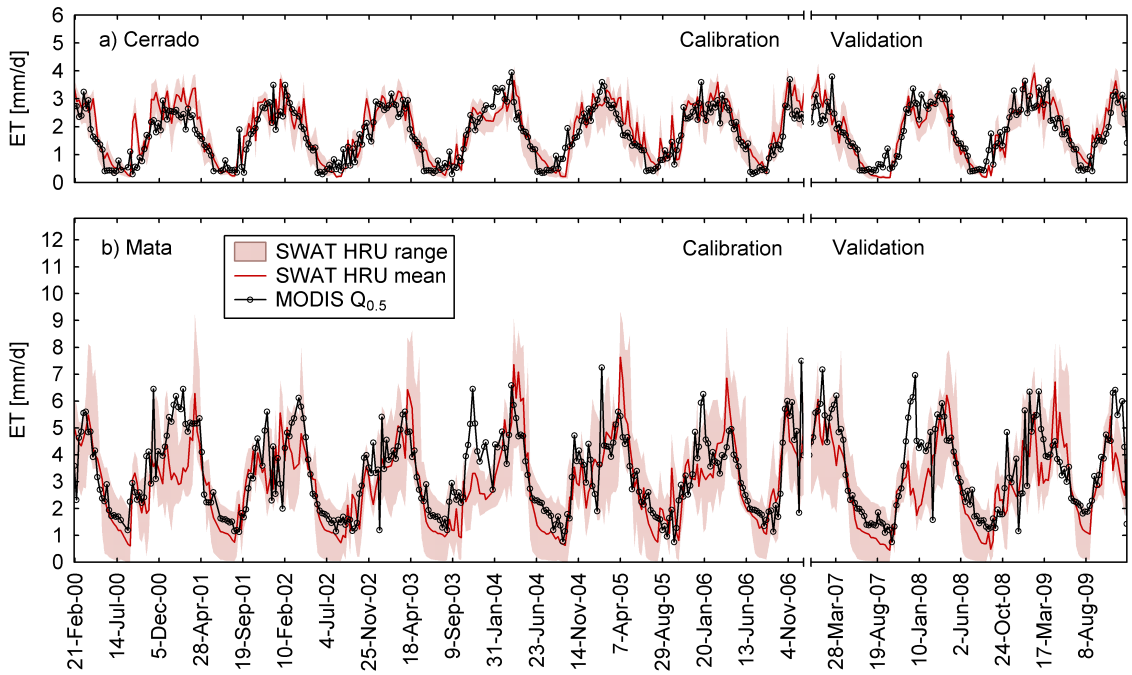

Figure 4.11: Simulated ET (range over HRUs and area weighted HRU mean) for (a) Cerrado and (b) Mata compared to the corresponding MODIS median.

April), where SWAT simulates highest ET values, would leave more water for ET during dry season.

In contrast, simulated ET for Campo and Cerrado were in good accordance with MODIS. Between Campo and Cerrado, the ET parameter values differ only for *CN2* and *GSI*, causing a slightly higher ET for Cerrado. Overall, it can be stated that the modified SWAT model performs satisfactorily and is able to reflect phenology and transpiration patterns of perennials and trees in the study area. To the authors' best knowledge, this is the first study in the field of watershed modeling that evaluated the model capability to simulate vegetation dynamics providing correlation-based model performance measures for LAI and ET.

In a last step, the model was proved for its ability to simulate streamflow, which is fundamental for nearly all SWAT watershed applications regardless of the focus of analysis (Gassman et al., 2007). In order to reduce the efforts for model calibration, we focused only on five commonly used streamflow parameters (cf. Table 4.4), which have been proven to be sensitive in the nearby Pipiripau River Basin (Strauch et al., 2012, 2013). For parameter *CH_K2*, the calibrated value (105 mm hr^{-1}) is relatively high representing a high streamflow loss rate to groundwater which is characteristic for influent streams with channel beds typically consisting of sand and gravel (Neitsch et al., 2010). In fact, the sand content of the alluvial sediments of the Torto River was found to be 50-90% according to Franz et al. (2011). However, it is hard to assess the feasibility of such parameter values on the catchment scale. Often, a stream is gaining water in some reaches and losing it in other reaches, while seasonal variations in precipitation patterns, as typically occuring in the study area, can also alter groundwater tables and stream stages and thereby cause changes in the direction of exchange flows (Kalbus et al., 2006). The value of 0.1 for *CH_N2* (Manning's "n") represents natural streams with heavy timber and brush (Chow, 1959) and is, therefore, a reasonable value for reaches of protected natural areas, such as the SMTW, with gallery forests (Mata) along large parts of the river system. The calibrated groundwater delay time (*GW_DELAY*) is 120 days for the main part of the study area (Campo and Cerrado). For the riparian sites, however, covered by Mata, we chose a much smaller value (10 days) to represent the proximity to the groundwater table. The final *CN2* values were increased by 5 units compared to the initial estimates based on Neitsch et al. (2010) in order to reach a better fit to observed peak flows. Note that our stepwise manual calibration approach, which first captured vegetation phenology, followed by evapotranspiration, and then streamflow, is far from identifying optimal parameter values by ignoring the problems of parameter dependence and equifinality (Beven, 1993). If one would aim at identifying near-optimum parameter solutions, calibration needs to be conducted within a comprehensive multi-objective sensitivity analysis and auto-calibration framework. Such a procedure would consider parameter dependence and objective functions for different model outputs (eg. LAI, ET, and streamflow) at the same time and would allow to estimate parameter uncertainty. That, however, was not the aim of this study. Here, it was appropriate to test the modified SWAT model for its ability to reach reasonable model simulations based on physically meaningful parameter settings.

The model performance values for predicting streamflow (Tab. 4.5) can be evaluated as 'good' according to Moriasi et al. (2007), who provided general performance ratings for watershed simulations on a monthly time step.

Table 4.5: SWAT model performance for predicting streamflow in the SMTW.

	Streamflow, daily [monthly] resolution	
	Calibration (00-06)	Validation (91-99)
NSE	0.65 [0.79]	0.57 [0.66]
R^2	0.67 [0.78]	0.57 [0.67]
PBIAS	-2.7	5.9

However, as shown in Figure 4.12, the model fails to accurately predict peak flows. This might be attributed to the large uncertainties associated with the rainfall input data. Strauch et al. (2012) have shown that a few point measurements may not adequately represent catchment rainfall in that region. Heavy rainfalls are mostly related to small convective cells, whose spatio-temporal distribution is highly variable. Given the catchment rainfall used in this study (also shown in Fig. 4.12), the simulated peak flows can be considered as plausible, whereas several measured peak flows, especially in the beginning of the validation period, can hardly be explained by measured rainfall. Furthermore, the reservoir system (Santa Maria – Torto) may strongly affect streamflow at the watershed outlet. Due to the lack of data, we simply assumed a constant reservoir outflow (Table 4.1) in our simulations. Nevertheless, it is shown that the modified SWAT version is able to simulate streamflow reasonably well.

Figure 4.12: Observed vs. simulated daily streamflow in calibration (2000-2006) and validation period (1991-1999) in the SMTW.

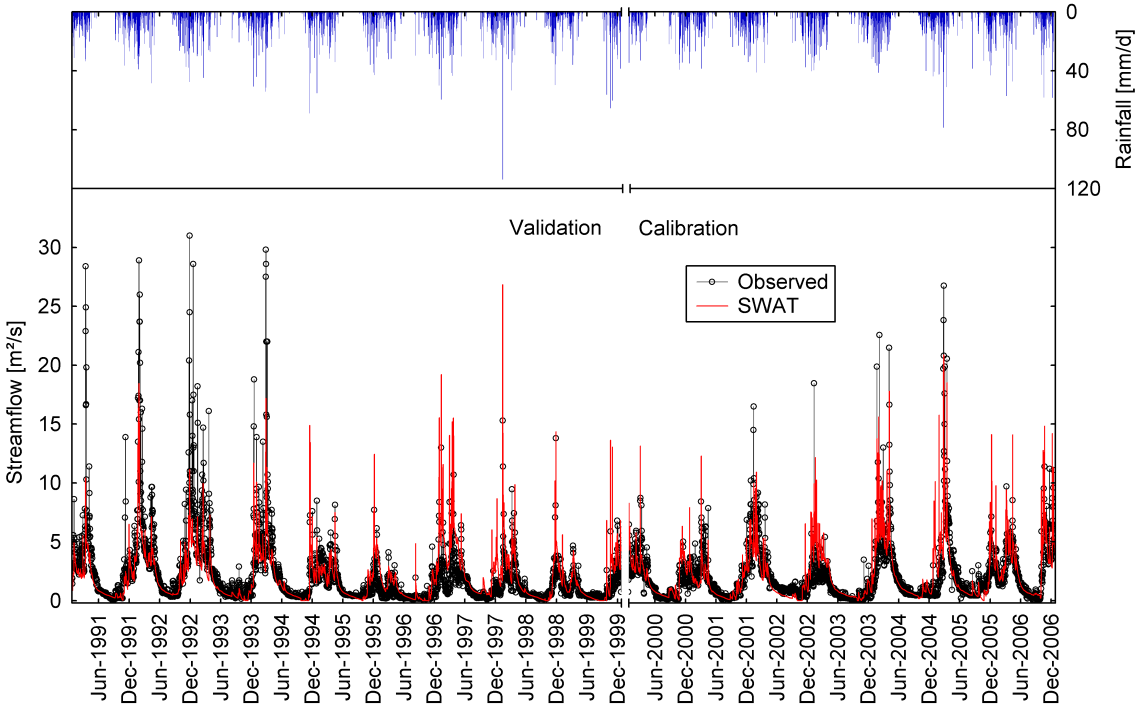

4.3.3 Added value of the modified plant growth module

A sound inference of the added value of the plant growth module modification is only possible by comprehensively testing the model in other tropical regions and against other approaches to represent perennial tropical vegetation in SWAT. This would exceed the scope of this study, but we tested at least the default version of SWAT, where fixed "kill" and "plant" dates must be defined in the management schedule to allow growing cycles in each simulation year.

In general, it was found that rather stable phenological cycles can be reflected satisfactorily by defining adequate "kill" and "plant" dates (Fig. 4.13). However, due to the fact that the minimum LAI cannot be considered, ET was underestimated during dry season (Fig. 4.14). Although there were no considerable effects on streamflow (due to the constant reservoir minimum outflow), this represents a model structural failure, which might be more influential in other regions. Varying lengths of dry seasons could be better reflected using the modified plant growth module (Fig. 4.15), which was to expect considering the start of growing cycles is dynamically coupled to simulated soil moisture and hence based on a physical premise.

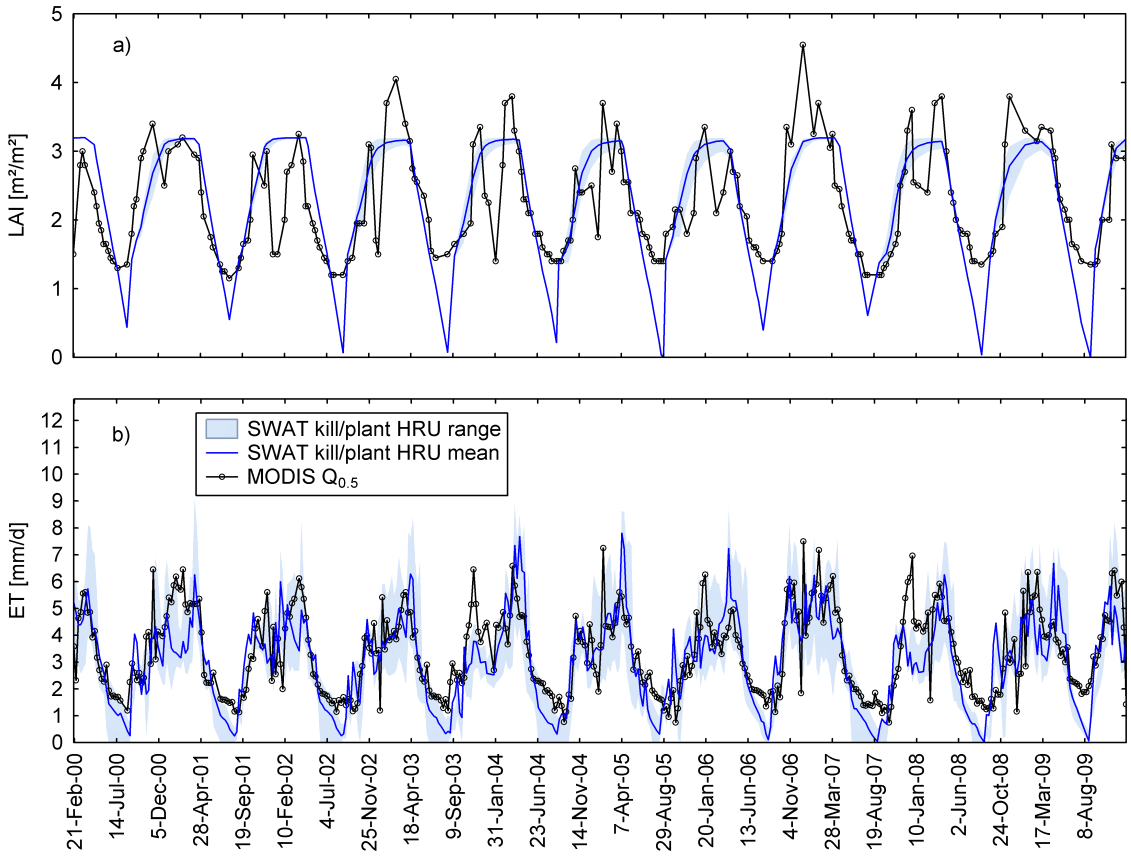

Figure 4.13: Simulated LAI (a) and ET (b) with its range over HRUs and the area weighted HRU mean for Mata using the default SWAT version (fixed "kill" and "start" dates) compared to the corresponding MODIS estimations. The simulated LAI drops to zero in each year (not obvious in the figure due to averaging over 8-day intervals).

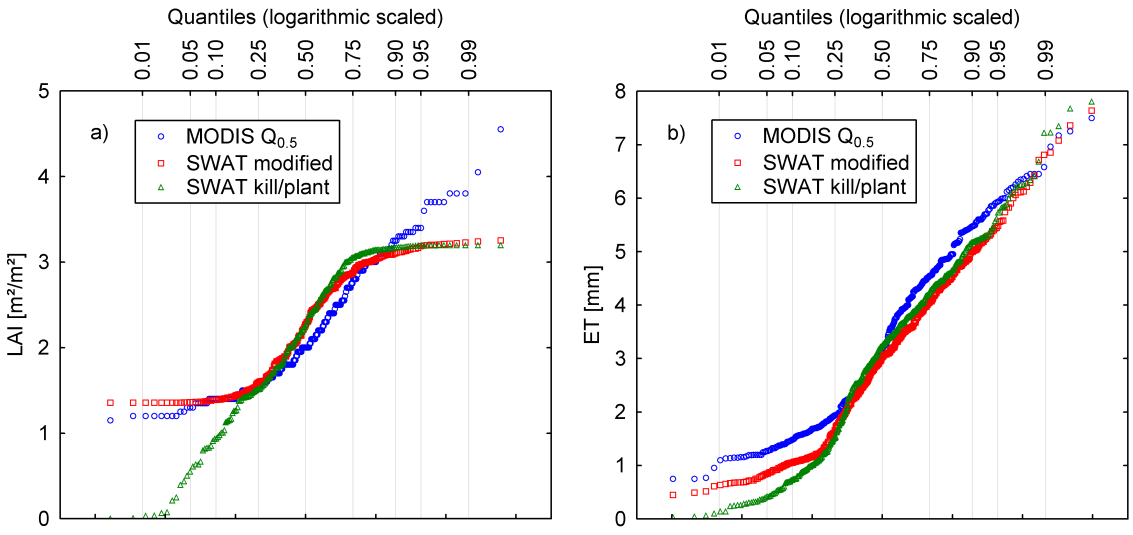

Figure 4.14: Quantile plots of average LAI (a) and ET (b) estimations for Mata in period 2000-2009 derived from (i) MODIS, (ii) the modified SWAT version for the tropics, and (iii) the SWAT default version using fixed "kill" and "start" dates.

Last but not least, the SWAT default version cannot be used for studies focused on biomass production of tropical perennials because likewise to LAI, the simulated biomass is reset to zero each year along with the "kill" operation (Fig. 4.16).

Wagner et al. (2011) defined an artificial dormancy period in the source code for their model application in India. With that, it was possible to account for the minimum LAI

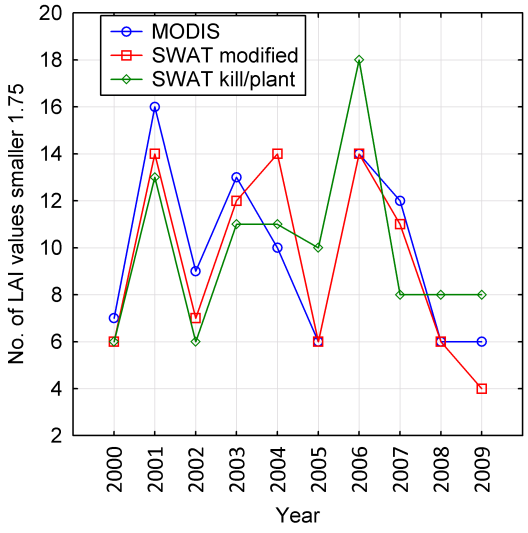

Figure 4.15: Number of LAI values smaller than 1.75 for Mata (indicating variable dry season length) for each year of period 2000-2009 derived from (i) MODIS, (ii) the modified SWAT version for the tropics, and (iii) the SWAT default version using fixed "kill" and "start" dates. The sum of the yearly absolute deviations from MODIS over the whole period is 26 for the default version, while it is only 13 for the modified model.

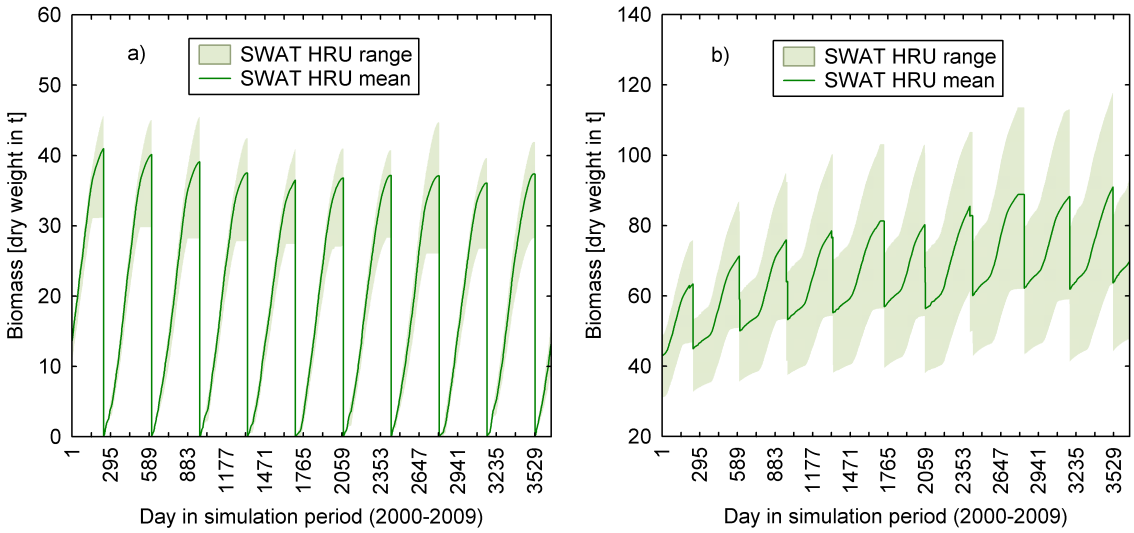

Figure 4.16: Daily biomass simulation for Mata in period 2000-2009 using (a) the SWAT default version with fixed "kill" and "start" dates and (b) the modified SWAT version for the tropics. Both models are not calibrated for biomass, but the figure shows the principal model behavior for the different approaches. Likewise to LAI, biomass is reset to zero each year along with the "kill" operation of the default model, while wooden biomass is stored and accumulated in the modified version.

and the accumulation of wooden biomass. However, it is still a static approach using a fixed dormancy period for each year and it requires programming skills (source code adaptation) that many users might not have. The different approaches are summarized in a qualitative comparison in Table 4.6, which depicts the advantages of the modified plant growth module presented in this study.

Table 4.6: Comparison of approaches representing perennial tropical vegetation in SWAT.

	Fixed "kill/plant" dates (SWAT2009)	Fixed dormancy (Wagner et al., 2011; SWAT2009)	Modified plant growth module (SWAT2009)
User settings	"kill" and "plant" in mgt-files corresponding to the mean greening onset date	Adequate definition of a mean dormant period in the source code (for many users not applicable)	Not necessary, but FR_{AWC} (crop.dat) and transition period (sub-files) can be adjusted
Varying greening onset dates	Can be partly reproduced, but not before „plant" date (later onset may be captured by water stress[a])	Can be partly reproduced, but not within dormant period (later onset may be captured by water stress[a])	Can be reproduced[a]
LAI decline	Linear towards zero	Linear towards zero (*ALAI_MIN* when dormancy is reached)	Sigmoidal to *ALAI_MIN*
Biomass	Reset to zero each year	Storage of wooden biomass	Storage of wooden biomass

[a]except for regions where the LAI is lower in wet season due to decreased radiation (Poulter and Cramer, 2009)

4.4 Conclusions

With this study, we propose changes in the SWAT plant growth module for improved simulation of perennial vegetation in tropical watersheds with distinct dry and wet seasons. The main change of the new module refers to the implementation of a soil moisture threshold that automatically triggers new growing seasons for perennials during the transition from dry to wet season. Furthermore, the LAI decline rate has been modified to a logistic function which provides a sigmoidal decrease towards the minimum LAI, which cannot be considered by the default version due to the absence of a dormant period. The "fixed dormancy" approach of Wagner et al. (2011) was a step in the right direction, but it was still a static approach not accounting for variable dry season lengths and not applicable for other SWAT users without changing the model code.

With the modified plant growth module, we provide a ready to use version, which was successfully tested for the Santa Maria - Torto watershed in Central Brazil on the basis of MODIS data for LAI and ET. It can be assumed that the changed plant growth module leads to improved SWAT simulations also in other tropical regions, especially in the outer tropics which are characterized by distinct seasonal variations in precipitation. The majority of the tropics experiences dry and wet seasons by either tropical savanna (Aw) or tropical monsoon climate (Am). This seasonality, however, depends mostly on latitude and can vary in terms of timing and the duration of dry and wet seasons. With the new model parameters introduced in this study, it should be possible to account for these variations. Model parameters $TRAMO_1$ and $TRAMO_2$ can be used to coarsely adjust the timing by defining the starting and ending month of the transition period from dry to wet season, in which then parameter FR_{AWC} (fraction of available water capacity when growing season is triggered) can be used for finer adjustments. However, the closer one gets to the equator, the shorter and less distinct are dry seasons (McGregor and Nieuwolt, 1998) leading to smaller phenological variations throughout the year. Equatorial evergreen rainforests (Af), finally, might not experience a seasonality at all. Smaller variations in LAI can be represented in SWAT by smaller differences between maximum and minimum LAI ($BLAI$ and $ALAI\_MIN$). Hence, the modified plant growth module might be applicable to large parts of the tropics. However, this must be proven by other case studies in different tropical climates.

The implementation of a logistic function which considers the minimum LAI should be seen as a general improvement, independent of whether the study area is located in the tropics or not. With this, the LAI of trees and perennials is not allowed to fall to zero before entering dormancy. Moreover, a sigmoidal LAI decline (instead of a linear) can be considered as more realistic also for annual plants, e.g. agricultural crops.

The study has also shown that remote sensing based data, such as MODIS, can serve as useful reference data to calibrate and validate the model regarding vegetation dynamics, even if filtering or smoothing techniques might be still necessary to correct cloud-contaminated data. Here, we applied the 'Best Index Slope Extraction' algorithm, with which most of the high-frequency noise could be eliminated for MODIS LAI.

Finally, the modified SWAT model was successfully calibrated for streamflow. The resulting parameter values were derived from a simple manual calibration procedure, which

was sufficient to check model plausibility in this study. Manual calibration helps to better understand model processes and parameter sensitivity (Arnold et al., 2012). However, in combination with an automatic approach, better and more robust model results including uncertainty estimations should be feasible. Future SWAT auto-calibration procedures should therefore not only consider gauge data, such as streamflow or loads of nutrients or sediments, but also at the same time spatial data on vegetation (LAI, ET). This is still missing in current model applications.

Good or satisfactory streamflow predictions might be possible even without any improvement of the plant growth module, since SWAT can probably be seen as one of the models that Kirchner (2006) described as "parameter-rich models that may succeed as mathematical marionettes, dancing to match the calibration data even if their underlying premises are unrealistic". Due to the process-based model changes, it was possible to reasonably account for seasonal vegetation dynamics and thus evapotranspiration, which is an important part of the hydrologic cycle. This study should therefore be considered as a crucial step towards more realistic SWAT model applications for tropical watersheds which include perennial vegetation, such as forests or savannas.

Acknowledgements

The study is part of the project IWAS-ÁGUA DF, which is funded by the German Ministry of Education and Science (BMBF) in scope of the initiative 'Excellent research and innovation in the New Länder'(FKZ: 02WM1166 and 02WM1070).

5 Summarizing discussion and conclusion

This dissertation presents three case studies using the SWAT model for meso-scale catchments in the *Distrito Federal*, Central Brazil. Each of the studies had a different focus, but can be integrated into the workflow presented in Figure 1.2, which includes technical steps relevant for utilizing the SWAT model in general. Therefore, central findings and limitations of the case studies and their implications for future research are discussed in an integrative manner with reference to each step of the modeling workflow.

5.1 Model setup

In general, data availability in the DF can be evaluated as good. For both watersheds, the Pipiripau and the Santa Maria / Torto watershed, it was possible to setup the SWAT model using the available data, even though data constraints often hamper the use of SWAT in Brazil (Garbossa et al., 2011). However, for precipitation, which is the key driver of hydrological models, the amount of available information appeared to be insufficient to represent highly variable spatio-temporal rainfall pattern, as they are typical for the model region. This shortcoming was addressed by generating an ensemble of four different precipitation datasets to be used as model input (Chapter 2). As a consequence, four different SWAT (rain input) models were setup and applied to the Pipiripau River Basin. The approach can be easily transferred to other data scarce regions and turned out to be advantageous in several respects for the modeling workflow as disscussed in more detail in sections 5.2 and 5.4.

A further important issue of input data uncertainty which was not explicitly tackled in this thesis refers to soil physical properties (e.g. bulk density, awailable water capacity, saturated hydraulic conductivity). At the time of conducting the studies, measured information on these properties was not available for the soils in the DF. As a workaround, pedotransfer functions (PTFs) were applied to derive unknown soil properties from other, available soil information, such as texture, organic carbon content and chemical properties. Although the PTFs used in the case studies were developed for tropical soils (e.g. Benites et al., 2007; Tomasella and Hodnett, 2004), large uncertainties remain regarding their accuracy and reliability. Recently, Lima et al. (2013) provided a database on measured soil hydraulic characteristics based on a comprehensive sampling of a wide range of soil types in the DF region. Data such as this might substantially help to define more reliable initial values and calibration ranges, and thus to reduce this source of uncertainty in future SWAT applications for the DF.

5.2 Model calibration

Model calibration, the process of adjusting parameter values to fit model outputs (e.g. streamflow predictions) to measured data, is a key challenge in watershed modeling. In their comprehensive review on SWAT model applications in Brazil, Garbossa et al. (2011) reported that model performance was poor for most of the studies when evaluating the model outputs on a daily basis, irrespective of the size of the watersheds. In this thesis, the SWAT model was calibrated for streamflow and sediment load (Chapters 2 and 3) as well as for Leaf Area Index (LAI) and evapotranspiration (ET) of perennial vegetation (Chapter 4). The model generally performed well in predicting daily streamflow, regardless of whether the original precipitation gauge data was used as input or other reasonably derived datasets. This showed that - to some degree - model calibration can compensate differences in input assumptions (precipitation datasets) which could not be defined as true or false due to the lack of data. This also implicates that in case of uncertain input data, one has to deal with a larger uncertainty of calibrated (best-fit) parameter values. Calibrated parameter values varied remarkably across the different rain input models. Therefore, the input ensemble approach should be also applied in scenario applications as it was done in the BMP scenario study (Chapter 3).

A further central finding regarding precipitation uncertainty (Chapter 2) was the fact that combining the model outputs (streamflow) of each of the rain input models can significantly improve the predictions. The simple arithmetic mean across the ensemble (ensemble mean) outperformed each individual model prediction as indicated by higher performance metrics (Nash-Sutcliff Efficiency (NSE) and R^2). By using Bayesian Model Averaging (BMA), one can infer the probability of each rain input model being the best streamflow predictor given the observations. It was shown that the resulting weighted model average (BMA mean) and the according BMA uncertainty estimation can be superior over simple ensemble combination methods, but not necessarily for all flow conditions (e.g. dry season flow uncertainty was reproduced more realistically by autocalibration uncertainty intervals). Literature provides many examples for the benefits from using ensembles in hydrological modeling, mostly for improved and more reliable short-term flood forecasts (e.g. Cloke and Pappenberger, 2009; Georgakakos et al., 2004; Wu et al., 2011) or - when used for long-term simulations - for considering model structural uncertainties (e.g. Franz et al., 2010; Viney et al., 2009; Zhang et al., 2009). However, to the author's best knowledge this was the first time that precipitation (input) uncertainty was addressed by ensemble methods for enhancing long-term hydrologic simulations. Pluntke et al. (2014) adopted this approach for a catchment in the Ukraine and confirmed its usefulness in case of rare meteorological data.

Even though ensemble combination also improved the predictions of daily sediment loads (Chapter 3), it was not possible to achieve a satisfactory model performance (NSE of 0.34). The problems encountered during sediment calibration showed, in first instance, how essential reliable reference data are. In absence of measured data, daily sediment loads (to be used as model reference) were derived using a rating-curve method which is highly error-prone (e.g. Walling, 1977). Moreover, since soil erosion and subsequent transport of sediment is strongly tied to heavy rainfalls, its prediction in high resolution

(e.g. days) is only reasonable with high-quality precipitation input data. Mismatches between single peaks of measured rainfall and measured runoff, however, showed that the available rainfall datasets for the Pipiripau River Basin are hardly appropriate to predict daily sediment transport. Such a failure cannot be solved by ensemble combination either.

While for the Pipiripau River Basin SWAT was calibrated for streamflow and sediments using an automated approach (SUFI-2, Abbaspour et al., 2004), model calibration for LAI, ET, and streamflow was done manually for the Santa Maria/Torto Watershed (Chapter 4). In general, automated or semi-automated calibration approaches are preferable over calibration solely based on manual trial-and-error adjustments, since they allow for a less subjective and more comprehensive search within the parameter space. In consequence, automated approaches can identify multiple parameter sets with similar model performance ("equifinality") and thus can be used to estimate parameter uncertainty (Beven, 1993). SUFI-2 has proven to be efficient and useful in this context (Chapters 2 and 3), as also reported by numerous other SWAT applications (among them the comparative study of Yang et al., 2008). In contrast, the manual procedure used for the Santa Maria/Torto model could not identify optimal parameter values and their uncertainty ranges, but this was also out of the scope of the study. There, the innovative value lies in model delevopment as discussed in the next section. However, what can be learned from this study is that SWAT can be also calibrated for ET and LAI in high temporal resolution (eight day intervals), after appropriately processing (e.g. filtering) readily available satellite data as provided by MODIS. Future SWAT applications should make use of this potential because model reliability in terms of process consistency can substantially increase when not only the output of interest (usually streamflow and/or pollutant loads) is considered in calibration, but also spatially distributed data on plant growth and evapotranspiration. This, however, raises further issues on how to integrate different calibration objectives at different spatial scales (HRUs, sub-basin, watershed) into coherent auto-calibration schemes. Such schemes must account for parameter dependencies within and among the objectives in order to further reduce model uncertainty.

5.3 Source code adaptation

In case the adjustment of parameters is not enough to ensure a consistent and reasonable simulation of processes, the failure is most likely related to wrong model assumptions. This typically occurs when the model is used for conditions it was neither designed nor approved for. Although SWAT has proven to reasonably simulate eco-hydrological processes across different scales and for a wide range of conditions (Gassman et al., 2007), model applications in this thesis have revealed shortcomings that required adaptation of the source code.

It was found that the model's assumptions for simulating perennial plant growth are not transferable to tropical regions, since there the daylength-driven dormancy approach cannot be used to reflect seasonal dynamics of vegetation. Therefore, the structural changes presented in Chapter 4 of this thesis might be seen as a fundamental model improvement. By considering simulated soil moisture development to initialize annual growing cycles, a more process-based approach could be introduced given the fact that tropical plant phe-

nology is usually driven by seasonal precipitation pattern. Furthermore, a logistic function for LAI decline toward a user-defined minimum value was implemented. Test runs in the savanna-dominated Santa Maria/Torto watershed showed that the modified model can sufficiently reflect temporal vegetation dynamics in the Cerrado region. However, due to the introduced model parameters FR_{AWC} (fraction of available water capacity at which a growing cycle is initiated) and $TRAMO_1$ and $TRAMO_2$ (beginning and ending month of the transition period in which FR_{AWC} is active), the modified plant growth module should also be transferable to other tropical regions.

The model code was further modified for simulating Barraginhas (Chapter 3), which are a characteristic sediment control practice for this region. Sediment retention basins in SWAT are treated as ponds (Waidler et al., 2011). However, routing all horizontal flows, i.e. surface, lateral and groundwater flow, and respective loads through ponds would have been an improper way to simulate Barraginhas. Due to their small size of approximately 35 m^3, it was convenient to route only the surface runoff through these retention basins.

These examples illustrate how important it is to have access to the model code. The open source philosophy of SWAT enables users to adjust the model structure to region-specific conditions. This is especially important for watershed model applications that are supposed to support decision making. If a model application is justified only by showing good matches of measured streamflow and/or pollutant loads at the watershed outlet, there remains a high risk of misrepresentation of internal processes. Model errors might compensate each other in such a way that the overall result appears reasonable compared to measured data. However, in the scenario case (e.g. considering a changed land use), these models likely lead to flawed predictions and wrong implications for policy.

5.4 Scenario simulation

The main objective of the thesis was to utilize the SWAT model for assessing the impact of land management changes on the water resources of the intensively cropped Pipiripau River Basin where conflicts arise among agricultural and urban water uses. The results of the scenario runs (presented and discussed in Chapter 3) indicate that structural BMPs, such as terraces and sediment retention basins ('Barraginhas') might significantly reduce sediment loads, while not adversely affecting water yield in the Pipiripau River. In contrast, introducing an economically viable multi-diverse crop rotation system as an alternative to the predominating soybean and corn monocultures led to strongly decreased streamflow predictions during dry season due to increasing irrigation demands.

Based on estimated costs for BMP implementation (BRASIL, 2010), the simulated effects could be related to the economic effort and by following the precipitation ensemble approach of the previous Pipiripau study (Chapter 2) it was also possible to provide uncertainty ranges for the BMP effectiveness. As an example, a one-million-USD investment for implementing Barraginhas was predicted to reduce average sediment loads of the Pipiripau River by 18 to 26% depending on which rain input model was used. This range is similar to the predicted effect of terraces (16 - 23%). However, while this was the maximum effect for Barraginhas (assuming the extreme scenario with ten Barraginhas per road kilometer), the maximum effect for terraces (when installed on total farmland) was a sediment

load reduction of 27 to 37% for an investment of approximately 1.75 million USD. The strongest reduction of average sediment load was predicted for a combined implementation of Barraginhas and terraces (each in maximum), ranging from 34 to 48%, but this was related with substantially decreased cost-effictiveness (2.75 million USD).

Even though the modeling approach presented here accounted, to some extent, for uncertainty in precipitation data, important other sources of uncertainty could not be addressed. Most notably is model structural uncertainty regarding the representation of BMPs, which is based on empirical studies in US watersheds. For example, to represent terraces the SCS curve number was reduced by 5 units and the USLE practice factor was reduced from 0.5 (representing contour farming or terraces in poor condition) to 0.12. These settings were based on values presented in literature (e.g. Arabi et al., 2008; Tuppad et al., 2010a; Wischmeier and Smith, 1978). However, the validity of these empirical values has to be questioned for the Pipiripau River Basin or tropical regions in general. The presented results must therefore be treated with caution, although they may currently constitute the best estimation possible. The only way to further increase model reliability is to conduct empirical studies in the region at hand. The Pipiripau River Basin is ideally suited for this purpose since BMPs (whatever these may be) will be implemented in near future due the pilot program "Produtor de Água". This, however, requires stronger efforts in monitoring, i.e. (1) long-term sampling of sediment concentration at several stream gauges and in appropriate intervalls (at least weekly as recommended by Johnes (2007) for sampling Phosphorus which is closely linked to sediment transport), (2) on-site sediment sampling campaigns, and (3) experiments using standardized Wischmeier plots (Wischmeier and Smith, 1978) to regionally adapt the factors of the USLE, which is in a modified version also used in SWAT to predict soil erosion, not to mention the need for (4) a denser rain gauge network.

The BMP scenario study did not consider the shortcomings in simulating perennial plant growth. In fact, the insufficient model behavior for Cerrado was just identified at that moment and solved later in the Santa Maria / Torto case study where reference data for vegetation phenology could be used. However, since perennial vegetation covers less than 25% of the Pipiripau catchment area, the model error due to this problem should be relatively low.

Nevertheless, future SWAT scenario applications in tropical regions should include the plant growth modification to minimize model structural errors in the catchment water balance. Future model applications in the DF should, moreover, focus on two further scenario aspects, urbanization and climate change. Climate change impact studies can be easily conducted based on recently available global multi-model ensemble projections analyzed for the DF (Borges et al., 2014b) or upcoming regional climate scenarios due to statistical downscaling of ECHAM5 projections (Borges et al., 2014a). In contrast, simulations considering the effects of urbanization would not lead to reasonable results by using SWAT alone. In urbanized areas, the Storm Water Management Model (SWMM) could be utilized to simulate urban drainage through a network of pipes, channels and storage/treatment devices (Gironás et al., 2010), providing that recently started efforts in high resolution precipitation monitoring in urban areas of the DF will continue. These urban areas, modeled by SWMM, could be nested as sub-basins into a broader SWAT

model framework for the whole Lake Paranoá Basin including Brasília and surrounding urban as well as agricultural and protected natural areas (e.g. the Santa Maria / Torto watershed in the north of Brasília). In such a way, changes in the Paranoá Basin (densification and expansion of urban areas) could be analyzed in terms of both, (1) stormwater runoff and pollutant loads in urbanized sub-basins and (2) - when aggregated to daily times steps and linked to corresponding SWAT sub-basins - long-term total water yield and pollutant loads as input into the lake. The development of such a process-based modeling framework and follow-up scenario analyses of water and pollutant fluxes for the whole Lake Paranoá Basin is a very challenging task. However, since population growth and urbanization in this basin are major threats for future water supply security, strong research and monitoring efforts remain justified.

5.5 Conclusion

In this thesis, the SWAT model was utilized to simulate hydrological processes and sediment transport in response to land management changes. Due to impact analysis, it was shown that structural Best Management Practices (BMPs), in particular terraces and Barraginhas, might substantially reduce sediment loads while maintaining water yield. The quantified effects of these measures in combination with estimated costs of implementation should be useful for the regional water supplier CAESB to identify potentials for saving water treatment costs, i.e. costs for removing suspended sediments and particle bound nutrients. The results should be especially useful for the program "Produtor de Água" in order to effectively allocate BMPs. It is still under discussion which BMPs shall finally receive support in the Pipiripau River Basin due to "payments for ecosystem services". Based on the results of this thesis, terraces and Barraginhas can be recommended. However, for a combined implementation, one must consider decreasing cost-effectiveness with increasing level of implementation. Any measures that are related with an increase of irrigation, in contrast, should be rejected to maintain environmental flow during dry season. Even if land cover and land use is only one aspect of IWRM among many, this work showed yet again the importance of this issue for future water management strategies in the DF.

Although urgent research questions were tackled concerning the impact of land management practices on water resources, the true value of this thesis lies much deeper than that. Methods were developed that explicitly address region-specific challenges. That is, (1) an ensemble approach to deal with uncertain precipitation input data and (2) the modification of the SWAT plant growth module to better reflect seasonal dynamics of tropical perennial vegetation. Both methods contribute toward more reliable model predictions and both methods are transferable to other regions with similar problems and characteristics, i.e. scarcity of precipitation input data or the presence of perennial land cover (forest, savanna, grassland, horticultures) in tropical areas. Although several sources of uncertainty remain that were not addressed (e.g. BMP process description), the thesis provided critical insights into and practical solutions for challenges crucial to sound watershed model applications.

References

Abbaspour, K. C., Johnson, C., van Genuchten, M., 2004. Estimating Uncertain Flow and Transport Parameters Using a Sequential Uncertainty Fitting Procedure. Vadose Zone Journal 3, 1340–1352.

Abbaspour, K. C., Yang, J., Maximov, I., Siber, R., Bogner, K., Mieleitner, J., Zobrist, J., Srinivasan, R., 2007. Modelling hydrology and water quality in the pre-alpine/alpine Thur watershed using SWAT. Journal of Hydrology 333 (2-4), 413–430.

ANA, 2009. Atlas Brasil: Abastecimento Urbano de Água - Resultados por Estado, Volume 2. Tech. rep., Agência Nacional de Águas, Ministério do Meio Ambiente.

Andréassian, V., Perrin, C., Michel, C., 2001. Impact of imperfect rainfall knowledge on the efficiency and the parameters of watershed models. Journal of Hydrology 250 (1-4), 206–223.

Arabi, M., Frankenberger, J. R., Engel, B., Arnold, J. G., 2008. Representation of agricultural conservation practices with SWAT. Hydrological Processes 22, 3042–3055.

Arabi, M., Govindaraju, R. S., Engel, B., Hantush, M. M., 2007a. Multiobjective sensitivity analysis of sediment and nitrogen processes with a watershed model. Water Resources Research 43 (6), W06409.

Arabi, M., Govindaraju, R. S., Hantush, M. M., 2006. Cost-effective allocation of watershed management practices using a genetic algorithm. Water Resources Research 42 (10), W10429.

Arabi, M., Govindaraju, R. S., Hantush, M. M., 2007b. A probabilistic approach for analysis of uncertainty in the evaluation of watershed management practices. Journal of Hydrology 333 (2-4), 459–471.

Arnold, J. G., Fohrer, N., 2005. SWAT2000: current capabilities and research opportunities in applied watershed modelling. Hydrological Processes 19 (3), 563–572.

Arnold, J. G., Gassman, P. W., White, M. J., 2010. New developments in the SWAT ecohydrology model. In: Proc. 21st Watershed Technology Conf.: Improving Water Quality and Environment. ASABE Publication No. 701P0210cd. St. Joseph, Mich.: ASABE. ASCE.

Arnold, J. G., Moriasi, D., Gassman, P. W., Abbaspour, K. C., White, M. J., Srinivasan, R., Santhi, C., Harmel, R., van Griensven, A., Van Liew, M. W., Kannan, N., Jha, M. K.,

2012. Swat: Model Use, Calibration, and Validation. Transactions Of The ASABE 55 (4), 1491–1508.

Arnold, J. G., Srinivasan, R., Muttiah, R., Williams, J., 1998. Large area hydrologic modeling and assessment part I: Model development. Journal of the American Water Resources Association 34 (1), 73–89.

Aster, S., Vasyukova, E., Ripl, K., Kuse, B., 2010. Developing an integrated water resources management (IWRM) concept for the Capital Brasília. Gwf-Wasser/Abwasser 151, 52–57.

Atkinson, P. M., Jeganathan, C., Dash, J., Atzberger, C., 2012. Inter-comparison of four models for smoothing satellite sensor time-series data to estimate vegetation phenology. Remote Sensing of Environment 123, 400–417.

Bárdossy, A., Das, T., 2008. Influence of rainfall observation network on model calibration and application. Hydrology and Earth System Sciences 12 (1), 77–89.

Beck, P. S. A., Atzberger, C., Hø gda, K. A., Johansen, B., Skidmore, A. K., 2006. Improved monitoring of vegetation dynamics at very high latitudes: A new method using MODIS NDVI. Remote Sensing of Environment 100 (3), 321–334.

Benites, V., Machado, P., Fidalgo, E., Coelho, M., Madari, B., 2007. Pedotransfer Functions for Estimating Soil Bulk Density from Existing Soil Survey Reports in Brazil. Geoderma 139, 90–97.

Beven, K. J., 1993. Prophecy, reality and uncertainty in distributed hydrological modelling. Advances in Water Resources 16 (1), 41–51.

Beven, K. J., 2001. Rainfall-Runoff Modelling. John Wiley & Sons, Ltd, Chicester.

Beven, K. J., 2012. Rainfall-Runoff Modelling: The Primer. Wiley.

Bicalho, C. C., Koide, S., Lima, J. E. F. W., 2006. Estudo preliminar do fluxo de sedimentos em suspensão na Bacia do Rio Descoberto. In: VII Encontro Nacional de Engenharia de Sedimentos. Porto Alegre, pp. 1–17.

Biswas, A. K., 2004. Integrated Water Resources Management: A Reassessment. Water International 29 (2), 248–256.

Borah, D. K., Yagow, G., Saleh, A., Barnes, P. L., Rosenthal, W., Krug, E. C., Hauck, L. M., 2006. Sediment and nutrient modeling for TMDL development and implementation. Transactions Of The ASABE 49 (4), 967–986.

Borchert, R., 1994. Soil and stem water storage determine phenology and distribution of tropical dry forest trees. Ecology 75, 1437–1449.

Borges, P. d. A., Barfus, K., Weiss, H., Bernhofer, C., 2014a. Statistical downscaling of daily mean temperature and precipitation for ECHAM5 scenarios in Central Brazil, In preparation.

Borges, P. d. A., Barfus, K., Weiss, H., Bernhofer, C., 2014b. Trend analysis and uncertainties of mean surface air temperature, precipitation and extreme indices in CMIP3 GCMs in Distrito Federal, Brazil. Submitted to Environmental Earth Sciences.

Bosch, D. D., Arnold, J. G., Volk, M., Allen, P. M., 2010. Simulation of a Low-Gradient Coastal Plain Watershed Using the SWAT Landscape Model. Transactions Of The ASABE 53 (5), 1445–1456.

Bossa, A., Diekkrüger, B., Igué, A., Gaiser, T., 2012. Analyzing the effects of different soil databases on modeling of hydrological processes and sediment yield in Benin (West Africa). Geoderma 173-174, 61–74.

Bracmort, K., Arabi, M., Frankenberger, J. R., Engel, B., Arnold, J. G., 2006. Modeling Long-Term Water Quality Impact of Structural BMPs. Transactions Of The Asabe 49 (2), 367–374.

BRASIL, 2010. Programa Produtor de Água - Relatório de Diagnóstico Socioambiental da Bacia do Ribeirão Pipiripau. Tech. rep., Agência Nacional de Águas, Nature Conservancy, Empresa de Assistência Técnica e Extensão Rural - DF, Secretaria de Agricultura, Pecuária e Abastecimento do Distrito Federal, Brasília, DF.

Breuer, L., Huisman, J., Willems, P., Bormann, H., Bronstert, A., Croke, B., Frede, H.-G., Gräff, T., Hubrechts, L., Jakeman, A., Kite, G., Lanini, J., Leavesley, G., Lettenmaier, D., Lindström, G., Seibert, J., Sivapalan, M., 2009. Assessing the impact of land use change on hydrology by ensemble modeling (LUCHEM). I: Model intercomparison with current land use. Advances in Water Resources 32 (2), 129–146.

Bucci, S. J., Scholz, F. G., Goldstein, G., Hoffmann, W. A., Meinzer, F. C., Franco, A. C., Giambelluca, T. W., Miralles-Wilhelm, F., 2008. Controls on stand transpiration and soil water utilization along a tree density gradient in a Neotropical savanna. Agricultural and Forest Meteorology 148 (6-7), 839–849.

Bullock, S., Solis-Magallanes, J., 1990. Phenology of canopy trees of a tropical deciduous forest in Mexico. Biotropica 22, 22–35.

Buric, B., Gault, J., 2011. Payment for Environmental Services: First global inventory of schemes provisioning water for cities. Tech. Rep. June, FAO, Natural Resources Management and Environment Department, Land and Water Division.

Burkart, C. S., Jha, M. K., 2012. Site-Specific Simulation of Nutrient Control Policies : Integrating Economic and Water Quality Effects. Journal of Agricultural and Resource Economics 37 (1), 20–33.

CAESB, 2002. SIÁGUA - Sinopse do Sistema de Abastecimento de Água - DF. Tech. rep., Companhia de Saneamento do Distrito Federal, Brasília, DF.

CAESB, 2004. SIÁGUA - Sinopse do Sistema de Abastecimento de Água - DF. Tech. rep., Companhia de Saneamento do Distrito Federal, Brasília, DF.

Campana, N., Monteiro, M., Koide, S., Neto, O., 1998. Avaliação Quantitativa dos Recursos Hídricos Superficiais do Distrito Federal. In: In: MMA/SRH, SEMATEC/DF, IEMA/DF, 1998, Inventário Hidrogeológico e dos Recursos Hídricos Superficiais do Distrito Federal, Relatório Técnico. Brasília.

Carvalho, A. M., 2009. O uso de plantas de cobertura em agroecossistemas no Cerrado. Tech. rep., Embrapa Cerrados, Planaltina DF. http://www.cpac.embrapa.br/noticias/artigosmidia/publicados/149/.

Carvalho, A. M., 2010. Adubação Verde e qualidade do solo no Cerrado. Tech. rep., Embrapa Cerrados, Planaltina DF. http://www.cpac.embrapa.br/noticias/artigosmidia/publicados/284/.

Chaplot, V., Saleh, A., Jaynes, D., 2005. Effect of the accuracy of spatial rainfall information on the modeling of water, sediment, and NO3 N loads at the watershed level. Journal of Hydrology 312 (1-4), 223–234.

Childes, S., 1989. Phenology of nine common woody species in semi-arid, deciduous Kalahari Sand vegetation. Vegetatio 79, 151–163.

Cho, J., Bosch, D. D., Lowrance, R. R., Strickland, T. C., 2009. Effect of Spatial Distribution of Rainfall on Temporal and Spatial Uncertainty of SWAT Output. Transactions Of The ASABE 52 (5), 1545–1555.

Chow, V. T., 1959. Open-channel hydraulics. McGraw-Hill, New York.

Cloke, H., Pappenberger, F., 2009. Ensemble flood forecasting: A review. Journal of Hydrology 375 (3-4), 613–626.

Codeplan, 1992. Mapas Topográficos Plani-altimétricos Digitais do Distrito Federal na escala de 1:10.000. Tech. rep., GDF, Brasília.

Crawford, C. G., 1991. Estimation of suspended-sediment rating curves and mean suspended-sediment loads. Journal of Hydrology 129, 331–348.

Daniel, E. B., Camp, J. V., Leboeuf, E. J., Penrod, J. R., Dobbins, J. P., Abkowitz, M. D., 2011. Watershed Modeling and its Applications : A State-of-the-Art Review. The Open Hydrology Journal 5, 26–50.

Darroch, B. A., Baker, R. J., 1990. Grain Filling in Three Spring Wheat Genotypes: Statistical Analysis. Crop Science 30 (3), 525.

Dawdy, D., Bergmann, J., 1969. Effect of Rainfall Variability on Streamflow Simulation. Water Resources Research 5 (5), 958–966.

Devineni, N., Sankarasubramanian, a., Ghosh, S., 2008. Multimodel ensembles of streamflow forecasts: Role of predictor state in developing optimal combinations. Water Resources Research 44 (9), W09404.

Douglas-Mankin, K., Srinivasan, R., Arnold, J. G., 2010. Soil and Water Assessment Tool (SWAT) Model: Current Developments and Applications. Transactions Of The ASABE 53 (5), 1423–1431.

Duan, Q., Ajami, N. K., Gao, X., Sorooshian, S., 2007. Multi-model ensemble hydrologic prediction using Bayesian model averaging. Advances in Water Resources 30 (5), 1371–1386.

Duncan, M., Austin, B., Fabry, F., Austin, G., 1993. The effect of gauge sampling density on the accuracy of streamflow prediction for rural catchments. Journal of Hydrology 142 (1-4), 445–476.

Easton, Z. M., Fuka, D. R., White, E. D., Collick, A. S., Biruk Ashagre, B., McCartney, M., Awulachew, S. B., Ahmed, A. A., Steenhuis, T. S., 2010. A multi basin SWAT model analysis of runoff and sedimentation in the Blue Nile, Ethiopia. Hydrology and Earth System Sciences 14 (10), 1827–1841.

EMBRAPA, 1978. Levantamento de reconhecimento dos solos do Distrito Federal, Boletim Técnico 53. Tech. rep., Empresa Brasileira de Pesquisa Agropecuária - Embrapa Solos, Rio de Janeiro.

Falkenmark, M., Rockström, J., 2004. Balancing Water for Humans and Nature. The New Approach in Ecohydrology. Earthscan, London.

FAO, 2004. Fertilizer use by crop in Brazil. Tech. rep., Food and Agriculture Organization of the United Nations - FAO, Rome.

Faramarzi, M., Abbaspour, K. C., Schulin, R., Yang, H., 2009. Modelling blue and green water resources availability in Iran. Hydrological Processes 501 (November 2008), 486–501.

Faures, J., Goodrich, D., Woolhiser, D., Sorooshian, S., 1995. Impact of small-scale spatial rainfall variability on runoff modeling. Journal of Hydrology 173 (1-4), 309–326.

Felizola, E. R., Lago, F. P. d. L. S., Galvão, W. S., 2001. Avaliação da dinâmica da paisagem no Distrito Federal. Projeto da Reserva da Biosfera do Cerrado - Fase I. In: Anais X Simpósio Brasileiro de Sensoriamento Remoto, Foz do Iguaçu, 21-26 abril 2001, INPE. Foz do Iguaçu, pp. 1593–1600.

Fortes, P. T. F. O., Oliveira, G. I. M., Crepani, E., de Medeiros, J. S. a., 2007. Geoprocessamento aplicado ao planejamento e gestão ambiental na Área de Proteção Ambiental de Cafuringa, Distrito Federal Parte 1: processamento de imagens. In: Anais XIII Simpósio Brasileiro de Sensoriamento Remoto, Florianópolis, Brasil, 21-26 abril 2007, INPE. pp. 2605–2612.

Franz, C., Makeschin, F., Roig, H. L., Schubert, M., Weiß, H., Lorz, C., 2011. Sediment characteristics and sedimentations rates of the Torto River, 'Planalto Western Central Brazil'. In: XII IWA International Specialised Conference on Watershed and River Basin Management, 11.-16. September 2001, Recife. Vol. 1.

Franz, C., Makeschin, F., Weiß, H., Lorz, C., 2013. Geochemical signature and properties of sediment sources and alluvial sediments within the Lago Paranoá catchment, Brasilia DF: A study on anthropogenic introduced chemical elements in an urban river basin. Science of the Total Environment 452-453, 411–20.

Franz, K. J., Butcher, P., Ajami, N. K., 2010. Addressing snow model uncertainty for hydrologic prediction. Advances in Water Resources 33 (8), 820–832.

Funatsu, B. M., Dubreuil, V., Claud, C., Arvor, D., Gan, M. A., 2012. Convective activity in Mato Grosso state (Brazil) from microwave satellite observations: Comparisons between AMSU and TRMM data sets. Journal of Geophysical Research 117, D16109.

Garbossa, L. H. P., Vasconcelos, L. R. C., Lapa, K. R., Blainski, E., Pinheiro, A., 2011. The use and results of the Soil and Water Assessment Tool in Brazil : A review from 1999 until 2010. In: 2011 International SWAT Conference, June 15-17, Toledo, Spain.

Gassman, P. W., Osei, E., Saleh, A., Rodecap, J., Norvell, S., Williams, J., 2006. Alternative practices for sediment and nutrient loss control on livestock farms in northeast Iowa. Agriculture, Ecosystems & Environment 117 (2-3), 135–144.

Gassman, P. W., Reyes, M., Green, C., Arnold, J. G., 2007. The Soil and Water Assessment Tool: Historical Development, Applications, and Future Research Directions. Transactions Of The ASABE 50 (4), 1211–1250.

Gassman, P. W., Williams, J. R., Benson, V. W., Izaurralde, R., Hauck, L. M., Jones, C. A., Atwood, J. D., Kiniry, J. R., Flowers, J., 2005. Historical Development and Applications of the EPIC and APEX Models. Working Paper 05-WP397. Tech. rep., Center for Agricultural and Rural Development Iowa State University.

GDF, 2012. Plano de Gerenciamento Integrado de Recursos Hídricos do Distrito Federal - PGIRH/DF. Relatório Síntese. Tech. rep., Governo do Distrito Federal, Brásilia, DF.

Georgakakos, K. P., Seo, D.-J., Gupta, H. V., Schaake, J. C., Butts, M. B., 2004. Towards the characterization of streamflow simulation uncertainty through multimodel ensembles. Journal of Hydrology 298 (1-4), 222–241.

Giambelluca, T. W., Scholz, F. G., Bucci, S. J., Meinzer, F. C., Goldstein, G., Hoffmann, W. A., Franco, A. C., Buchert, M. P., 2009. Evapotranspiration and energy balance of Brazilian savannas with contrasting tree density. Agricultural and Forest Meteorology 149 (8), 1365–1376.

Gironás, J., Roesner, L. A., Rossman, L. A., Davis, J., 2010. A new applications manual for the Storm Water Management Model (SWMM). Environmental Modelling & Software 25 (6), 813–814.

Gourley, J., Vieux, B., 2006. A method for identifying sources of model uncertainty in rainfall-runoff simulations. Journal of Hydrology 327 (1-2), 68–80.

Gupta, H. V., Sorooshian, S., Yapo, P. O., 1999. Status of Automatic Calibration for Hydrologic Models: Comparison with Multilevel Expert Calibration. Journal of Hydrologic Engineering 4 (2), 135–143.

GWP, 2000. Integrated Water Resources Management. TAC Background Paper 4. Tech. Rep. 4, Global Water Partnership, Stockholm.

Hernandez, M., Miller, S., Goodrich, D., 2000. Modeling runoff response to land cover and rainfall spatial variability in semi-arid watersheds. Environmental Monitoring and Assessment 64 (1), 285–298.

Hoeting, J. A., Madigan, D., Raftery, A. E., Volinsky, C. T., 1999. Bayesian Model Averaging: A Tutorial. Statistical Science 14 (4), 382–401.

Hoff, H., 2009. Challenges in upland watershed management: the green-blue water approach. In: Garrido, A., Dinar, A. (Eds.), Managing water resources in a time of global change: mountains, valleys and flood plains. Routledge Chapman & Hall, Oxford, pp. 167–190.

Hoffmann, W. A., da Silva Jr, E. R., Machado, G. C., Bucci, S. J., Scholz, F. G., Goldstein, G., Meinzer, F. C., 2005a. Seasonal leaf dynamics across a tree density gradient in a Brazilian savanna. Oecologia 145 (2), 307–16.

Hoffmann, W. A., Franco, A. C., Moreira, M., Haridasan, M., 2005b. Specific leaf area explains differences in leaf traits between congeneric savanna and forest trees. Functional Ecology 19 (6), 932–940.

Hsu, K.-l., Moradkhani, H., Sorooshian, S., 2009. A sequential Bayesian approach for hydrologic model selection and prediction. Water Resources Research 45, W00B12.

Huffman, G. J., Adler, R. F., Bolvin, D. T., Gu, G., Nelkin, E. J., Bowman, K. P., Hong, Y., Stocker, E. F., Wolff, D. B., 2007. The TRMM Multisatellite Precipitation Analysis (TMPA): Quasi-Global, Multiyear, Combined-Sensor Precipitation Estimates at Fine Scales. Journal of Hydrometeorology 8 (1), 38.

IBGE, 2011. Sinopse do Censo Demográfico 2010. Tech. rep., Instituto Brasileiro de Geografia e Estatística, Rio de Janeiro.

Jajarmizadeh, M., Harun, S., Salarpour, M., 2012. A Review on Theoretical Consideration and Types of Models in Hydrology. Journal of Environmental Science and Technology 5 (5), 249–261.

Jakeman, A. J., Letcher, R. A., 2003. Integrated assessment and modelling: features, principles and examples for catchment management. Environmental Modelling & Software 18 (6), 491–501.

Jewitt, G., 2006. Integrating blue and green water flows for water resources management and planning. Physics and Chemistry of the Earth 31 (15-16), 753–762.

Johnes, P., 2007. Uncertainties in annual riverine phosphorus load estimation: Impact of load estimation methodology, sampling frequency, baseflow index and catchment population density. Journal of Hydrology 332 (1-2), 241–258.

Jolly, W. M., Running, S. W., 2004. Effects of precipitation and soil water potential on drought deciduous phenology in the Kalahari. Global Change Biology 10, 303–308.

Justice, C., Townshend, J., Vermote, E., Masuoka, E., Wolfe, R., Saleous, N., Roy, D., Morisette, J., 2002. An overview of MODIS Land data processing and product status. Remote Sensing of Environment 83 (1-2), 3–15.

Kalbus, E., Reinstorf, F., Schirmer, M., 2006. Measuring methods for groundwater, surface water and their interactions: a review. Hydrology and Earth System Sciences 10, 873–887.

Kalin, L., Hantush, M. M., 2006. Hydrologic Modeling of an Eastern Pennsylvania Watershed with NEXRAD and Rain Gauge Data. Journal of Hydrologic Engineering 11 (6), 555–569.

Kirchner, J. W., 2006. Getting the right answers for the right reasons: Linking measurements, analyses, and models to advance the science of hydrology. Water Resources Research 42, W03S04, doi:10.1029/2005WR004362.

Klink, C. A., Machado, R. B., 2005. Conservation of the Brazilian Cerrado. Conservation Biology 19 (3), 707–713.

Knyazikhin, Y., Martonchik, J. V., Diner, D. J., Myneni, R. B., Verstraete, M., Pinty, B., Gobron, N., 1998. Estimation of vegetation canopy leaf area index and fraction of absorbed photosynthetically active radiation from atmosphere-corrected MISR data. Journal of Geophysical Research 103 (D24), 32239–32256.

Koch, H., Grünewald, U., 2009. A Comparison of Modelling Systems for the Development and Revision of Water Resources Management Plans. Water Resources Management 23 (7), 1403–1422.

Krause, P., Boyle, D., Bäse, F., 2005. Advances in Geosciences Comparison of different efficiency criteria for hydrological model assessment. Advances In Geosciences 5, 89–97.

Krysanova, V., Arnold, J. G., 2008. Advances in ecohydrological modelling with SWAT - a review. Hydrological Sciences Journal/Journal des Sciences Hydrologiques 53 (5), 939–947.

Lam, Q., Schmalz, B., Fohrer, N., 2011. The impact of agricultural Best Management Practices on water quality in a North German lowland catchment. Environmental monitoring and assessment 183 (1-4), 351–79.

Lange, M., Doktor, D., 2013. R-Package 'phenex' - Auxiliary functions for phenological data analysis.

Lautenbach, S., Volk, M., Strauch, M., Whittaker, G., Seppelt, R., 2013. Optimization-based trade-off analysis of biodiesel crop production for managing an agricultural catchment. Environmental Modelling & Software 48, 98–112.

Li, J., Heap, A. D., 2008. A Review of Spatial Interpolation Methods for Environmental Scientists. Tech. rep., Geoscience Australia, Record 2008/23.

Lima, J. E. F. W., 2010. Modelagem numérica do fluxo da água no solo e do escoamento de base em uma bacia experimental em área agrícola no Cerrado (Distrito Federal). Diss. In: PTARH.TD 08/10, Departamento de Engenharia Civil e Ambiental, Universidade de Brasília, Brasília-DF. Phd, Universidade de Brasília.

Lima, J. E. F. W., da Silva, C. L., Oliveira, C. A. d. S., 2001. Comparação da evapotranspiração real simulada e observada em uma bacia hidrográfica em condições naturais de cerrado. Revista Brasileira de Engenharia Agrícola e Ambiental 5 (1), 33–41.

Lima, J. E. F. W., Lopes, W. T. A., Oliveira-Filho, E. C., de Muniz, D. H., 2011. Relação entre a tubidez e a concentração de sedimentos em suspensão em uma bacia agrícola típica do Cerrado: o caso da Bacia Experimental do Alto Rio Jardim , DF. In: XIX Simpósio Brasileiro de Recursos Hídricos. Maceió.

Lima, J. E. F. W., Silva, E. M., Strauch, M., Lorz, C., 2013. Development of a soil database for applying SWAT in the Brazilian Savanna region. In: International SWAT Conference 2013, July 17-19, Toulouse, France.

Lima, W. d. P., Zakia, M. J. B., Libardi, P. L., Filho, A. P. d. S., 1990. Comparative evapotranspiration of Eucalyptus, Pine and natural "Cerrado" vegetation measure by the soil water balance method. IPEF International 1, 5–11.

Liu, T., Merrill, N. H., Gold, A. J., Kellogg, D. Q., Uchida, E., 2013. Modeling the Production of Multiple Ecosystem Services from Agricultural and Forest Landscapes in Rhode Island. Agricultural and Resource Economics Review 42 (1), 251–274.

Liu, Y., Gupta, H., Springer, E., Wagener, T., 2008. Linking science with environmental decision making: Experiences from an integrated modeling approach to supporting sustainable water resources management. Environmental Modelling & Software 23 (7), 846–858.

Lopes, V. L., 1996. On the effect of uncertainty in spatial distribution of rainfall on catchment modelling. Catena 28 (1-2), 107–119.

Lorz, C., Abbt-braun, G., Bakker, F., Borges, P., Börnick, H., Fortes, L., Frimmel, F. H., Gaffron, A., Hebben, N., Höfer, R., Makeschin, F., Neder, K., Roig, H. L., Steiniger, B., Walde, D. H., Weiß, H., Worch, E., Wummel, J., 2011a. Challenges of an integrated water resource management for the Distrito Federal, Western Central Brazil: climate, land-use and water resources. Environmental Earth Sciences 65 (5), 1575–1586.

Lorz, C., Bakker, F., Neder, K., Roig, H. L., Weiß, H., Makeschin, F., 2011b. Landnutzungswandel und Wasserressourcen im Bundesdistrikt, Zentral Brasilien. Hydrologie und Wasserbewirtschaftung 2, 75–87.

Madaleno, I. M., 1996. Brasilia: the frontier capital. Cities 13 (4), 273–280.

Maringanti, C., Chaubey, I., Arabi, M., Engel, B., 2011. Application of a Multi-Objective Optimization Method to Provide Least Cost Alternatives for NPS Pollution Control. Environmental Management 48 (3), 448–461.

Marshall, L., Nott, D., Sharma, A., 2007. Towards dynamic catchment modelling : a Bayesian hierarchical mixtures of experts framework. Hydrological Processes 861 (October 2006), 847– 861.

Martine, G., Camargo, L., 1997. Growth and Distribution of the Brazilian Population: Recent Trends. Brazilian Journal of Population Studies 1, 59–83.

McGregor, G. R., Nieuwolt, S., 1998. Tropical Climatology: An Introduction to the Climates of the Low Latitudes. John Wiley & Sons, Ltd, Chichester.

Memarian, H., Tajbakhsh, M., Balasundram, S. K., 2013. Application of SWAT for impact assessment of land use/cover change and best management practices: A review. International Journal of Advancement in Earth and Environmental Sciences 1 (1), 36–40.

Milewski, A., Sultan, M., Yan, E., Becker, R., Abdeldayem, A., Soliman, F., Gelil, K. A., 2009. A remote sensing solution for estimating runoff and recharge in arid environments. Journal of Hydrology 373 (1-2), 1–14.

Millenium Ecosystem Assessment, 2005. Ecosystems and Human Well-being: Synthesis. Island Press, Washington, DC.

Monasterio, M., Sarmiento, G., 1976. Phenological strategies of plant species in the tropical savanna and the semi-deciduous forest of the Venezuelan llanos. Journal of Biogeography 3, 325–355.

Monteith, J. L., 1965. Evaporation and the environment. In: Fogg, G. E. (Ed.), Symposium of the Society for Experimental Biology. The State and Movement of Water in Living Organisms, 19. Academic Press, Inc., NY, pp. 205–234.

Monteith, J. L., 1977. Climate and the efficiency of crop production in Britain. Philosophical Transactions of the Royal Society of London B 281, 277–294.

Moon, J., Srinivasan, R., Jacobs, J., 2004. Stream flow estimation using spatially distributed rainfall in the Trinity River basin, Texas. Transactions Of The ASABE 47 (5), 1445–1451.

Moriasi, D., Arnold, J. G., Van Liew, M. W., Bingner, R., Harmel, R., Veith, T. L., 2007. Model Evaluation Guidelines for Systematic Quantification of Accuracy in Watershed Simulations. Transactions Of The ASABE 50 (3), 885–900.

Mu, Q., Heinsch, F. A., Zhao, M., Running, S. W., 2007. Regional evaporation estimates from flux tower and MODIS satellite data. Remote Sensing of Environment 111, 519–536.

Mu, Q., Zhao, M., Running, S. W., 2011. Improvements to a MODIS global terrestrial evapotranspiration algorithm. Remote Sensing of Environment 115 (8), 1781–1800.

Myneni, R. B., Hoffman, S., Knyazikhin, Y., Privette, J. L., Glassy, J., Tian, Y., Wang, Y., Song, X., Zhang, Y., Smith, G. R., Lotsch, A., Friedl, M., Morisette, J. T., Votava, P., Nemani, R. R., Running, S. W., 2002. Global products of vegetation leaf area and fraction absorbed PAR from year one of MODIS data. Remote Sensing of Environment 83 (1-2), 214–231.

Naramngam, S., Tong, S. T. Y., 2013. Environmental and economic implications of various conservative agricultural practices in the Upper Little Miami River basin. Agricultural Water Management 119 (0), 65–79.

Nash, J., Sutcliffe, J., 1970. River flow forecasting through conceptual models part I - A discussion of principles. Journal of Hydrology 10 (3), 282–290.

Neitsch, S., Arnold, J. G., Kiniry, J. R., Srinivasan, R., Williams, J., 2005. Soil and Water Assessment Tool: Input/Output File Documentation: Version 2005. Tech. rep., Grassland, Soil and Water Research Laboratory, Agricultural Research Service, Blackland Research Center, Texas Agricultural Experiment Station, Temple, Texas.

Neitsch, S., Arnold, J. G., Kiniry, J. R., Srinivasan, R., Williams, J., 2010. Soil and Water Assessment Tool Input/Output File Documentation Version 2009. Texas Water Resources Institute Technical Report No. 365. Tech. rep., Grassland, Soil and Water Research Laboratory - Agricultural Research Service, Blackland Research Center - Texas AgriLife Research, College Station, Texas.

Neitsch, S., Arnold, J. G., Kiniry, J. R., Williams, J., 2011. Soil & Water Assessment Tool Theoretical Documentation Version 2009. Texas Water Resources Institute Technical Report No. 406. Tech. rep., Grassland, Soil and Water Research Laboratory - Agricultural Research Service, Blackland Research Center - Texas AgriLife Research, College Station, Texas.

Oliveira, R., Bezerra, L., Davidson, E., Pinto, F., Klink, C. A., Nepstad, D., Moreira, A., 2005. Deep root function in soil water dynamics in cerrado savannas of central Brazil. Functional Ecology 19, 574–581.

Oliveira-Filho, A. T., Ratter, J. A., 2002. Vegetation Physiognomies and Woody Flora of the Cerrado Biome. In: Oliveira, P. S., Marquis, R. J. (Eds.), The Cerrados of Brazil. Columbia University Press, New York, Ch. II 6, pp. 91–120.

Pappenberger, F., Beven, K. J., 2006. Ignorance is bliss: Or seven reasons not to use uncertainty analysis. Water Resources Research 42 (5), W05302.

Phalan, B., Onial, M., Balmford, A., Green, R. E., 2011. Reconciling food production and biodiversity conservation: land sharing and land sparing compared. Science 333 (6047), 1289–91.

Phomcha, P., Wirojanagud, P., Vangpaisal, T., Thaveevouthti, T., 2011. Suitability of SWAT Model for Simulating of Monthly Streamflow in Lam Sonthi Watershed. Journal of Industrial Technology 7 (2), 49–56.

Plesca, I., Timbe, E., Exbrayat, J.-F., Windhorst, D., Kraft, P., Crespo, P., Vaché, K., Frede, H.-G., Breuer, L., 2012. Model intercomparison to explore catchment functioning: Results from a remote montane tropical rainforest. Ecological Modelling 239, 3–13.

Pluntke, T., Pavlik, D., Bernhofer, C., 2014. Reducing uncertainty in hydrological modelling in a data sparse region. Submitted to Environmental Earth Sciences.

Poulter, B., Cramer, W., 2009. Satellite remote sensing of tropical forest canopies and their seasonal dynamics. International Journal of Remote Sensing 30 (24), 6575–6590.

Raftery, A. E., Gneiting, T., Balabdaoui, F., Polakowski, M., 2005. Using Bayesian Model Averaging to Calibrate Forecast Ensembles. Monthly Weather Review 133, 1155–1175.

Rahaman, M. M., Varis, O., 2005. Integrated water resources management : evolution , prospects and future challenges. Sustainability: Science, Practice, & Policy 1 (1), 15–21.

Reatto, A., Martins, E. d. S., Farias, M. F. R., da Silva, A. V., de Carvalho Jr, O. A., 2004. Mapa Pedológico Digital - SIG Atualizado do Distrito Federal Escala 1:100.000 e uma Síntese do Texto Explicativo. Tech. rep., EMBRAPA-Cerrados, Planaltina, DF.

Refsgaard, J. C., Henriksen, H. J. r., 2004. Modelling guidelines - terminology and guiding principles. Advances in Water Resources 27 (1), 71–82.

Refsgaard, J. C., van der Sluijs, J. P., Hø jberg, A. L., Vanrolleghem, P. a., 2007. Uncertainty in the environmental modelling process - A framework and guidance. Environmental Modelling & Software 22 (11), 1543–1556.

Regonda, S. K., Rajagopalan, B., Clark, M. P., Zagona, E., 2006. A multimodel ensemble forecast framework: Application to spring seasonal flows in the Gunnison River Basin. Water Resources Research 42 (9), 1–14.

Rizzi, R., Rudorff, B., Shimabukuro, Y., Doraiswamy, P., 2006. Assessment of MODIS LAI retrievals over soybean crop in Southern Brazil. International Journal of Remote Sensing 27 (19), 4091–4100.

Rocha, E. O., Calijuri, M. L., Santiago, A. F., Assis, L. C., Alves, L. G. S. o., 2012. The Contribution of Conservation Practices in Reducing Runoff, Soil Loss, and Transport of Nutrients at the Watershed Level. Water Resources Management 26 (13), 3831–3852.

Rostamian, R., Jaleh, A., Afyuni, M., Mousavi, S.-F., Heidarpour, M., Jalalian, A., Abbaspour, K. C., 2008. Application of a SWAT model for estimating runoff and sediment in two mountainous basins in central Iran. Hydrological Sciences Journal/Journal des Sciences Hydrologiques 53 (5), 977–988.

Santana, A. O., Cuniat, G., Imaña Encinas, J., 2010. Contribuição da vegetação rasteira na evapotranspiração total em diferentes ecossistemas do bioma Cerrado, Distrito Federal. Ciência Florestal 20 (2), 269–281.

Schaap, M., Leij, F., van Genuchten, M., 2001. Rosetta: A Computer Program for Estimating Soil Hydraulic Parameters with Hierarchical Pedotransfer Functions. Journal of Hydrology 251, 163–176.

Schaffrath, D., Barthold, F. K., Bernhofer, C., 2010. Spatiotemporal variability of grassland vegetation cover in a catchment in Inner Mongolia, China, derived from MODIS data products. Plant and Soil 340 (1-2), 181–198.

Scholz, F. G., Bucci, S. J., Goldstein, G., Meinzer, F. C., Franco, A. C., Salazar, A., 2008. Plant- and stand-level variation in biophysical and physiological traits along tree density gradients in the Cerrado. Brazilian Journal of Plant Physiology 20 (3), 217–232.

Schuol, J., Abbaspour, K. C., Srinivasan, R., Yang, H., 2008. Estimation of freshwater availability in the West African sub-continent using the SWAT hydrologic model. Journal of Hydrology 352 (1-2), 30–49.

Schwab, G. O., Fangmeier, D. D., Elliot, W. J., 1995. Soil and Water Management Systems, 4th Edition. John Wiley & Sons, New Jersey.

Secchi, S., Gassman, P. W., Jha, M. K., Kurkalova, L., Feng, H. H., Campbell, T., Kling, C. L., 2007. The cost of cleaner water: Assessing agricultural pollution reduction at the watershed scale. Journal of Soil and Water Conservation 62 (1), 10–21.

Seghieri, J., Floter, C., Pontanier, R., 1995. Plant phenology in relation to water availability: herbaceous and woody species in the savannas of northern Cameroon. Journal of Tropical Ecology 11, 237–254.

Setegn, S. G., Srinivasan, R., Melesse, A. M., Dargahi, B., 2010. SWAT model application and prediction uncertainty analysis in the Lake Tana Basin , Ethiopia. Hydrological Processes 24, 357– 367.

Sexton, A., Sadeghi, A., Zhang, X., Srinivasan, R., Shirmohammadi, A., 2010. Using NEXRAD and Rain Gauge Precipitation Data for Hydrologic Calibration of SWAT in a Northeastern Watershed. Transactions Of The ASABE 53 (5), 1501–1510.

Sharma, A., Chowdhury, S., 2011. Coping with model structural uncertainty in medium-term hydro-climatic forecasting. Hydrology Research 42 (2-3), 113–127.

Shirmohammadi, A., Chaubey, I., Harmel, R. D., Bosch, D. D., Munoz-Carpena, R., Dharmasri, C., Sexton, A., Arabi, M., Wolfe, M. L., Frankenberger, J., Graff, C., Sohrabi, T. M., 2006. Uncertainty in TMDL models. Transactions Of The Asabe 49, 1033–1049.

Silva, J., Fariñas, M., Felfili, J. M., Klink, C. A., 2006. Spatial heterogeneity, land use and conservation in the cerrado region of Brazil. Journal of Biogeography 33 (3), 536–548.

Simon, A., Trentin, G., Cunha, C., 2010. Avaliação da dinâmica do uso da terra na bacia do Arroio Santa Bárbara Pelotas (Brasil), no período de 1953 a 2006. Revista electrónica de geografía y ciencias socials XIV 14 (327).

Singh, V. P., 1995. Computer models of watershed hydrology. Water Resources Publications.

Singh, V. P., Frevert, D. K., 2006. Watershed Models. NetLibrary, Inc. Taylor & Francis.

Sohrabi, T. M., Shirmohammadi, A., Chu, T. W., Montas, H., Nejadhashemi, A. P., 2003. Uncertainty Analysis of Hydrologic and Water Quality Predictions for a Small Watershed Using SWAT2000. Environmental Forensics 4, 229–238.

Strauch, M., Bernhofer, C., Koide, S., Volk, M., Lorz, C., Makeschin, F., 2012. Using precipitation data ensemble for uncertainty analysis in SWAT streamflow simulation. Journal of Hydrology 414-415, 413–424.

Strauch, M., Lima, J. E. F. W., Volk, M., Lorz, C., Makeschin, F., 2013. The impact of Best Management Practices on simulated streamflow and sediment load in a Central Brazilian catchment. Journal of Environmental Management 127 Suppl, S24–36.

Thampi, S. G., Raneesh, K. Y., Surya, T. V., 2010. Influence of Scale on SWAT Model Calibration for Streamflow in a River Basin in the Humid Tropics. Water Resources Management 24 (15), 4567–4578.

Thornley, J. H., France, J., 2005. An open-ended logistic-based growth function. Ecological Modelling 184 (2-4), 257–261.

Tian, Y., Knyazikhin, Y., Myneni, R. B., Glassy, J., Dedieu, G., Running, S., 2000. Prototyping of MODIS LAI and FPAR algorithm with LASUR and LANDSAT data. IEEE Transactions on Geoscience and Remote Sensing 38 (5), 2387–2401.

Tobin, K. J., Bennett, M. E., 2009. Using SWAT to Model Streamflow in Two River Basins With Ground and Satellite Precipitation Data. JAWRA Journal of the American Water Resources Association 45 (1), 253–271.

Tomasella, J., Hodnett, M. G., 2004. Pedotransfer Functions for Tropical Soils. Developments in Soil Science 30, 415–429.

Troutman, B. M., 1983. Runoff Prediction Errors and Bias in Parameter Estimation Induced by Spatial Variability of Precipitation. Water Resources Research 19 (3), 791–810.

Tuppad, P., Douglas-Mankin, K., Koelliker, J., Hutchinson, J., Knapp, M., 2010a. NEXRAD Stage III Precipitation Local Bias Adjustment for Streamflow Prediction. Transactions Of The ASABE 53 (5), 1511–1520.

Tuppad, P., Kannan, N., Srinivasan, R., Rossi, C. G., Arnold, J. G., 2010b. Simulation of Agricultural Management Alternatives for Watershed Protection. Water Resources Management 24 (12), 3115–3144.

Uhlenbrook, S., Seibert, J., Leibundgut, C., Rodhe, A., 1999. Prediction uncertainty of conceptual rainfall-runoff models caused by problems in identifying model parameters and structure. Hydrological Sciences Journal/Journal des Sciences Hydrologiques 44 (5), 779–797.

Ullrich, A., Volk, M., 2009. Application of the Soil and Water Assessment Tool (SWAT) to predict the impact of alternative management practices on water quality and quantity. Agricultural Water Management 96 (8), 1207–1217.

Ullrich, A., Volk, M., 2010. Influence of different nitrate-N monitoring strategies on load estimation as a base for model calibration and evaluation. Environmental Monitoring and Assessment 171 (1-4), 513–527.

UN-Water, 2008. Status Report on IWRM and Water Efficiency Plans for CSD16. Tech. Rep. May.

UNESCO, IHP, WWAP, NARBO, 2009. IWRM Guidelines at River Basin Level. Part 2-1: The Guidelines for IWRM Coordination. Tech. rep., United Nations Educational, Scientific and Cultural Organization - UNESCO, International Hydrological Programme - IHP, World Water Assessment Programme - WWAP, Network of Asian River Basin Organizations - NARBO.

USDA-SCS, 1972. Section 4 hydrology. In: National Engineering Handbook. USDA Soil Conservation Service, Washington, Ch. 10.1-10.24.

Vaché, K. B., Eilers, J. M., Santelmann, M. V., 2002. Water Quality Modeling of Alternative Agricultural Scenarios in the U.S. Corn Belt. Journal of the American Water Resources Association 38 (3), 773–787.

van Griensven, A., Meixner, T., Grunwald, S., Bishop, T., Diluzio, M., Srinivasan, R., 2006. A global sensitivity analysis tool for the parameters of multi-variable catchment models. Journal of Hydrology 324 (1-4), 10–23.

Vandenberghe, V., Goethals, P. L. M., van Griensven, A., Meirlaen, J., De Pauw, N., Vanrolleghem, P. A., Bauwens, W., 2005. Application of automated measurement stations for continuous water quality monitoring of the Dender river in Flanders, Belgium. Environmental Monitoring and Assessment 108 (1-3), 85–98.

Vanmaercke, M., Poesen, J., Verstraeten, G., de Vente, J., Ocakoglu, F., 2011. Sediment yield in Europe: Spatial patterns and scale dependency. Geomorphology 130 (3-4), 142–161.

Vasyukova, E., Uhl, W., Braga, F., Simões, C., Baylão, T., Neder, K., 2012. Drinking water production from surface water sources in the tropics: Brasília DF, Brazil. Environmental Earth Sciences 65 (5), 1587–1599.

Viney, N. R., Bormann, H., Breuer, L., Bronstert, A., Croke, B., Frede, H.-G., Gräff, T., Hubrechts, L., Huisman, J., Jakeman, A., Kite, G., Lanini, J., Leavesley, G., Lettenmaier, D., Lindström, G., Seibert, J., Sivapalan, M., Willems, P., 2009. Assessing the impact of land use change on hydrology by ensemble modelling (LUCHEM) II: Ensemble combinations and predictions. Advances in Water Resources 32 (2), 147–158.

Viovy, N., Arino, O., Belward, A. S., 1992. The Best Index Slope Extraction (BISE): A method for reducing noise in NDVI time-series. International Journal of Remote Sensing 13 (8), 1585–1590.

Volk, M., Fohrer, N., Schmalz, B., Ullrich, A., 2011. Application of the SWAT Model for Ecohydrological Modelling in Germany. In: Shukla, M. (Ed.), Soil Hydrology, Land Use and Agriculture. pp. 176–195.

Vrugt, J. A., Robinson, B., 2007. Treatment of uncertainty using ensemble methods: Comparison of sequential data assimilation and Bayesian model averaging. Water Resources Research 43 (1), W01411.

Wagner, P. D., Kumar, S., Fiener, P., Schneider, K., 2011. Hydrological modeling with SWAT in a Monsoon-driven environment: Experience from the Western Ghats, India. Transactions Of The ASABE 54 (5), 1783–1790.

Waidler, D., White, M. J., Steglich, E. M., Wang, S., Williams, J., Jones, C. A., Srinivasan, R., 2011. Conservation Practice Modeling Guide for SWAT and APEX. Texas Water Resources Institute Technical Report No. 399. Tech. rep., College Station, Texas.

Walling, D. E., 1977. Limitations of the rating curve technique for estimating suspended sediment loads, with particular reference to British rivers. In: Erosion and Solid Matter Transport in Inland Waters - Symposium. IAHS-Publication No. 122. International Association of Hydrological Sciences, Dorking, Surrey, UK, pp. 34–48.

Williams, J. R., Jones, C. A., Dyke, P. T., 1984. A modeling approach to determining the relationship between erosion and soil productivity. Transactions of the ASAE 27, 129–144.

Williams, J. R., Jones, C. A., Kiniry, J. R., Spanel, D. A., 1989. The EPIC crop growth model. Transactions of the ASAE 32, 497–511.

Winchell, M., Srinivasan, R., Di Luzio, M., 2007. ArcSWAT interface for SWAT2005 - Users Guide. Tech. rep., Blackland Research Center, Grassland, Soil and Water Research Laboratory, Temple, TX.

Wischmeier, W., Smith, D., 1978. Predicting rainfall losses: A guide to conservation planning. USDA Agricultural Handbook No. 537. U.S. Gov. Print. Office, Washington, D.C.

Woznicki, S. A., Nejadhashemi, A. P., 2012. Sensitivity Analysis of Best Management Practices Under Climate Change Scenarios. JAWRA Journal of the American Water Resources Association 48 (1), 90–112.

Wu, L., Seo, D.-J., Demargne, J., Brown, J. D., Cong, S., Schaake, J., 2011. Generation of ensemble precipitation forecast from single-valued quantitative precipitation forecast for hydrologic ensemble prediction. Journal of Hydrology 399 (3-4), 281–298.

Yang, J., Reichert, P., Abbaspour, K. C., Xia, J., Yang, H., 2008. Comparing uncertainty analysis techniques for a SWAT application to the Chaohe Basin in China. Journal of Hydrology 358 (1-2), 1–23.

Young, A., 1976. Tropical soils and soil survey. Cambridge University Press, Cambridge.

Zhang, X., Friedl, M. A., Schaaf, C. B., Strahler, A. H., Hodges, J. C. F., Gao, F., Reed, B. C., Huete, A., 2003. Monitoring vegetation phenology using MODIS. Remote Sensing of Environment 84 (3), 471–475.

Zhang, X., Srinivasan, R., Bosch, D. D., 2009. Calibration and uncertainty analysis of the SWAT model using Genetic Algorithms and Bayesian Model Averaging. Journal of Hydrology 374 (3-4), 307–317.